Dissertation

A microsystem for on-chip droplet storage and processing

Ausgeführt zum Zwecke der Erlangung des akademischen Grades eines Doktors der technischen Wissenschaften von

Mahmuda Akhtar

eingereicht an der Universität Bremen Institut für Mikrosensoren, -aktoren und -systeme, Fachbereich Physik und Elektrotechnik

The research presented in this thesis was carried out at the Institute of Microsensors, - actuators and -systems, University of Bremen, Germany

Date of thesis defense : 10 September 2020

Erstbegutachter : Prof. Dr. Michael J. Vellekoop

Zweitbegutachter : Prof. Dr.-Ing. Karl-Ludwig Krieger

Abstract

Droplet microfluidics is a useful tool that can be used to carry out biological and chemical experiments at high speed and with enhanced efficiency. Many applications such as biological cell culturing and chemical analysis and screening require on-chip storage and manipulation of the droplets. The goal of this thesis work was to design a microfluidic chip that can store droplets on-chip and to explore its potential applications.

The primary aim of this research was to develop a microfluidic system where droplets could be stored on the same chip from which they were generated. With this aim, several materials were investigated and examined to realize such a microchip. A Parylene AF4 coated polydimethylsiloxane (PDMS) chip was finally produced to generate and store the droplets. The main applications of on-chip storage droplets are related to cell storage and cell culture. These uses require a microchip that is made out of a biocompatible material, and both PDMS and Parylene are biocompatible. Droplets containing biological cells were generated and stored to evaluate the on-chip storage system. The droplets were stored more than four days on the developed chip.

In addition to the on-chip storage of water droplets, agarose droplets were also generated and stored. Agarose is often used as a support to culture human and animal cells. Agarose solution can form a stable gel at low concentrations, it is free of contamination, and does not adhere to cells. The elasticity of the microenvironment has a significant impact on cellular growth. The agarose droplets allow the encapsulation of cells, which can then be cultured in different elastic environments. This enables the investigation of the impact that the mechanical properties of the environment can have on cell behavior. A primary study was conducted by encapsulating yeast cells in agarose.

The ability to carry out reactions and culture cells in microdroplets depends on being able to merge microdroplets from different sample fluids. The sorting of required droplets is another important aspect of a microfluidic network. A chip was designed and realized to generate droplets with fresh

nutrients that could be merged with the stored droplets to supply nutrients to the cells.

Droplets containing *Escherichia coli* and *Enterococcus faecalis* were stored on-chip in AF4 coated PDMS channels for several hours, and cell growth was observed for up to 5 hours. However, mammalian cells cannot be stored in an AF4 coated channel for an extended period due to the lack of oxygen and carbon dioxide. A method of supplying oxygen to the stored droplets in a microchannel was therefore developed. Air bubbles were placed close the aqueous droplets, separated by fluorinated oil, in the same microfluidic channel to modulate the oxygen level by means of diffusion. The oxygen level in the aqueous droplets was monitored by the redox indicator methylene blue. Madin-Darby Canine Kidney (MDCK) cells were encapsulated and stored in the droplets with the presence of air bubbles.

In conclusion, the applicability of AF4 coated PDMS chips for cell storage and culturing was experimentally proven. All the devices were fabricated using low-cost, rapid prototyping fabrication techniques.

Kurzfassung

Die Tropfen-Mikrofluidik ist ein nützliches Verfahren, mit dem biologische und chemische Experimente mit hoher Geschwindigkeit und verbesserter Effizienz durchgeführt werden können. Viele Anwendungen, wie die biologische Zellkultivierung sowie die chemische Analyse und das Screening erfordern die Positionierung und die Handhabung der Tröpfchen in dem Chip. Das Hauptziel dieser Forschungsarbeit war es, einen Mikrofluidik-Chip zu entwerfen, der Tröpfchen auf dem Chip generieren und speichern kann, um weitere Untersuchungen zu ermöglichen und potentielle Applikationen zu erforschen. Zu diesem Zweck wurden mehrere Materialien ausgewählt und untersucht. Letztendlich wurde ein Parylene AF4-beschichteter Polydimethylsiloxan (PDMS)-Chip hergestellt, der diese Anforderungen erfüllt. Die Hauptanwendungen von On-Chip-Speichertröpfchen stehen im direkten Zusammenhang mit der Zellspeicherung und der Zellkultivierung. Diese Anwendungen erfordern einen Mikrochip, der aus einem biokompatiblen Material, wie PDMS oder Parylene hergestellt ist. Um das On-Chip-Speichersystem zu bewerten, wurden Tröpfchen, die biologische Zellen enthielten, erzeugt. Diese verblieben mehr als vier Tage in dem entwickelten Chip.

Neben der On-Chip-Speicherung von wässrigen Tröpfchen wurden auch Agarosetröpfchen hergestellt und platziert. Agarose wird häufig als Träger für die Kultivierung menschlicher und tierischer Zellen verwendet. Eine Agaroselösung kann bei geringen Konzentrationen ein stabiles Gel bilden, welches frei von Verunreinigungen ist und nicht an den Zellen haftet. Die Elastizität der Mikroumgebung hat einen signifikanten Einfluss auf das Zellwachstum. Die Agarosetröpfchen ermöglichen die Einkapselung von Zellen, die dann in verschiedenen elastischen Umgebungen kultiviert werden können. In einer durchgeführten Primärstudie wurden Hefezellen in Agarose eingekapselt. Diese Untersuchungen dienten dem Nachweis, dass mechanische Eigenschaften der Umgebung das Zellverhalten beeinflussen können.

Um chemische Reaktionen anzuregen und Zellkulturen in Mikrotröpfchen zu realisieren, müssen Mikrotröpfchen aus verschiedenen Flüssigkeitsproben zusammengeführt werden. Die Handhabung der erforderlichen Tröpfchen ist

ein weiterer wichtiger Aspekt der tropfenbasierten Mikrofluidik. Es wurde ein Chip entworfen und hergestellt, der Tröpfchen mit frischen Nährstoffen produziert und die gespeicherten Tröpfchen zusammenführt, um deren Zellen mit-Nährstoffen zu versorgen.

Tröpfchen, die *Escherichia coli* und *Enterococcus faecalis* enthielten, wurden mehrere Stunden in dem Chip in AF4-beschichteten PDMS-Kanälen aufbewahrt. Dabei wurde ein bis zu 5 Stunden andauerndes Zellwachstum beobachtet. Da Säugetierzellen jedoch aufgrund des Mangels an Sauerstoff und Kohlendioxid nicht über einen längeren Zeitraum in einem AF4-beschichteten Kanal gelagert werden können, wurde ein Verfahren zur Zufuhr von Sauerstoff zu den in einem Mikrokanal gespeicherten Tröpfchen entwickelt. Nahe den durch fluoriertes Öl getrennten wässrigen Tröpfchen wurden Luftblasen in demselben Mikrofluidikkanal positioniert, um den Sauerstoffgehalt mittels Diffusion anzupassen. Die Überwachung des Sauerstoffgehaltes in den wässrigen Tröpfchen erfolgte mittels des Redoxindikators Methylenblau. Des Weiteren wurden Madin-Darby Canine Kidney (MDCK)-Zellen eingekapselt und in Gegenwart von Luftblasen den Tröpfchen hinzugefügt.

In der vorliegenden Forschungsarbeit konnte die Anwendbarkeit von AF4-beschichteten PDMS-Chips für die Speicherung und Kultivierung von Zellen experimentell nachgewiesen werden. Die Herstellung aller Testvorrichtungen erfolgte unter Verwendung schneller und kostengünstiger Methoden.

Contents

Nomenclature

0.1 List of abbreviations

Symbol	Description
CO_2	carbon dioxide
CVD	chemical vapor deposition
DI	de-ionized
DNA	deoxyribonucleic acid
DRIE	deep reactive ion etching
E. coli	Escherichia coli
E. faecalis	Enterococcus faecalis
LB	lysogeny broth
MEMS	microelectromechanical systems
O_2	oxygen
PBS	phosphate-buffered saline
PCR	polymerase chain reaction
PDMS	polydimethylsiloxane
PMMA	polymethyl methacrylate
PVC	polyvinyl chloride
RNA	ribonucleic acid
rpm	revolutions per minute
Ti	titanium
UV	ultraviolet
vol.%	volume percent
YEPD/YPD	yeast extract peptone dextrose

0.2 List of variables

Symbol	Description	Unit
Re	Reynolds number	-
ρ	fluid density	kg/m^2
υ	characteristic velocity	m/s
D_h	hydraulic diameter	m
P_{wet}	wetted perimeter	m
k	Boltzmann's constant	J/K
T	absolute temperature	J
μ	viscosity	Pa.s
φ	molar concentration	mol/m^3
D	diffusion coefficient	m$^2/s$
U	cohesive energy	N
δ	molecular dimension	m
γ	surface tension	N/m
θ_s	static contact angle	radians
θ_s	static contact angle	radians
λ	mean free path	m
B_0	Bond number	-
R	droplet radius	meter
g	gravitational acceleration	m/s^2

Chapter 1

Introduction

Droplet microfluidics came into the spotlight at the beginning of this century. When a new technology emerges, scientists attempt to apply it in their respective fields. Microfluidics technology is of interest in many fields, especially in biology and chemistry because of its high reproducibility, fast reaction time, and its ability for high-throughput analysis. This thesis work focuses on the design and realization of a microsystem for the on-chip manipulation of droplets and its applications.

For several decades, the concept of miniaturization has been employed in every branch of science. Miniaturized systems have been realized in the mechanical, electrical, fluidics and biological fields. In the 1980s, the notion of miniaturization led to the development of a new field known as MEMS (microelectro-mechanical systems). MEMS endeavors to make systems less complex, more reliable and cost-effective, and highly sensitive. A smart system is defined by its simplicity and portability. It is often considered that the history of micro- and nanotechnologies began in the year 1959. During the APS (American Physical Society) at Caltech (USA) of that year, Richard P. Feynman gave a visionary speech, entitled 'There is plenty of room at the bottom'. He mentioned that there is no physical reason why the 50 volumes of the Encyclopedia Britannica could not be inscribed on the head of a needle. His prediction did not remain a fantasy. In 1995, the word "IBM" was spelled out using only a few atoms.

Chemists and biologists have continuously searched for methods to further miniaturize their analytical systems. The miniaturization of analytical systems is advantageous for many biological applications where reagents are very expensive and the sample volumes are often limited. In the drive for the miniaturization of analytical systems, the bioanalytical and microelectronics disciplines have merged, which can be considered as the birth of the microfluidics field. In 1979, the first silicon-based gas chromatography analysis

system was published [1]. This work revealed that the combination of MEMS and microfluidics has tremendous potential. In early 1990, the concept of *micro Total Analysis Systems (μTAS)* was introduced by Manz and others [2]. This led to a boom in microfluidics. In the past 25 years, researchers have developed many new concepts and applications based on microfluidic technology. Sample volumes were reduced to the microliter range. For instance, consider that 10^5 components need to be screened in a microplate consisting of 20 wells, each containing 10 μl. The required analysis time would be several months. The microfluidic system reported in [3] can reduce the screening time to one week and sample volume to 100 milliliters; droplet microfluidics further reduces the required sample volume to 1 milliliter. A graphical representation of the evolution of microfluidic systems is depicted in Fig.1.1.

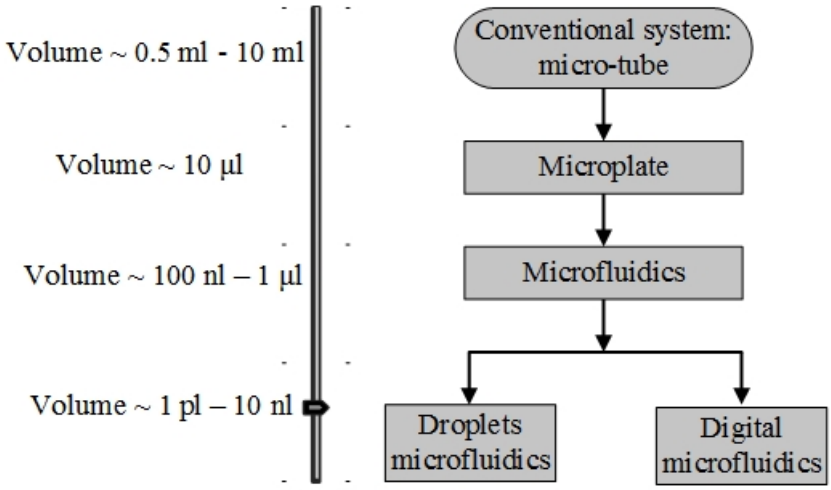

Figure 1.1: Scheme of different scales of fluidic systems [4].

1.1 Microflow to microdrops

According to the definition of microfluidics, microliters (10^{-6} liter) of fluid can be controlled and manipulated in the networks of a channel with dimensions from tens to hundreds of micrometers [5]. In conventional microfluidics, a fluid sample is injected into a microchannel for investigation. Therefore, reagents are in direct contact with the microchannel. In contrast, the sample is surrounded by another immiscible fluid in droplet microfluidics. Hence, the sample has very little or no contact with the microchannel (Fig.1.2). Therefore, one of the advantages of droplet microfluidics over conventional

microfluidics is its property of compartmentalization. A single droplet in a microfluidic channel can be considered as a micro-reactor with an extremely small fluid volume (pico- to nanoliter), yielding little or no cross-contamination between different compartmentalized samples, which reduces the interactions of reagents with the channel walls. It also improves the heat and mass transfer due to high surface area to volume ratios. The frequency of droplet generation (i.e., the throughput) can reached up to 10 kHz, whereas robotic microtiter plate platforms can reach a throughput of approximately 1 Hz. The ultrahigh throughput and an extremely small volume of required sample make droplet microfluidics desirable in the field of biotechnology.

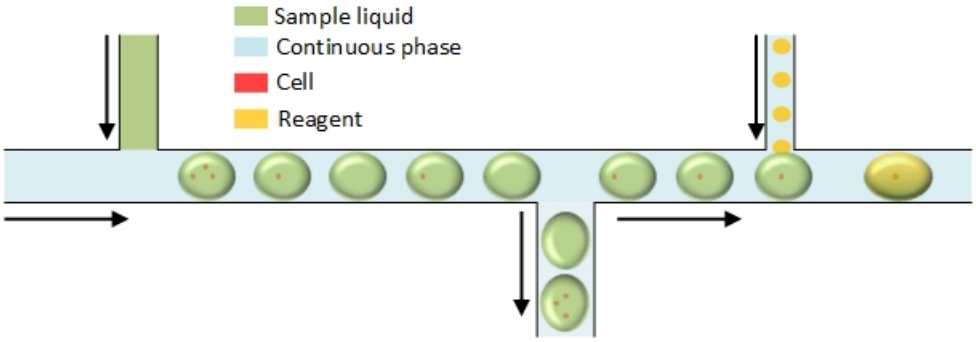

Figure 1.2: Schematic diagram of on-chip manipulation of droplets including generation, sorting, and merging.

Along with the high-throughput analysis and reduced sample volume, droplet microfluidics offers on-chip processing of a sample. After loading the sample in a droplet, reagents can be added to the sample, droplets of interest can be sorted, chemical reactions of different liquids can be conducted, and the sample droplet can be separated into several smaller droplets. For instance, cells have been encapsulated in droplets using the Poisson distribution ratio, where some droplets contain a single cell, some contain two or three cells, and some droplets are empty. To further investigate the cells encapsulated in droplets (e.g., to verify cell viability), it is often necessary to add reagents. This can be accomplished by following the protocols presented in [6, 7]. Before adding reagents to the sample, droplets can be sorted to save reagents and investigation time. For example, if single-cell droplets are of interest, it is possible to sort those droplets from the train of droplets using available methods [8, 9]. The on-chip manipulation of droplets gives more possibilities and opportunities for applications in different branches of science.

1.2 Digital and droplet microfluidics

Digital and droplet microfluidics both work with a very small volume of liquid, in the range of micro- to picoliter. However, they differ significantly in how they deal with the liquid. Digital microfluidics is referred to as a parallel system, whereas droplet microfluidics is referred to as a serial system. The idea of digital microfluidics was inspired by the concept of a microplate. In digital microfluidics, microdrops are generated and treated individually on a planar surface. Therefore, an actuation force (electric or acoustic) is needed to perform the mixing, pumping, and drop generation (Fig.1.3). It deals only with sample liquid (one phase); in contrast, droplet microfluidics deals with two liquids: a continuous phase and droplet phase. In general, an oil-based liquid is used as a continuous phase, and the sample liquid is used as a droplet phase, and they are immiscible with each other. The sample droplets are generated in the continuous phase at the T- or flow-focusing junction [10, 11]. The generation of droplets in a microchannel requires a continuous flow system; therefore, microfluidic pumps and valves, actuated by electrical, mechanical, magnetic, or acoustic force, are needed. The physics behind the creation and manipulation of droplets in droplet microfluidics will be discussed in the following chapter.

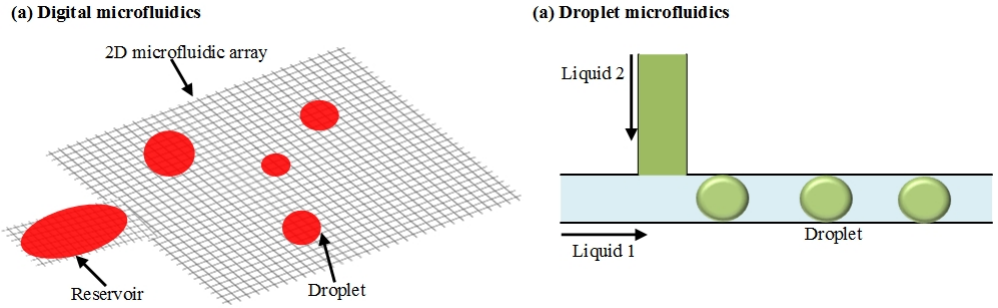

Figure 1.3: Schematic diagram of (a) digital microfluidics (droplets on a surface), (b) droplet microfluidics (droplets in a channel).

1.3 Droplet microfluidics and cell culture

In cell biology, cells are cultured in bulk medium where cells can be contaminated by the surrounding environment. Culturing and investigating a single cell during its growth is impossible in traditional bulk medium. Droplet microfluidics offers the possibility to compartmentalize single cells and investigate them while they are growing. Water-in-oil droplets can carry out

a large number of experiments in a controlled environment. Researchers are attempting to automate the whole droplet system, including the generation, mixing, sorting, and means of readout. These developments could lead to more possibilities and greater reliability in applying droplet microfluidics in cell biology. Researchers have been able to demonstrate applications of droplets as miniaturized laboratories for biological measurements. It has been reported that a single *Escherichia coli* (*E. coli*) cell was encapsulated in a droplet that contained all the nutrients needed for a cell to grow [12–14]. Mammalian cells also have been encapsulated and grown in droplets [15, 16].

Cell culturing and cellular investigation using droplets requires the on-chip storage of droplets, but most of the methods mentioned above describe the storage of droplets off-chip. In the off-chip storage methods, after generating cells encapsulated in droplets, they are taken out of the chip for storage and incubation and then brought back to the chip for further investigation. The continuous investigation of cells is not possible in this process. Furthermore, there is the possibility of liquid displacement during the droplet transfers. One of the research topics of this work is to develop on-chip storage of droplets, where droplets can be generated and stored on the same chip.

1.4 Possibilities offered by droplets

Owing to the high-throughput analytical performance, droplet microfluidics has been employed in conducting chemical reaction, sorting particles, cell culturing, cell investigation, drug delivery, and drug discovery. For instance, they can be applied to PCR based analysis, where a single droplet serves as a PCR reactor for single copy DNA molecule amplification [17, 18]. Because of the low sample volume and large number of experiments to be carried out at the same time, droplet microfluidics is being used for protein crystallization and drug screenings [19, 20]. Key features of droplet microfluidics can be summarized as follows,

1. The sample volume is reduced down to 10^{-12} liter, which is 10^2 - 10^6 less than the conventional assays.

2. Ultrahigh throughput analysis, droplets generation frequency is up to 10 kHz.

3. Compartmentalization of individual reactions makes the analysis process less or footprint free.

4. Higher surface-to-volume ratios of droplets increases effective thermal dissipation.

5. Thousands of experiments can be conducted at the same time.

6. Precise control of the sample volume. Reliable manipulation of individual droplets such as coalescence, mixing of their contents, and sorting.

1.5 Objectives of this work

Applicability of droplet microfluidics for the diagnostic and synthesis of the biological and chemical sample is yet to be explored. The goal of this Ph.D project is to develop a droplet platform where droplets can be stored and manipulated on-chip to be used in medical and biological studies. The main research objectives are:

- Droplet microfluidics chip design for the manipulation and on-chip storage of droplets.
- Finding suitable materials and fabrication techniques for the fabrication of the devices.
- Characterization of the fabricated device.
- Verifying the fabricated prototype for real biological samples.

1.6 Organization of the text

This thesis consists of six technical chapters and a chapter for conclusions and outlook.

In chapter 2, entitled 'Fundamentals', consequences of the miniaturization of the fluidic system are described from a physical point of view. The physics of the micro scale differs from the macroscale in many aspects. For instance, the gravitational force is a dominating force in macroscale, whereas the microfluidic world tends to be dominated by surface forces like capillarity. The Reynold number at this scale is very low, which leads to the laminar flow regime of the liquid and diffusion becomes the main way of mixing of two liquids in a microchannel. Droplets generation methods and the physics behind the droplets generation will be discussed in this chapter.

Microfabrication methods are introduced in chapter 3. Nowadays, microchip production methods include a diversity of fabrication approaches. The fabrication technology depends on the material that is being selected for a specific device. The selection of he material depends on the application of the device, which is addressed in this chapter. This chapter is particularly dedicated to the soft technology based elastomer. A substantial portion of this chapter is also dedicated to Parylene deposition technology. Parylene has been used to overcome some drawbacks of PDMS, which is the base material for droplet chip fabrication.

Chapter 4 is devoted to the on-chip storage of droplets. Cell culturing, chemical synthesis, and drug screening are the major applications of droplet microfluidic among many other applications in the field of biology and chemistry. PDMS, the base substrate for droplet-microfluidic devices, is a porous material that causes water molecules to diffuse into the bulk and consequently causes fast aqueous droplet shrinkage. The proposed method, in this study, prevents droplet shrinkage by coating the PDMS channels with Parylene AF4. The obtained results are discussed at the end of this chapter.

Chapter 5, entitled 'Agarose droplets', generation of agarose droplets in a microchannel and their applications are presented. The biocompatibility and easy processing steps make agarose attractive to the *in vitro* cell culture. Agarose has been used to culture cells in a petri dish for many decades. Generation of agarose droplets in a microchip requires very a specific temperature during the pumping of the agarose solution, the droplet generation setup especially for agarose droplets is presented in this chapter. The size and shape of the agarose droplets, and the yeast encapsulation procedure are discussed.

Chapter 6 is dedicated to the principle of droplet merging and sorting, and their necessity. Many chemical and biological reactions, and cell analysis require the addition of reagents to the empirical droplets as well as sorting of droplets which are of interest. A chip has been designed and fabricated for the on-chip manipulation of droplets. The functionality of the chip is demonstrated by merging nutrient droplets to the cell containing droplets.

In chapter 7, a method to supply oxygen to the on-chip stored aqueous droplets is presented. By generating air-droplets (air-bubbles) in between the aqueous droplets in a microchannel, oxygen is supplied to those aqueous droplets. The proposed method and device are a step towards long-term on-chip cultivation of mammalian cells and aerobic grown bacteria in droplets.

The result of MDCK cells survival in the on-chip stored droplets for 12 hours will be presented.

In chapter 8, some conclusions are presented and some further perspectives are sketched.

Chapter 2

Fundamentals

2.1 Introduction

The importance of droplets in the field of biology and chemistry has been discussed in the preceding chapter. This chapter focuses on the principles of droplet generation and their behavior in microchannels.

The basic physics of fluid dynamics at the microscale, where shear forces dominate the gravitational force, is investigated in the first section. The flow profile and mixing of liquids at a low Reynolds number are also presented.

The second section focuses on droplet microfluidics, where basic terms of fluid dynamics, such as surface tension, capillary force, and contact angle, are introduced and discussed. These terms are essential to understand the principle of droplet generation, and their subsequent flow through a microchannel. In the latter part of the second section, droplet-generation techniques are discussed, such as those utilizing a T-junction and a flow-focusing junction. At the T-junction, droplet breakup is triggered by the pressure drop across the droplet. In contrast, the viscous stress and squeezing pressure cause droplet breakup in a continuous phase at the flow-focusing junction. In both cases, the capillary number is less than unity. The variation in droplet size in each case is also be described in this section.

Finally, droplet flow through a microchannel is described. The material properties of the channel, such as its hydrophobicity, hydrophilicity, and surface smoothness, are important factors affecting the shape and flow of droplets in a microchannel, which are described in the last section of this chapter.

2.2 Microfluidics

Microfluidics involves the study of very small volumes of fluids, usually in the range of microliters (10^{-6}) to picoliters (10^{-12}). At the microscale, very different forces from those experienced in everyday life become dominant, such as the viscous force, which overwhelms the force of gravity [21]. Therefore, in microfluidics experimentation, channel sizes are in the range of micrometers, with the fluid flow on the order of microliters per second (μl/s). The flow of a fluid through a microfluidic channel can be characterized by its Reynolds number. The dimensionless Reynolds number (Re) states the ratio between the magnitude of the inertial and viscous forces:

$$Re = \frac{\rho \upsilon D_h}{\mu}, \tag{2.1}$$

where ρ is the fluid density, υ is the characteristic velocity of the fluid, μ is the fluid dynamic viscosity, and D_h is the hydraulic diameter [22]. The hydraulic diameter (D_h) depends on the channel's cross-sectional geometry, and the following equation can compute the value,

$$D_h = \frac{4A}{P_{wet}}, \tag{2.2}$$

where A is the cross-sectional area and P_{wet} is the wetted perimeter of the cross-section. Rectangular microchannels are commonly used in microfluidic applications because of the well established and convenient fabrication techniques. D_h of a rectangular microfluidic channel of width w and height h can be calculated as follows

$$D_h = \frac{2wh}{(w+h)}. \tag{2.3}$$

An example with the dimension of one of the microfluidic chips presented in this work elaborates the flow behavior. When introducing water (ρ=1.0 g/cm^3 and μ= 0.001 Pa s) to a microfluidic channel of cross-sectional area 100×100 μm^2 at an average velocity (υ) of 0.01 m/s, the calculated Reynolds number is 1, which is clearly in the laminar regime, since the empirical observations defined $Re \approx 2300$ as the transition between laminar and turbulent flow behavior [23]. At a low Reynolds number, with the laminar flow, surface tension becomes a powerful force, diffusion becomes the basic method for mixing, and evaporation acts quickly on exposed liquid surfaces.

When a Newtonian liquid, where viscosity is independent of the applied shear stress, flows through two parallel plates, the forces acting on the fluid particles are (i) pressure force, (ii) gravity force, and (ii) shear stress force.

According to Newton's law ($F = ma$), the addition of all these forces is equal to the mass of the fluid times the acceleration. This law has been extended to fluid mechanics by Navier-Stokes equation, which is

$$\rho\frac{\partial\vec{v}}{\partial t} = -\nabla P + \mu\nabla^2\vec{v} + \rho\vec{g}, \tag{2.4}$$

The right-hand side of the equation (2.4) contains pressure gradient ($-\nabla P$), viscosity($\mu\nabla^2\upsilon$), and gravity ($\rho\vec{g}$) for per unit volume. The left hand gives the mass per unit volume(ρ) times the acceleration of the fluid. In the microfluidic system, the channel for fluid transport is in the range of micrometers. Hence the viscous force dominates over the inertial force and almost no effect of the gravitational force. Therefore, the Navier-Stokes equation for incompressible fluid dynamic becomes simple [24],

$$\mu\nabla^2\upsilon = \nabla P. \tag{2.5}$$

2.2.1 Flow profile

Fluid actuation through a microchannel can be achieved through both pressure-driven flows and electroosmotic pumping. In pressure-driven flows, a fluid is pumped through a device via a positive-displacement pump—such as a syringe pump—which is often used in microfluidic experimentation. One of the basic laws of fluid mechanics for pressure-driven laminar flow is the no-slip boundary condition at a channel wall [24]. The no-slip boundary condition assumes that a viscous fluid has zero velocity at any fluid–solid interface. The physical explanation for this is that, at the fluid–solid interface, the force between the fluid and solid particles is greater than the force between the fluid particles. In this work, the channel width used is in the micrometer range, and the fluid is viscous. Therefore, the no-slip boundary condition is applicable. Figure 2.1a shows that the flow velocity of zero at the walls produces a parabolic flow profile within the channel.

Electroosmotic pumping is also capable of providing a constant flow profile in a channel [24]. In this type of pumping system, an electric field is applied across the channel, which creates a uniform flow profile across its entire width (2.1b).

In this study, a pressure-driven flow system has been used to pump the fluid into the microchannel.

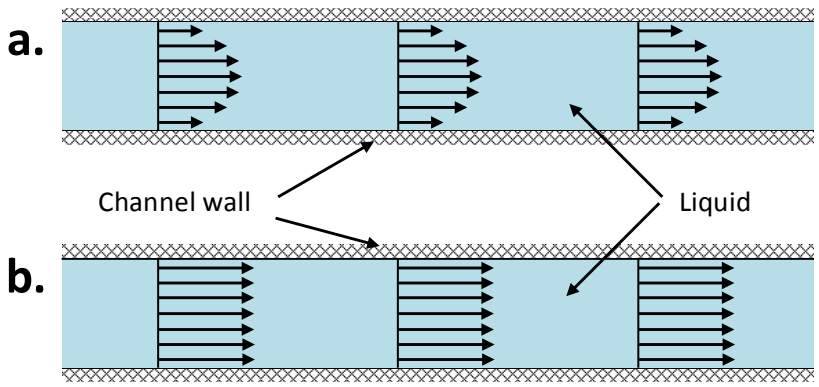

Figure 2.1: Flow profile in a microchannel. (a) Cross sectional flow profile under pressure driven flow. The flow velocity at the channel wall is zero. (b) Cross sectional flow profile under electro-osmosis flow.

2.2.2 Mixing of fluids in microscale

In a microchannel of width and height in the order of micrometers and with a low Reynolds number, fluids flow parallel to each other. If the flow velocity is constant with time, the mass transfer occurs between two liquids only in the direction of of their flow. Therefore, the mixing of liquids in a microchannel is only occurred by passive molecular diffusion. Diffusion is the process of the movement of molecules or atoms from a higher concentration region to a lower concentration region by Brownian motion, resulting in the mixing of materials. According to Fick's law, the amount of substance that will flow through a unit area in one second can be calculated as follows,

$$J = -D\frac{\partial \varphi}{\partial x}, \tag{2.6}$$

where φ is the species concentration, x is the position of the species, and D is the diffusion coefficient. Diffusion coefficient of large molecules in a viscous fluid can be calculated according to Stokes-Einstein equation,

$$D = \frac{kT}{6\pi\mu r}, \tag{2.7}$$

where k is Boltzmann's constant, T is the absolute temperature, r is the radius of the particles (or molecules) and μ is the viscosity of the medium

[25]. In a simple microfluidic channel, the average diffusion time (t) of a molecule over distance x can be calculated as follows,

$$t = \frac{x^2}{2D}. \tag{2.8}$$

As x represents the stream width of a fluid to be mixed in a microfluidic channel, the diffusion time drastically increases with the increase of x. Therefore, the mixing will be fast in a narrow capillary [26]. For instance, sucrose of typical diffusivity $D \sim 4.4 \times 10^3$ in water flowing through a channel of width 100 μm at velocity $v = 100\mu/s$ takes 2.3 seconds to be mixed. The mixing of fluids in a microchannel, particularly the mixing of droplets, will be discussed in chapter 6.

2.3 Droplet microfluidics

Droplet microfluidics is a branch of microfluidics that studies a sample liquid that takes the form of a drop in another immiscible, continuous liquid. The volume of each drop is in the range of nanoliters; however, fluid dynamics at the microscale is still valid in droplet microfluidics. Since two immiscible liquid phases are involved in droplet microfluidics, the surface tension, capillary number, and contact angle play a vital role in the droplet-breakup mechanism and their flow through the channel. This concept is also applicable to bubble generation in different liquids and their subsequent flow through microchannels. Before providing a detailed description of the droplet-generation mechanism, a brief discussion on the concepts of surface tension, capillary number, and contact angle is necessary.

2.3.1 Surface tension

Surface tension occurs at the interface between two immiscible fluids. To understand the underlying mechanism of surface tension, molecular interactions must be investigated. Inter-molecular attraction (cohesive and adhesive forces) in a liquid cause surface tension. As an example, it can be assumed that a water molecule in the bulk of the liquid is in contact with four other water molecules at any given time. However, at the interface between water and a gas, such as air, one molecule of water is in contact with two molecules of air and two molecules of water. Owing to the lower density of gases, the adhesive force between air and water is lower than the cohesive force in the bulk of the liquid. This causes a force imbalance in the water molecules at the interface, as they experience more force toward the inner water molecules.

This effect is called surface tension, which is a direct measure of surface energy. A simplified view of the water–air interface at the molecular level is shown in Fig.2.2.

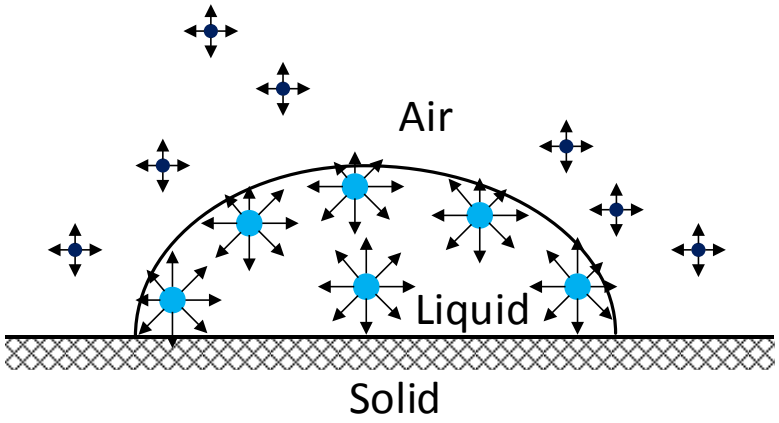

Figure 2.2: Schematic view of an interface of water/air at molecular level.

Surface tension can be defined as follows

$$\gamma = \frac{U}{2\delta^2}, \tag{2.9}$$

where, U is the total cohesive energy per molecule and δ is a characteristic molecular dimension [27]. The unit of surface tension is N/m. This relation shows that liquids with smaller molecules and higher cohesive energy creates higher surface tension.

The same principle applies to the interface between two immiscible liquids, such as water and oil, which is called interfacial tension. At the two liquids interface, surface molecules experience less imbalance force because, in liquids, molecules are closer compared to the molecules in air/gas. The surface tension between water/oil is 50 mN/m [28]. Figure 2.3 illustrated a schematic diagram at the interface of water/oil in a microchannel.

Surface tension also arises at the interface of liquid and solid. Molecules in the water usually attracted to a solid surface by the van der Walls forces, but they do not stick to the wall surface because of the Brownian motion [27].

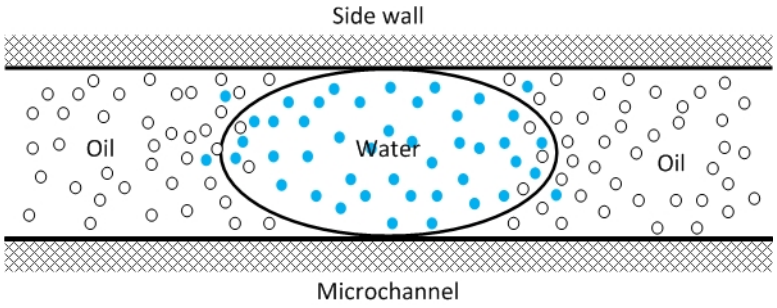

Figure 2.3: Schematic view of an interface of water/oil at the molecular level in a microfluidic channel.

2.3.2 Contact angle

The contact angle is another fundamental concept in droplet microfluidics. When a liquid drop sits on a solid surface, an angle forms at the interface of the liquid drop,-solid surface, and -air, which is called contact angle (Fig.2.4). In droplet microfluidics, the contact angle forms at the interface of a solid wall of a microchannel and the two immiscible fluids (Fig.2.5). The contact angle is divided into static (θ_s) and dynamic (θ_d) angles, considering the motion of a liquid. The Young's equation defines the static contact angle at the interface of solid/liquid/gas in terms of the three surface tension: solid/liquid (γ_{sl}), liquid/gas(γ_{lg}), and solid/gas(γ_{sg}),

$$cos\theta = \frac{\gamma_{sg} - \gamma_{sl}}{\gamma_{lg}}. \tag{2.10}$$

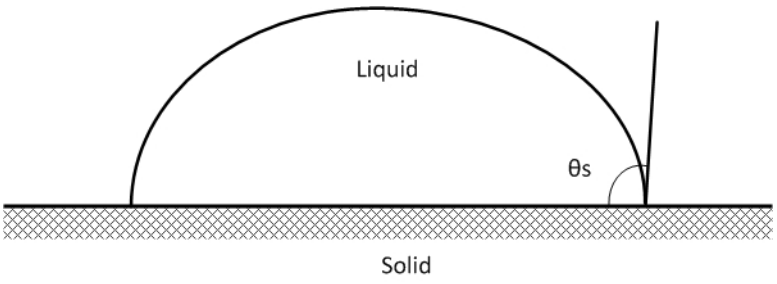

Figure 2.4: Schematic view of a liquid drop on a solid surface.

Materials with a contact angle (<90°) are called hydrophilic, while materials with a contact angle (>90°) are called hydrophobic. The details of hydrophilic and hydrophilic materials and their importance in droplet microfluidics will be discussed in chapter 4.

The contact angle at the resting position (static contact angle) of a liquid drop is well defined, whereas it appears to be complicated when liquid flows in a microchannel. The dynamic contact angle of a flowing liquid is a balance between capillary force and viscous force, which can be described by the capillary number (C_a). The relation between dynamic and static contact angle is

$$\theta_d{}^3 - \theta_s{}^3 = ACa, \tag{2.11}$$

where A is a coefficient, the value of A is approximately 94 when θ is expressed in radians [29]. Linearization of equation (2.11) has been done by [30, 31], which yields,

$$\theta_d - \theta_s \approx \frac{1}{3}\frac{ACa}{\theta_s{}^2} \tag{2.12}$$

When a droplet moves through a microchannel, it forms two contact angles with the solid surface (i) advancing contact angle and (ii) receding contact angle. A schematic view of a droplet in a microchannel is shown in Fig.2.5.

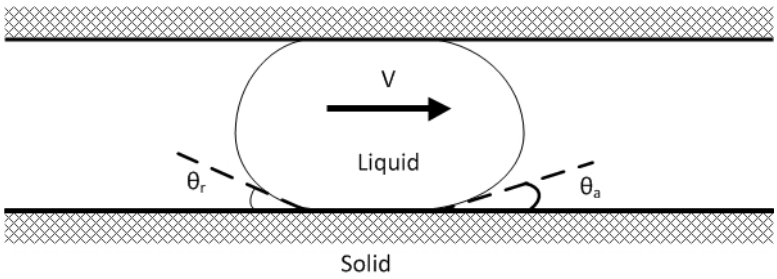

Figure 2.5: Schematic view of a liquid droplet in a microchannel with the advancing and receding contact angle.

According to the experimental observation, an advancing contact angle is larger than a static contact angle, and a receding contact angle is smaller than a static contact angle. The advancing (θ_a) and receding (θ_r) contact angle can be calculated based on the following equations,

$$\theta_a \approx \theta_s + \frac{1}{3}\frac{A|Ca|}{\theta_s{}^2}, \tag{2.13}$$

$$\theta_r \approx \theta_s - \frac{1}{3}\frac{A|Ca|}{\theta_s{}^2}. \tag{2.14}$$

The static and dynamic contact angles for the microfluidic systems that have been used in this study will be discussed in chapters 4 and 5 in detail.

2.3.3 Capillary force

The capillary action occurs in a microscale, where the surface tension dominates the gravitational force. Because of the capillary force, a liquid can flow through a narrow tube without any external force. If a liquid flows between two parallel plates, where the distance between two plates is h and the liquid flow profile is parabolic, then the capillary force between them can be calculated by Laplace's law [27],

$$F \approx \frac{2\gamma cos\theta}{h}\pi R^2, \tag{2.15}$$

where the radius of the curvature is R and the angle between the liquid and solid surface is θ (Fig.2.6).

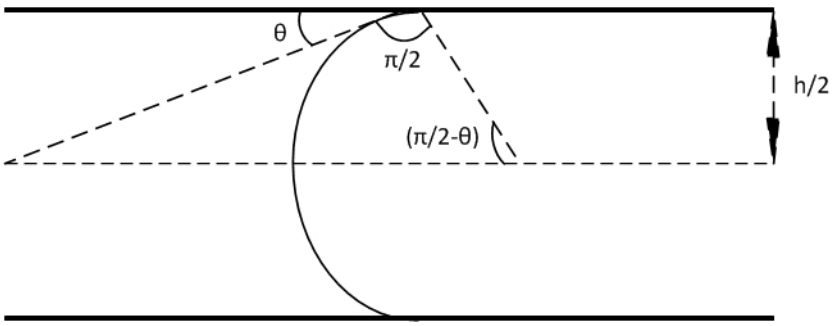

Figure 2.6: Schematic view of a liquid between two parallel plates.

2.3.4 Droplets generation

The generation of uniform droplets of a sample liquid in a continuous flow of an immiscible is a challenge in microfluidics. Droplets can be produced either in a T-junction or in a flow focusing device. Two different types of instabilities lead to droplets breakup in a microchannel. In a T-junction, the creation of droplets is governed by the pressure drop created by the merging droplets. In a flow focusing device, the capillary instability causes the generation of droplets. In this section, the mechanism of droplet generation is discussed.

Droplets generation in a T-junction

A T-junction (Fig.2.7) is formed by two rectangular channels of the same depth and usually merged at an angle of 90°. The droplets formation in a T-junction proceeds in several steps: the liquid enters the main channel, forms a blob and develops a neck. As the blob advances downstream, the neck elongates and becomes thinner. Eventually, it breaks up and the droplets are generated in a continuous flow. Figure 2.8 depicts a water droplet generation in oil.

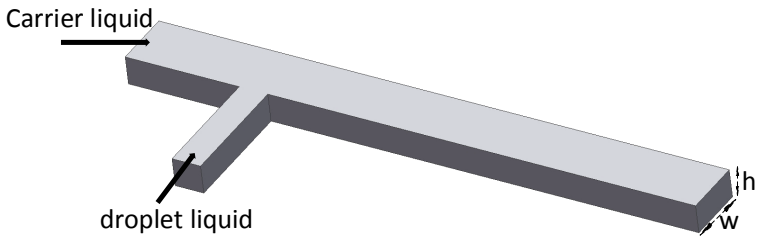

Figure 2.7: Sketch of a T-junction comprised of a rectangular channel.

The droplets generation in a T-junction depends on the capillary number (Ca). The capillary number is defined as the ratio of the viscous force to the capillary force,

$$Ca = \frac{\mu v}{\gamma}. \tag{2.16}$$

where μ is the dynamic viscosity, v is a characteristic velocity, and γ is the surface tension [32].

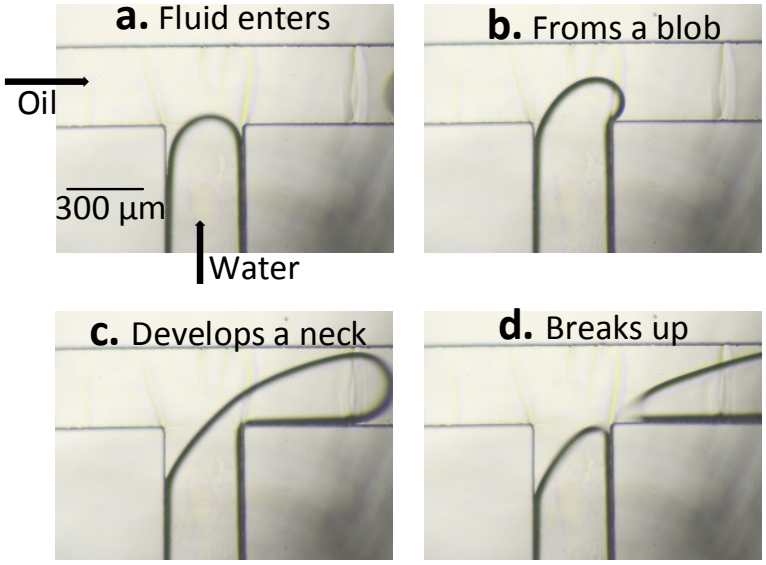

Figure 2.8: Water enters the channel (a); the water phase forms a blob in oil (b); droplet elongates downstream and develops a neck (c); the water phase breaks up and a droplet generates (d).

Droplet microfluidics usually functions with a low flow rate. Therefore, the capillary number is less than 10^{-2}, where the interfacial force dominates the shear stresses. In a T-junction, the size of the droplets determined by the ratio of the volumetric rates of flow of the two immiscible liquids. For a rectangular microchannel, the length of the droplet can be determined as follows

$$\frac{L}{w} = 1 + \alpha \frac{Q_{drop}}{Q_{cont}}, \tag{2.17}$$

where L is the length of a droplet, w is the width of a channel, Q_{drop} and Q_{cont} are the flow rates of the droplet and continuous phase, respectively. In equation (2.17), α is a positive constant and of the order of one, whose particular value depends on the geometry of the T-junction [33]. Therefore, the length of the droplet L is always larger than the width of the channel w. The relation (2.17) is not valid for the entire domain of variation of the ratio Q_{drop}/Q_{cont}. For small values of this ratio, L is constant. In practical, this equation is not valid anymore. Hence, correction is required. According to [27], the proposed solution is

$$\frac{L}{w} = 1 + \alpha \frac{Q_{drop}}{Q_{cont}} H(Q_{drop} - Q_{cont}) \tag{2.18}$$

where H is the Heaviside function: $H(x) = 1$ if $x > 0$, else $H(x) = 0$ [34].

Droplets generation in a flow focusing device

In a flow focusing device, the continuous phase flow rate has the most significant impact on the mechanism of the droplets formation and the size of the droplets. At the interface of two liquids, the viscous stress and the squeezing pressure from the continuous phase liquid force the droplet phase liquid to break into droplets. The flow focusing microfluidic devices are categorized into three types depending on the channel geometry, which are presented in Fig.2.9.

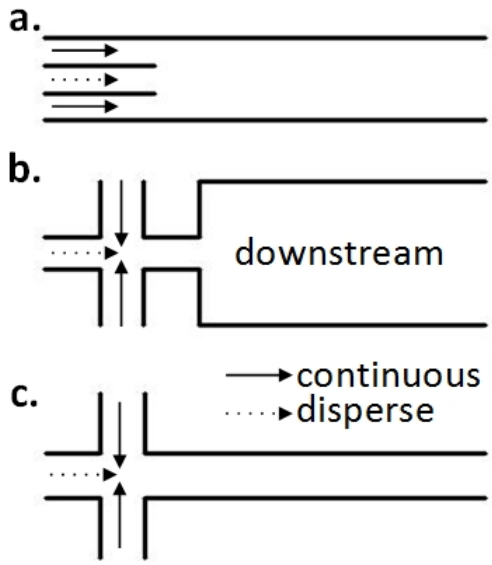

Figure 2.9: Different types of microfluidic flow focusing devices for droplets generation.

(a) Figure 2.9a presents a co-flowing device, in which the dispersed phase flow channel is sandwiched between two continuous phase flow channels [35, 36]; (b) the dispersed phase channel positioned with both the continuous phase channels at 90° angle (Fig.2.9b), which is aligned to a short-narrow channel and then to a wide downstream [10, 37]; (c) in this cross junction geometry (Fig.2.9c), all the channels dimensions are the same. The disperse phase channel is also positioned at the right angle with both the continuous phase channels [38, 39]. To date, little is known about the role of all relevant dimensionless parameters of droplet formation in a flow focusing

device. So far, the functioning of such devices has been mostly approached experimentally [36, 40, 41].

The droplet formation regimes in the flow focusing device are squeezing, dripping, and thread formation. The squeezing regime occurs at a low flow rate and the droplet size is larger than the channel through which it is injected. In this regime, the droplet phase coming from the channel blocks the flow of continuous phase liquid. Therefore, high upstream pressure of the continuous phase arises that squeezes the neck of this blockage and pinch off a droplet [33, 42]. As the flow rate increases, viscous stress increasingly deforms the droplet phase liquid, which forms an elongated cylindrical neck that is narrower than the channel width. Droplets pinch-off from the end of the neck due to a combination of end-pinching and capillary instabilities [43]. At still high flow rates, the continues phase flow stabilizes the neck of the droplet phase flow, elongated it further downstream. At the end of the thread, the droplet pinch off. In the thread formation regime, non uniform droplets are formed.

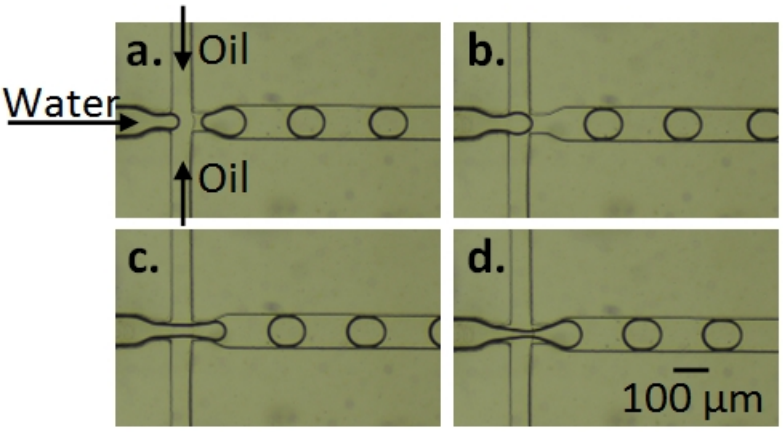

Figure 2.10: Droplets break up at flow focusing device. Water enters the disperse phase channel (a); the water phase blocks the flow of continuous phase (oil) liquid (b); droplet elongates down stream and develops a cylindrical neck (c); water phase breaks up and a droplet generates (d).

Considering the width of the channels, the viscosity of the two liquids, and the flow velocity of both continuous and droplet phase, the capillary number is redefined for the flow focusing device as follows [37].

$$Ca \equiv \frac{\mu_c w \Delta U}{\sigma \Delta z} \tag{2.19}$$

where Δz is the distance between the end of the droplet phase inlet and

the contraction, and ΔU is the difference between the average velocity of the continuous phase and the droplet phase.

$$\Delta U = \frac{Q_{cont}}{w_{or}h} - \frac{Q_{cont}}{2w_c h} \tag{2.20}$$

The above defined capillary number of equation (2.19) for a flow focusing device encompasses all the upstream dimensions along with the continuous phase flow rate, viscosity, and interfacial tension. The size of the droplets generated in a flow focusing device depends on the ratio of volumetric flow rates, viscosity, and expansion ratio. These three variables are defined as follows, the ratio of volumetric flow rate,

$$\phi \equiv \frac{Q_{drop}}{Q_{cont}} \tag{2.21}$$

the ratio of viscosity,

$$\lambda \equiv \frac{\mu_{drop}}{\mu_{cont}} \tag{2.22}$$

and the ratio of expansion,

$$\Lambda \equiv \frac{w_{main}}{w_{break}}. \tag{2.23}$$

Several studies have examined the dependence of droplet size, formation time, transitions between regimes, and thread length on the volumetric flow rate ratio [11, 44, 45]. These studies suggested that the droplet's diameter and the time of formation both increase with the increase of ϕ. The thread formation regime occurs at a very small flow rate ratio ($\phi \ll 1$) and the thread length decreases with increasing of the flow rate ratio. In the squeezing and thread formation regime, studies show that the droplet diameter is unaffected by the viscosity ratio [46, 47]. In contrast to this, viscous stresses become increasingly important in the dripping regime. In the dripping regime, the droplet size decreases as the viscosity ratio increases above $\lambda > 0.01$ [37].

2.4 Transportation of droplets through a microchannel

Droplets flow in a microchannel depends on the density of the fluids, the flow rate of both fluids, and the interfacial tension between them. It can be explained by the Weber number,

$$We = \frac{\rho v^2 l}{\gamma}, \tag{2.24}$$

where ρ density of a fluid, v velocity of the fluid, l characteristic length (typically droplet diameter), and γ surface tension. Additionally, the mobility of the droplets depends on the surface properties of the channel wall, such as surface smoothness and hydrophobicity/hydrophilicity of the microchannel surface. Water affinity of material defines its hydrophobicity or hydrophilicity, and this is measured by the contact angle, which has been explained in section 2.3.2. The contact angle of a water droplet in oil in a microchannel depends on the composition of the oil phase as well as the water phase.

The flow of water droplets in oil will be described in detail in chapter 4 and air/oil/water flows in microchannel will be described in chapter 5.

2.5 Summary

This chapter focused on discussing the basic terminology and principles of fluid dynamics in the context of microfluidics, the different droplet-generation methods, and the flow of droplets through a microchannel. Fluids at the microscale have very different features than those at the macroscale. At the microscale, the gravitational force has almost no effect, whereas the viscous force, capillary force, and surface tension dictate fluid behavior in a microchannel. The behavior of droplets in a microchannel also differs from that in conventional fluid mechanics. In droplet microfluidics, interfacial forces are more dominant than other forces.

The following chapter focuses on the selection of materials in droplet microfluidics, chip designs, and fabrication technologies. These factors are highly dependent on the fluid behavior in a microchannel. All of the fluid parameters discussed in this chapter have been investigated thoroughly and considered in chip design and material selection.

Chapter 3

Fabrication

3.1 Introduction

An principles of fluid dynamics at the microscale were discussed in the previous chapter. The effects of channel material and dimensions on the behavior of a fluid in a microchannel were also presented. This chapter outlines the materials conventionally used in fabricating microfluidic devices and the techniques developed for their fabrication. In the latter part, the materials and fabrication methods used to develop the microfluidic chip in this study will be discussed.

To date, the techniques used for fabricating microfluidic devices include micromachining, soft lithography, injection molding, laser ablation, and embossing [48–53]. Each of these techniques has its own advantages and disadvantages. Therefore, the selection of a material and fabrication method often depends on the application of the device. The first part of this chapter focuses on the materials used to fabricate microfluidic chips and the parameters to be investigated before selecting a material.

The soft lithography technique will be discussed in the second section of this chapter, with particular focus on the replica molding process of Polydimethylsiloxane (PDMS), which includes the preparation of an SU-8 mold on a silicon wafer and the casting of PDMS.

Microchannels were fabricated on silicon to measure the penetration depth of Parylene C and Parylene AF4. The third section of this chapter presents the fabrication method of a silicon channel using reactive-ion etching techniques. A PDMS channel surface was coated with Parylene AF4, which prevents the evaporation of droplets in microchannels. As a result, the droplets can be stored in a microchannel for an extended period of time. The deposition process for Parylene is discussed in section four.

3.2 Materials used to fabricate microfluidic devices

A wide range of materials is used to fabricate microfluidic devices, such as conventional silicon or glass and, more recently, polymers or paper [54–57]. The first generation of microfluidic devices was fabricated using standard photolithography with silicon or glass [54, 58]. These two materials are preferable for use in capillary electrophoresis and applications involving solvents. Both silicon and glass are biocompatible, resistant to organic solvents, and adhere sufficiently to metals [59]. However, the high-cost fabrication technology, complex bonding process, and use of dangerous chemicals (such as hydrofluoric acid) in the fabrication process limit their applicability in microfluidics [60].

Polymers gained widespread usage in the fabrication of microfluidic devices several years after the use of silicon and glass. They have garnered attention in the field of microfluidics because of their accessibility, inexpensiveness, and simple fabrication process. Various polymer materials are available in the market, such as PDMS, Parylene, poly(methylmethacrylate) (PMMA), polycarbonate (PC), SU-8 photoresist, and polyimides, providing great flexibility in choosing the appropriate material. Based on their physical properties, polymer materials are classified into three groups: thermosets, thermoplastics, and elastomers. SU-8 photoresist and polyimides belong to the thermoset group. Typically, thermosets are optically transparent, resistant to most solvents, and stable at high temperatures [61, 62]. However, their stiffness and high cost limit their usage in some microfluidic applications.

Polymethylmethacrylate (PMMA), Teflon, and polycarbonate (PC) belong to the thermoplastics group. Some thermoplastics, such as Teflon, are optically transparent and shows excellent resistance to organic solvents. Unlike thermosets, thermoplastics can be reshaped multiple times by reheating, and can therefore be used in thermomolding fabrication processes. The thermomolding process can produce thousands of replicas at a high rate and low cost. However, it requires metal or silicon templates. Therefore, it is excellent for commercial production but is not economical for producing small batches.

Polydimethylsiloxane (PDMS) is the most commonly used elastomer in microfluidic applications [63, 64]. Unlike thermosets and thermoplastics, PDMS is flexible. Further, it is biocompatible, relatively inexpensive, and has a simple fabrication process, making it preferable for the production of prototypes.

Recently, hydrogels have been garnering increased attention, particularly in the culturing of 3D cells, owing to their biocompatibility and high porosity with controllable pore size [65, 66]. However, hydrogels support a lower resolution than polymers in microfabrication.

Further, paper-based devices have recently been introduced for microfluidic applications. The preparation of these devices is very cost-effective and simple, as most processes do not require specific laboratory conditions. Therefore, such devices are promising for use as commercial point-of-care devices.

All the materials mentioned above have been used to fabricate droplet-generation chips, with the exception of hydrogels and paper. This thesis focuses on droplet microfluidics and its applications, particularly cell culturing in droplets. The material suitable for the purpose of this study must be biocompatible, transparent, and inexpensive for rapid prototyping. Biocompatibility is necessary as it is a critical requirement for cell culturing. Droplet investigation and analysis methods are primarily based on image processing, which necessitates optical transparency of the chip. In research, designed devices are often fabricated in small batches and need their designs altered frequently, which requires a low-cost and simple fabrication technique. Among the materials discussed earlier in this chapter, PDMS fulfills these requirements. However, like any other material, PDMS has certain advantages and disadvantages, which will be discussed in chapter 4. It is often necessary to use a hybrid material to overcome these disadvantages. A hybrid microfluidic chip fabricated using both PDMS and Parylene is used in this study. The fabrication process of the microfluidic chip using these two materials is discussed in this chapter.

3.3 Fabrication of a PDMS chip

PDMS is suitable for laboratory uses and the rapid prototyping of microfluidic devices. It is nontoxic to proteins and cells as well as permeable to oxygen and carbon dioxide. This permeability also has drawbacks, which will be discussed in the following chapter. Another significant advantage of PDMS is its optical transparency. It is optically transparent from 240 nm to 1100 nm [63].

The PDMS devices are fabricated using soft lithography techniques [67–70]. It is an alternative microfabrication approach to conventional photolithography. The development and expansion of soft lithography techniques took place in the last two decades. These techniques include cast molding [71], embossing [72], injection molding [73], and replica molding [68]. The

replica molding technique is typically used for PDMS device fabrication and also used for the development of chips that are used in this study. It consists of two processes: a master mold preparation and a stamp preparation. The master mold is a template that carries an inverse replica of the desired structure. Conventional lithography is the most general way to prepare mold on a silicon substrate. The stamp is an elastomer, such as PDMS. Several materials can be used as a mold such as SU-8, PMMA, polystyrene (PS), and Ordyl- dry film photoresist. SU-8 on silicon is used as a master mold in this study. Therefore, further discussion will be focused on the preparation of the SU-8 mold.

3.3.1 SU-8 master mold preparation

After introducing the SU-8 product in 1996 by MicroChem, it is gaining interest in photolithography. It is a negative photoresist designed for micromachining. Its high viscosity allows for film thicknesses of 4 to 120 μm in a single coat. Moreover, it is capable of producing very high aspect ratio structures (over 5:1) [74]. It is also possible to get a SU-8 film thickness of below 2 μm and above 3 mm. The resist solution needs to be diluted with the solvent to obtain a film thickness of fewer than 2 μm. Multicoating is necessary to achieve film thickness above 120 μm. Fabricated SU-8 structures are chemically inert and provide a high degree of biocompatibility [75].

In this study, 100 μm depth SU-8 channel structures of different width (25 μm, 50 μm, 100 μm, 200 μm, 300 μm) were prepared on a silicon wafer (4$''$ diameter, 525 μm thickness). Surface adhesion between a substrate and a photoresist is crucial for uniform and stable coatings. SU-8 is an organic material, and the contact angle of cured SU-8 is 73°, which is hydrophobic [74]. Therefore, the adhesion between SU-8 and hydrophilic inorganic substances (oxidized silicon wafer) is not good enough. Studies suggest that SU-8 shows the most robust adherence with titanium (Ti) and titanium dioxide (TiO_2) [76]. Therefore, before the deposition of SU-8 on the silicon substrate, Ti-prime (adhesion promoter) was spin-coated and cured at 120°C for 2 mins on a hot plate. Ti-prime adsorbed by the inorganic silicon substrate and formed a thin organic layer, which can be wetted by SU-8. Afterward, SU-8 film was deposited on the substrate and soft-baked to remove the solvent and to improve resist-substance adhesion. A hot plate is preferable than a conventional oven for soft baking, as a thin skin may form on the surface of the resist in the oven. This skin prevents solvent evaporation, resulting in the incomplete drying process, which can cause high film stress during post-exposure baking.

After soft baking, the resist was exposed to UV-light (350 nm wave-

lengths) through a mask using contact lithography, mask directly in contact with the substrate, to achieve optimal resolution. A post bake was done to increase the cross-link of the exposed resist and to stabilize against the solvent during the development process. Immersion development of the SU-8 was done with MicroChem′s SU-8 developer. After development, the wafer was rinsed with isopropanol and dried with compressed nitrogen. In the case, where the SU-8 is exposed to a higher temperature during regular operation, a hard bake is necessary. It improves the mechanical property of the SU-structures. The temperature of the hard bake should be 10° higher than the expected device operating temperature, and it also helps to anneal any surface crack of the SU-8 structure.

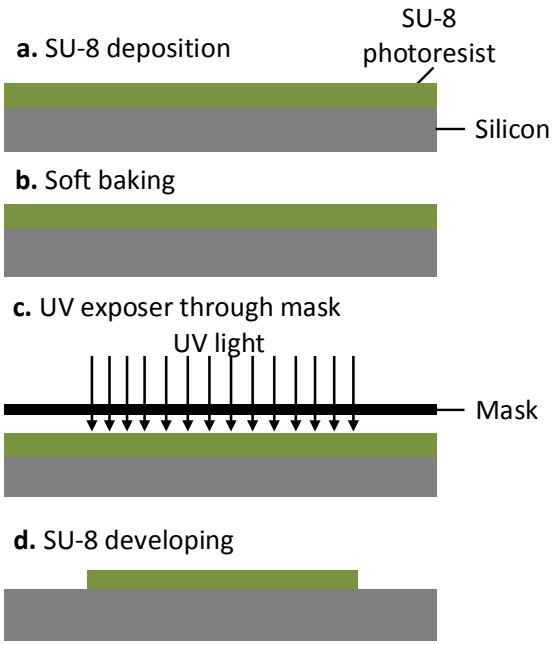

Figure 3.1: Fabrication steps of SU-8 master mold.

The main process steps for the fabrication of SU-8 layers with a thickness of 100 μm are as follows,

- Pre-bake of the silicon wafer on a hot plate at 120°C for 2 mins.
- Spin coat of an adhesion promoter (Ti-prime) and cure on a hot plate at 120°C for 2 mins.
- Spin coating of SU-8 3025 at 1500 rpm for 30 seconds.

- Soft bake on a hot plate at 65°C for 1 min and 95°C for 120 mins.
- Exposure to UV light for 130 seconds (depends on the wavelength and thickness of the SU-8 structure).
- Post exposure bake on a hot plate at 65°C for 1 min and 95°C for 10 mins.
- Developing SU-8 for approx. 15 mins.

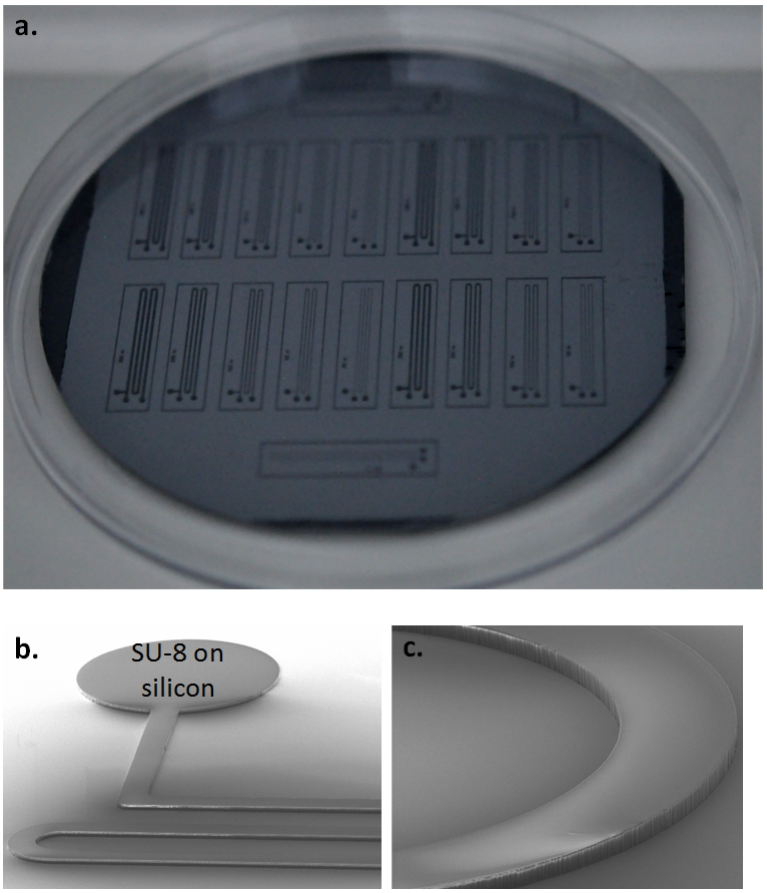

Figure 3.2: Photograph of SU-8 structure on a silicon wafer (a); Scanning electron microscopic (SEM) photograph of a meander shape channel including an inlet (b); SEM image at the corner of a channel structure (c).

Inverse SU-8 microchannels of different width (25 μm, 50 μm, 100 μm, 200 μm and 300 μm) and height of 100μm on a silicon wafer can be seen in Fig.3.2. Twenty channels, of length 85 mm each, are accumulated on a silicon

wafer of diameter 100 mm, which will be used as a master mold for PDMS casting. Scanning electron microscopic (SEM) photographs of fabricated SU-8 structure is presented in Fig.3.2(b & c). From the SEM images, it can be seen that the fabricated SU-8 structure has a smooth surface. Surface roughness hinders the droplets generation and transportation through the PDMS microchannel. The PDMS channel surface smoothness depends on the surface smoothness of the SU-8 structure. Therefore, in the following chapters for the analysis of the droplets generation and transportation in a microchannel, the surface roughness effect will be ignored.

3.3.2 PDMS-stamp preparation

After the commercialization of PDMS in the early 70s of the last century, it is gaining interest from different branches of science because of its biodegradability [77]. It is a silicon-based organic polymer. At room temperature and pressure, PDMS is a colorless, odorless, and highly viscous liquid. The chemical structure of PDMS is presented in Fig.3.3.

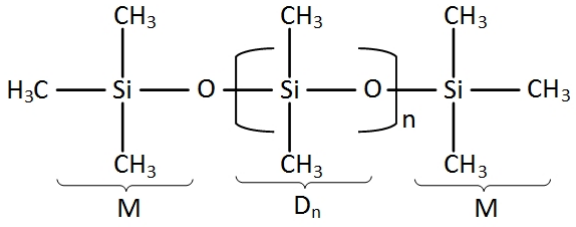

Figure 3.3: Polydimethylsiloxane (PDMS) chemical structure.

The general formula of PDMS is MD_nM, where D_n represents the number of dimethylsiloxy units and M represents trimethysiyl [78]. The viscosity of the liquid PDMS depends on the number of D-units in the molecule. D-unit also defines the molecular weight of the PDMS. The D unit is capable of expanding within the polymer. The polymerization of this material is possible by hydrolysis [78]. Nowadays, the hydrosilylation addition has been commonly used to prepare cross-linked PDMS materials [79]. PDMS contains two vinyl end groups, which can react with cross-linker leading to a three-dimensional cross-linked network [80]. The rate of the hydrosilylation reaction depends on the type and molecular structure of the catalytic complex, the vinyl groups of the PDMS, and the number of Si-H groups on the cross-linker. In this work, sylgard 184 silicone elastomer kit was purchased from Dow corning, USA, which consists of a liquid linear PDMS and a cross-linking reagent. To prepare solid PDMS, the liquid PDMS was mixed with

the cross-linker at a mass ratio of 10:1. Depending on the applications of the fabricated device, the PDMS/cross-linker mixing ratio can be varied. During the mixing, it is common that air bubbles trapped in the mixer due to the high viscosity of the PDMS, which later on causes degradation of the device performance. Therefore, it is necessary to remove the trapped air bubbles. The mixer was degassed in a vacuum desiccator until all trapped bubbles were removed. Afterward, the degassed PDMS was poured on the previously prepared SU-8 mold containing channel structures in a Petri dish. The PDMS can be cured at room temperature, which requires approximately 24 hours. To shorten the curing time, PDMS can also be cured at an elevated temperature and the curing time reduced with the applied temperature. The curing time and temperature, used to fabricate the microdroplets production and the processing chips in this work, is 4 hours and 65°C, which have been found the optimal temperature and time for further processing of the device. After curing, the PDMS structure was gently peeled off from the wafer and each PDMS channel structure was separated by a sharp scalpel. Inlet and outlet holes were made with a hollow needle of 800 μm inner diameter by punching through the PDMS.

Sealing a microfluidic channel is very crucial, as leakage of liquid from a channel can destroy the whole measurements. Like glass or silicon, sealing of channels made in PDMS does not require high temperature (600°C for glass to glass and 800°C for silicon to silicon) and pressure [81]. The typical method of sealing a PDMS channel on glass is oxygen [O_2] plasma processing of the surface of both materials. This is an irreversible sealing technique of a PDMS channel. Exposure to oxygen plasma creates silanol (Si-OH) groups on the PDMS surface, and -OH functional group on the glass surface. When the surfaces are bought into contact, the polar group form covalent -O-Si-O- bonds with oxidized PDMS. Therefore, the bonding is irreversible. It should be noted that the two surfaces must be cleaned and dried before the plasma process for better sealing. As well as the two surfaces must be brought into contact quickly after the plasma process since the oxidized PDMS surface reconstructs in contact with air. The main process steps for the PDMS casting are as follows

- Mixing PDMS with curing agent at 10:1 mass ratio.
- Degassed trapped bubble in the mixed PDMS using vacuum desiccator.
- Pouring the mixed PDMS on to the previously prepared SU-8 mold seated in a Petri dish and degassed again to remove bubbles.
- Heat the PDMS on a hot plate at 65°C for four hours.

- Peel off the PDMS from the mold and cut each individual chip.
- Make inlet and outlet holes with a hollow needle of 800μm inner diameter.
- Clean glass slides of width and length of 25×76 mm with isopropanol and dry at 100°C for 2 min.
- Bond the PDMS channel on the glass slide by plasma treatment of the both surface at 250 Watt for 10 sec.

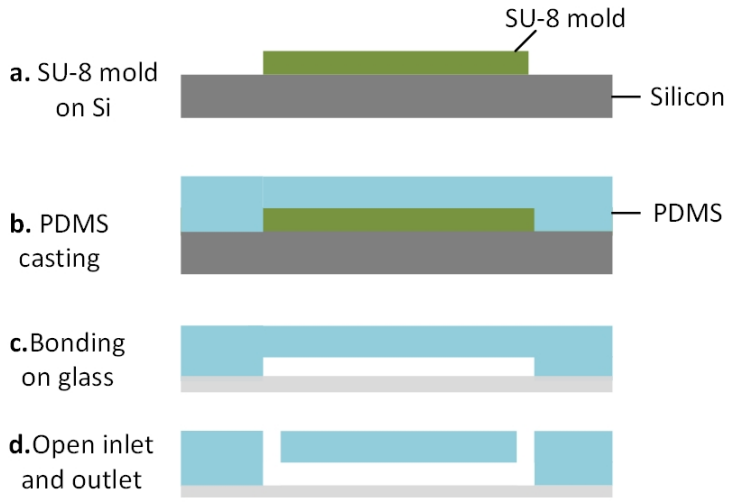

Figure 3.4: Additional fabrication step for a PDMS chip, starting from the SU-8 mold on silicon.

3.4 Fabrication of microfluidic channels on silicon

Microfluidic channels on silicon are fabricated to measure the penetration depth of Parylene into the channel and thickness of the deposited Parylene layer along the channel. The fabrication process begins with a spin coating of a 10 μm positive photoresist on a silicon wafer (4″ diameter, 525 μm thickness) followed by soft baked for 3 min. Soft bake is necessary to remove the solvent and to improve resist-substance adhesion. Afterward, the photoresist was exposed to UV-light (MA6 Karl Süss KG.GmbH) through the channel containing mask and developed (AZ400K) to remove the exposed resist. A

100 μm depth rectangular channel in silicon was achieved by reactive ion etching (DRIE) (ALCATEL etching tool). DRIE is an anisotropic etch with a very high aspect ratio (width to height). It allows fabricating a vertical wall of the silicon wafer at almost 90°. One cycle of a DRIE process is a combination of three steps: an etch step of silicon, a passivisation step of a polymer, and an etch step of the passivation layer. In the silicon etch step, particles (argon) are ionized and accelerated, which hit the silicon substrate from the vertical direction and remove materials. The ionized particles can also attack the sidewall of the silicon and destroy, which is prevented by depositing a thin chemically inert polymer layer on the substrate (Si). This deposition process is called the passivation step. The polymer layer on the sidewall of silicon can not be etched by radicals (sulfur hexafluoride). But, it can be destroyed by the direct impact of the radicals, which allows etching the passivation layer on the bottom of the trench. These three steps switch back and forth through the whole DRIE process until the desired depth of the channel reached. Finally, the remaining photoresist has been removed from the silicon surface by oxygen plasma.

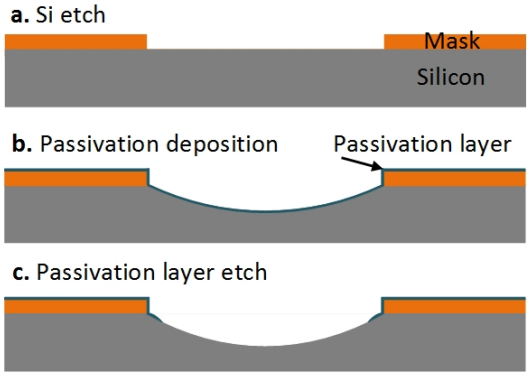

Figure 3.5: One cycle of the deep reactive ion etching process.

The main process steps of the fabrication of 100μm silicon channel are as follows

- Spin coating of 10 μm positive photoresist on a silicon wafer.
- Soft bake on a hot plate at 110°C for 3 min.
- Exposure to UV-light for 130 seconds.
- Developing the exposed photoresist.
- DRIE etching of the silicon.

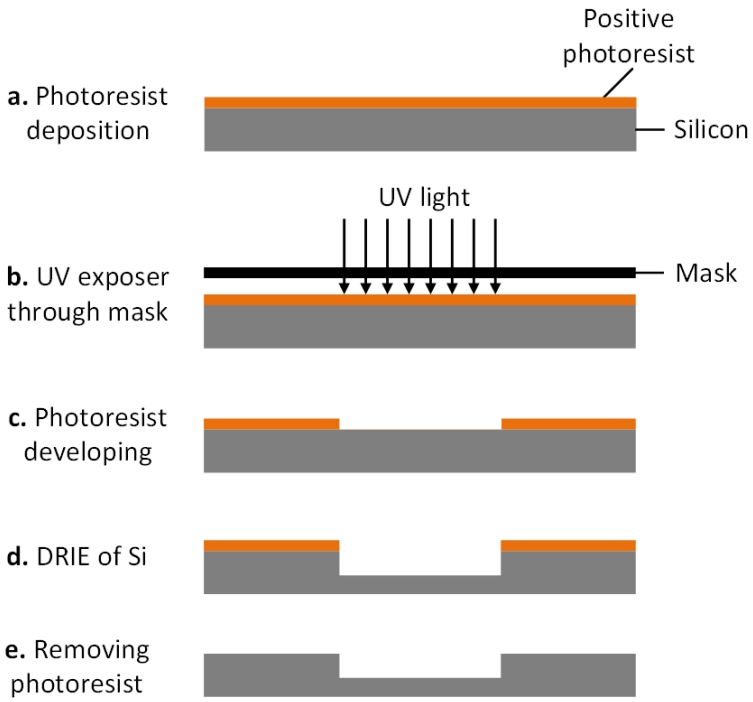

Figure 3.6: Fabrication of a microchannel on a silicon wafer.

- Plasma removal of the photoresist.

3.5 Parylene deposition

Parylene is another potential polymer, which is being used to fabricate microfluidic devices because of its biocompatibility, chemical inertness, and optical transparency [82, 83]. Properties of Parylene and the necessity to be used together with the PDMS will be described in chapter 4. Parylene can be vapor-deposited on a substrate, which facilitates to coat an uneven surface, an assembled microfluidic channel, and the surface where other deposition methods cannot be used (cardiac assist devices, electrosurgical tools, etc). The deposition thickness of a Parylene layer is in the range of several hundred angstroms to 75 μm [84]. In this study, Parylene AF4 is deposited on an assembled PDMS channel (PDMS channel is bonded on a glass slide). The deposition of Parylene on PDMS has three main steps: (i) PDMS surface cleaning and activation, (ii) Primer deposition, and (iii) Parylene deposition. Surface cleaning is crucial for the adhesion between the two materials. The surface of the PDMS channel was cleaned by oxygen plasma. The adhesion

of PDMS requires silanol (Si-OH) groups on the PDMS surface and -OH functional group on the other material. The silanol group on the PDMS surface was created by oxygen plasma. Since Parylene does not have any -OH functional group, a secondary layer is necessary between PDMS and Parylene for better adhesion. Silane-174 (PPS, Germany) is a coupling agent with the general formula $R_nSiX(4-n)$, where X represents hydrolizable alkoxy group (CH_3O-) and R is a nonhydrolyzable organic radical that enables the Silane-174 to bond with Parylene [85]. During the hydrolysis process X group creates -OH functional group and bonded on silanol (Si-OH) groups on the PDMS surface. When the polymer Parylene comes to the contact of the silane, R groups react and bonded with the Parylene. In this work, the PDMS surface was activated by an O_2/CF_4 plasma for 3 minutes at 50 Pa, followed by an oxygen plasma exposure for 5 minutes and finally, primer silane -174 (PPS, Germany) was deposited.

For the Parylene deposition on a silicon channel, the channel surface was activated by the oxygen plasma exposure for 5 minutes at 50 Pa. A 2% (v/v) silane-174 of pH 4.5 - 5.5 solution was prepared by adding 95% ethanol and 5% water. Afterward, plasma-activated silicon was dip-coated in the silane solution for 10 min, followed by air-dried for 24 hours at room temperature.

The deposition process of Parylene takes place in three steps: (i) the solid dimer is vaporized at a temperature of 150°C; (ii) the vapor is pyrolysed at a temperature of 680°C and the dimer becomes a stable monomeric diradical; (iii) the monomeric vapor is deposited on the sample in a vacuum deposition chamber at room temperature [86, 87]. The pressure and temperature for each step is summarized in Fig.3.7.

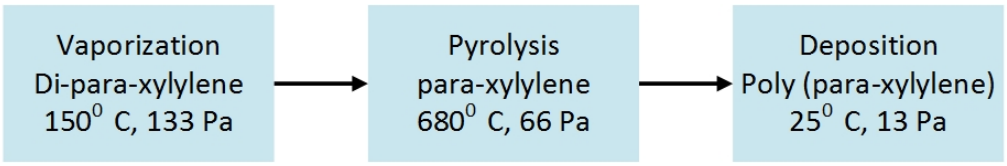

Figure 3.7: Simplified scheme of Parylene deposition process.

The deposition of Parylene was conducted on the assembled channel of both silicon and PDMS. Since it is a chemical vapor deposition method, the vaporized Parylene enters through the openings of the channel and deposits on the channel surface. The silicon channel was covered with polyvinyl chloride (PVC) foil, and the inlets and outlets were opened by removing the foil using a sharp scalpel. A schematic diagram of a Parylene coated PDMS channel and a silicon channel can be seen in Fig.3.8.

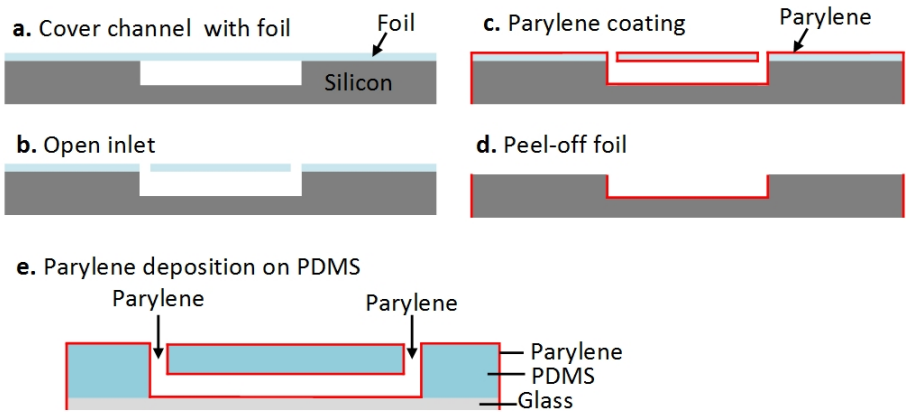

Figure 3.8: Parylene deposition on an assembled silicon (a-d) and PDMS channel (e).

3.6 External interface

Lab-on-a-chip technology aims to integrate laboratory function on a single chip. Nowadays, several biological and chemical processes are being carried out in a single chip, which previously was done in a test tube or well plates. Nevertheless, an external interface is still required to inject liquids in a microfluidic chip and their analysis. In this study, fluidic connections are used to feed fluids into the microchannel using a pressure-driven flow method, which was discussed in section 2.21.

Fluidic connection

Droplet generation in a microchip requires a continuous pressure-driven flow of both continuous and droplet phase liquids into the microchannel. External syringe pumps are used to supply the liquids to the microfluidic chip inlets. Microtubes carry liquids from a syringe to the microfluidic chip inlets. A photograph of a microfluidic chip with connected microtube is presented in Fig.3.9.

A fluidic connection is very crucial for the droplet generation setup. The size of the droplets in a microfluidic channel depends on the flow rate of the continuous phase and the droplet phase. During the generation process of droplets, if there is a slight change in the flow rate of any phase, the droplet size will be changed immediately. The pulsating characteristic of the fluidic pump is another critical factor in the variation of the size of the generated droplets. The choosing of a microfluidic pump for the droplets generation

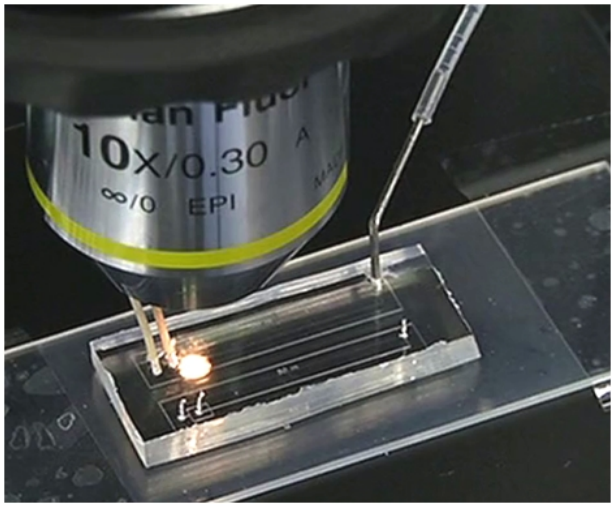

Figure 3.9: Microtubes are connected to inlets of a PDMS chip.

set up depends on the flow stability, settling times, and flow rate depending on the applications. The flow rate required for microfluidic set up in the range nano- to milliliter per minute. A pulsating free micropump with a flow rate of min. 0.6 nl/min. to 3 ml/min. for 1 ml syringe, has chosen for the droplets generation setup. The experimental setup of each experiment will be discussed in the following chapters.

3.7 Summary

This chapter presented the fabrication technologies used to produce microfluidic devices. It focused on the selection of materials for a microfluidic device and fabrication technologies. Both the material and fabrication technology required depend on the applications of a particular device. For instance, a cell-culturing microfluidic device must be biocompatible, a droplet-generation device must be hydrophobic, and a droplet-storage microfluidic chip should be liquid-impermeable. In research, the exact design specifications of a microfluidic device are seldom known in advance; they often change as the project matures. Therefore, the fabrication technologies involved in producing a microfluidic chip should be as simple as possible. The fabrication technology presented in this chapter was PDMS casting, a SU-8 replica mold, a silicon channel, and the deposition process of Parylene. A hybrid-material microchip of PDMS and Parylene were used in the droplet-storage application. The details of the PDMS–Parylene device will be discussed in the following chapters.

Chapter 4

On-chip droplet storage

To facilitate chemical reactions and analyze living cells in droplets, it is necessary to develop a method for droplet storage. Droplets can be stored either on-chip or off-chip, depending upon the system itself and the intended application. This chapter introduces a new on-chip droplet storage method and describes its applications. The introduction section of this chapter gives an overview of existing droplet storage methods and their advantages and disadvantages.

The basic-aspect section focuses on the working principle of the surfactant and the properties of different variants of Parylene. During storage, neighboring droplets tend to merge—using a surfactant with a continuous-phase liquid prevents this. Further, PDMS and Parylene are the base materials for the storage chip. Parylene coated PDMS channels prevent the diffusion of aqueous droplets into the PDMS, inhibiting droplet shrinking. The fabrication procedure of the storage chip has been presented in chapter 3.

This chapter is divided into two main parts: (i) characterization of Parylene coated PDMS channels and (ii) investigation of droplet generation and on-chip storage in the Parylene coated PDMS channels. The experimental procedure and resulting Parylene properties, such as hydrophobicity, penetration depth, and absorption barrier, are discussed in the characterization section. The droplet generation and on-chip storage section presents the experimental results of long-term on-chip droplet storage and biological cell survival in these droplets. The theory of droplet generation and their flow through a microchannel have been discussed in detail in chapter 2.

Finally, an outline of the current limitations and future perspectives of this storage method are presented. The work presented in this chapter has been published in [88, 89].

4.1 Introduction

New applications of droplet microfluidics are continually emerging because of the unique properties of micro-droplets, such as high reproducibility, high throughput, and uniform size [90, 91]. In the fields of chemistry, biology, and pharmacology, scientists are developing a system with a fast reaction time, low sample volume, and high throughput. Droplet microfluidics offers suitable alternative solutions that meet these requirements. It is heavily applied in microparticle synthesis, biomedical analysis, cell culturing, and drug delivery. Wang et al. synthesized fluorescent silica nanoparticles with a flow-focusing microfluidic system, where they improved nanoparticle-size uniformity by using droplet-microfluidic techniques [92]. Nisisako et al. have developed a droplet-based method to produce oil-filled polymeric microcapsules, where the system is capable of tuning the size and shell thickness of each individual capsule [93]. Another droplet-based platform has been developed that facilitates the culture and encapsulation of mammalian cells [94]. These experimental processes often demand on-chip storage of droplets for longer periods of time.

To date, the materials used for fabricating microfluidic devices include silicon, glass, PMMA, SU-8, polycarbonate, Parylene, and PDMS. The advantages and disadvantages of each material have been discussed in section 3.2. From these materials, PDMS is the most widely used material for droplet-generation chips because it is chemically inert, biocompatible, hydrophobic, transparent, cost-effective, and porous. This porosity makes PDMS permeable to both gases and liquids. Gas permeability makes its use convenient for cell-based studies since oxygen and carbon dioxide can diffuse through [95, 96]. However, liquid permeability allows water to diffuse through PDMS and eventually evaporate, which limits its application to microfluidic channels for the storage of droplets on-chip [94, 97].

A method has been reported in literature, where after generating hundreds of droplets in a PDMS chip, the droplets were transferred to polyvinyl chloride (PVC) tubes for storage by using electrovalves. This type of system is complex to use because it involves manipulating valves that affect droplet handling. An on-chip storage method, where sample droplets were stored, used water-filled PDMS channels to reduce sample evaporation in adjacent PDMS channels [98]. However, the reservoirs did not fully surround the storing channels, which led to only a partial reduction in sample evaporation. In another sample-storage method, the PDMS chip was stored in a water bath after the generation of droplets [99]. However, continuous monitoring of the stored droplets was not possible in this case [100]. Therefore, we aim to develop a solution to on-chip droplet storage, where the properties of the

PDMS channel can be improved.

In recent years, Parylene (poly p-xylylene) has been receiving increased attention for use in microfabrication technology. Parylene can be deposited in vapor form on a post-fabricated (assembled) PDMS channel. This vapor penetrates into the microchannel and covers the walls. Such Parylene coated PDMS channels are used for on-chip droplet storage and facilitate the storage of droplets for two days on the same chip in which they are generated. A microchannel used for droplet-storage measurements is shown in Fig.4.1

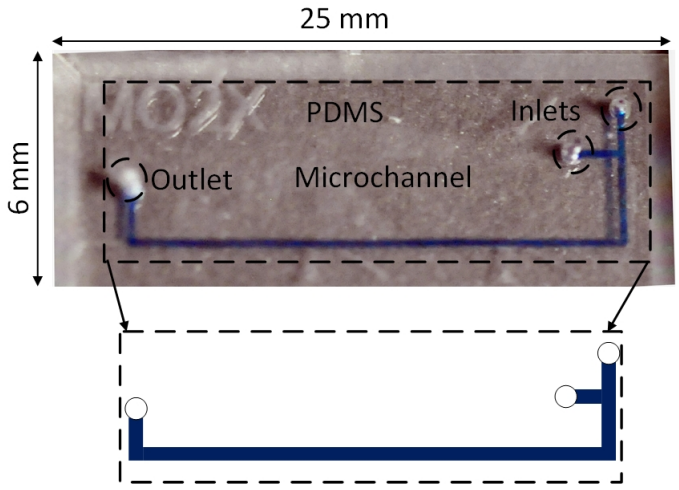

Figure 4.1: Parylene AF4 coated PDMS microchannel.

4.2 Basic aspects

4.2.1 Surfactant in droplet microfluidics

Droplets must be stored on a chip for the length of time required to complete an assay, which can be on the order of hours or days. During the storage of aqueous droplets in a microchannel, it has been found that, with time, neighboring droplets begin to come closer and eventually merge. Water (H_2O) is a polar inorganic compound, the oxygen and hydrogen in a water molecule have a high difference in electronegativity, resulting in its polarization. Hydrogen can form a “hydrogen bond", which is capable of creating a very strong intermolecular force and is the cause of the strong cohesive forces of water molecules. Because of this force, neighboring water droplets are attracted to each other and the oil phase between them drains out. Eventually, they merge and produce one large water droplet. In several applications of

droplet microfluidics, such as cell culturing or protein crystallization, merging of stored droplets is not desired; therefore, a surfactant is essential for such applications. A surfactant is an amphiphilic organic substance with a hydrophilic head and a hydrophobic tail. Hence, it has an affinity to both water and oil. Usually, a surfactant is mixed with the continuous phase (oil) prior to droplet generation. During the storage of droplets in a microchannel, surfactants gather at the interface between water and oil, forming an interfacial surfactant layer (Fig.4.2). This stabilizes the droplets and prevents coalescence. This surfactant layer also decreases the surface tension between the two phases [101]. Further, it rigidifies droplets by slowing them down. In accordance with the Marangoni effect, as a droplet moves, the distribution of the surfactant becomes non-uniform [102]. Excess surfactant gathered at the rear of the droplet results in a decrease in surface tension in this region. This generates a stress opposed to the direction of flow and makes droplets slower.

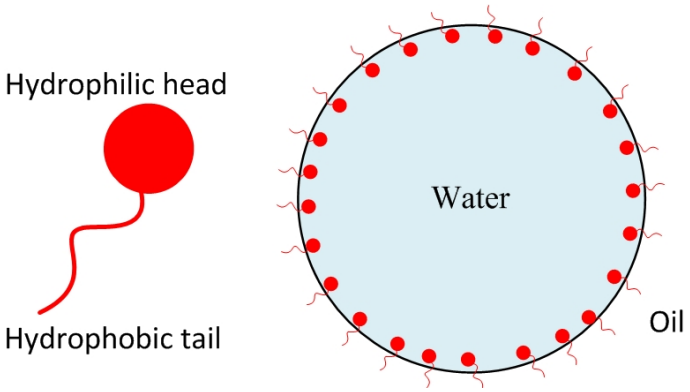

Figure 4.2: Surfactant gathered at the water-oil interface of a water droplet.

Over the past few years, several surfactant molecules have been developed for application in microfluidics. Two factors must be considered when selecting a surfactant for use in droplet microfluidics: biocompatibility—which allows cells to be stored and cultured in a droplet—and the characteristic that allows aqueous droplets to be generated in oil within a microchannel.

4.2.2 Properties of Parylene

Parylene is a relatively new biomaterial used in the production of microfluidic chips, although it has been used in non-biological applications for several decades. The application of Parylene has drastically increased after the development of the Gorham process, which facilitates the deposition of Parylene

via chemical vapor deposition (CVD) [103]. Using this method, the Parylene film thicknesses of several hundred angstroms to 75 μm can be achieved. Several variants of Parylene have been developed, including Parylene N, C, D, and AF4/HT [84]. These variants of Parylene have been developed by replacing the aromatic or aliphatic hydrogen atoms with other atoms or chemical groups. The chemical structures of Parylene N, C, D, and AF4/HT are shown in Fig.4.3. Parylene provides a pinhole-free barrier to protect against bodily fluids, moisture, chemicals, and atmospheric gases. It also offers some unique properties such as being biocompatible and pinhole-free, along with having the ability to form a highly conformal film. Parylene possesses a low sticking coefficient ($<1\times10^{-3}$) at room temperature, which allows it to easily pass through narrow microchannels [103].

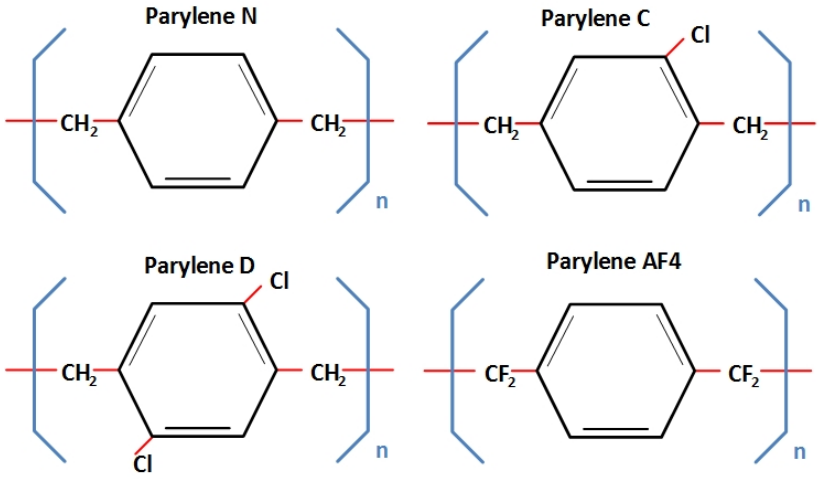

Figure 4.3: Parylene structure

Parylene C is used in several applications because of its high deposition rate, conformal coating, and low cost. A Parylene C coated PDMS channel has been documented in literature, where the Parylene C suppressed the absorption of fluorescent dye into the PDMS [104]. The penetration depth (depth into a tubing) of Parylene C is low; therefore only a short distance of an assembled PDMS channel can be covered with it (typically only a few millimeters) [105]. Very often in biochemical analysis, a large number of samples must be processed simultaneously; therefore, a longer channel is required. Longer Parylene coated PDMS channels can be achieved by coating an open channel and a microscope glass slide separately with a layer of Parylene, and bonding them afterward. Nevertheless, bonding Parylene on Parylene requires high pressures and elevated temperatures (200°C for

Parylene C and 350°C for Parylene AF4), which PDMS cannot withstand [106].

In the chemical structure of Parylene AF4, a hydrogen atom of the aromatic group is replaced by fluorine. The advantages of fluorination are high-temperature stability (up to 450°C), a low coefficient of friction, and a high penetration depth. Among all variants of Parylene, AF4 has the highest penetration depth, which allows it to coat a longer length of the channel [86]. However, there is a lack of research on the applications of Parylene AF4 in microfluidics. A preliminary investigation on droplet storage in AF4-coated PDMS channels has been addressed in [89]. Further, the properties of the different variants of Parylene are summarized in Table 4.1.

Table 4.1: Parylene properties [84, 86]

Properties	Parylene AF4/HT	Parylene C	Parylene N	Parylene D
Continuous service temperature	350°C	80°C	60°C	100°C
Short-term service temperature	450°C	100°C	80°C	120°C
Penetration ability*	50x dia	5x dia	40x dia	2x dia
Water absorption (% after 24 hours)	<0.01	<0.1	<0.1	<0.1

*Depth into tubing

4.3 Chip design

The primary function of the chip is to generate droplets and store them for an extended period. A T-junction device with a 23-mm-long channel (width and depth of 300×100 μm) has been used to generate and store the droplets. The droplet-generation principle at a T-junction has already been discussed in chapter 2. For the storage of droplets, the PDMS channel was coated with Parylene AF4. The penetration depth of Parylene depends on the width and depth of the channel. An experiment was conducted to measure the Parylene thickness by varying the channel width. Silicon channels of various widths were fabricated, sealed, and coated by Parylene. The thickness of the Parylene was then measured. The results are shown in Fig.4.5. Parylene AF4 can penetrate more than 25 mm from one end of a channel (with a width and depth of 300×100 μm). Another experiment was conducted to examine the absorption barrier of Parylene by storing indigo-carmine solution in the Parylene coated channel, the result of which is presented in Fig.4.6. The experimental results revealed that a Parylene AF4 with a thickness of 1.2 μm can prevent the diffusion of indigo carmine solution. Based on the

experimental results, an optimum droplet-storage channel length, width, and depth were chosen. Subsequently, a PDMS channel was fabricated using standard soft lithography and plasma bonded onto another layer of PDMS, which was then bonded with a glass slide. The inside of this PDMS-on-PDMS bonded channel was then coated with Parylene by CVD. The channel-fabrication process and Parylene-deposition process have been discussed in detail in chapter 3. The fabricated chip used for droplet-storage experiments is shown in Fig.4.1.

4.4 Characterization of Parylene coated PDMS channels

Several experiments were conducted to characterize the Parylene coated PDMS channels. In particular, they were used to store aqueous droplets and biological samples. Droplet generation and subsequent droplet transport through the microchannel require hydrophobic channel surfaces. The hydrophobicity of the Parylene coated PDMS channel was analyzed by measuring the contact angle of a water droplet on its surface. The experimental procedure and results are presented in the following section.

The absorption of molecules into the PDMS surface prevents PDMS microchannels from being used in many biological and chemical applications. A pinhole-free Parylene coating can prevent this absorption. Herein, the barrier properties of Parylene were investigated by storing Rhodamine B solution in a Parylene coated PDMS channel.

4.4.1 Hydrophobicity of channel materials

Hydrophobicity is a physical property of a material that defines its tendency to repel water from its surface. Generally, hydrophobic substances are non-polar. Therefore, they are attracted to neutral or nonpolar solvents and repel polar solvents such as water. Since hydrophobic surfaces prevent water from sticking to channel walls, hydrophobic channel materials are required to generate water droplets in oil and transport them through the channel [107, 108]. Although a material's hydrophobic property is dependent on its molecular structure, its surface profile can also affect this property. A rough surface is more hydrophilic than a smooth one. Since CVD of Parylene produces pinhole- and prone-free surfaces, the effect of surface roughness on hydrophobicity can be neglected.

The hydrophobicity of a material can be ascertained by measuring the contact angle of a water droplet on the surface of the material using Young's

law. The mathematical explanation of the contact angle has been covered in section 2.3.2. The contact angle of a water droplet resting on the material surface (Parylene C coated PDMS, AF4 coated PDMS, and uncoated PDMS) was measured using a goniometer (KRÜSS GmbH, Germany).

When a drop rests on the surface of a material, an angle is formed at the interface between the liquid drop, the solid surface, and air, which is called the static angle. The static contact angle can be simply measured using Young's equation (equation 2.1). In the case of droplets moving through a microchannel, two contact angles form with the solid surface—the advancing and receding contact angle—which have been discussed in chapter 2. To determine the hydrophobicity of the material, the static contact angle of a water drop on its surface was measured. The hydrophobicity of uncoated PDMS, Parylene AF4 coated PDMS, and Parylene C coated PDMS was measured. Five consecutive measurements were made for each material at room temperature. The contact angle of a water droplet on the PDMS surface was 105±4°, which is consistent with values found in the literature [109]. The measured average contact angles of Parylene C coated- and AF4-coated PDMS were 95±4° and 120±4°, respectively (Fig.4.4). Parylene AF4 coated PDMS shows a significantly higher degree of hydrophobicity, resulting in an improved droplet flow through the channel.

Although PDMS is a hydrophobic material, its hydrophobic properties change with droplet storage time. Further, cleaning and heat treatment are required to reuse PDMS chips. For some applications, such as cell storage in a microchannel, PDMS channels cannot be reused. This is because the cells stick to the channel walls and cannot be washed away. On the other hand, the hydrophobicity of Parylene AF4 does not change over time. In the droplet-storage experiments, water droplets were stored in the Parylene AF4 coated channel for more than two days. After two days, the stored droplets did not adhere to the channel wall. This facilitates the reuse of the device for several measurements.

4.4.2 Parylene thickness measurement in a microchannel

During the chemical vapor deposition of Parylene, the vaporized Parylene molecules enter into the assembled PDMS channel through the openings (inlets and outlet) and deposit. The thickness of the deposited Parylene C and AF4 was measured along the channel length. Both PDMS and the thin Parylene layer are elastic; to make sharp cuts in AF4 coated PDMS channels is difficult using general dicing technologies. Therefore, the thickness

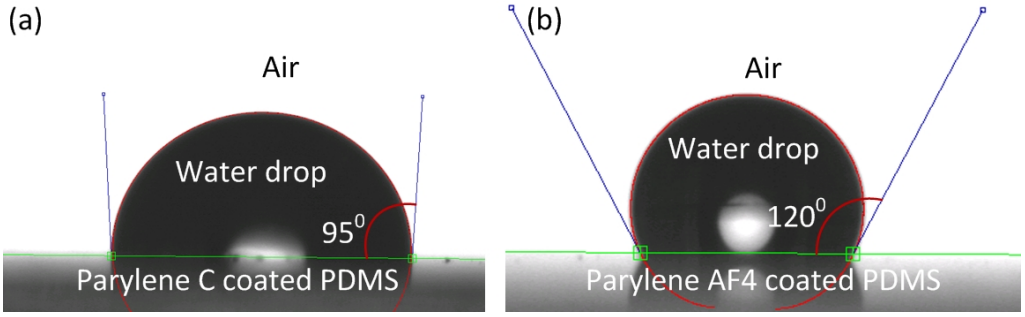

Figure 4.4: Contact angle measurement of (a) Parylene C coated PDMS and (b) Parylene AF4 coated PDMS.

of deposited Parylene was measured in silicon channels. Microchannels of different widths 300 μm, 200 μm, 100 μm and 50 μm were prepared on a 100 mm diameter silicon wafer of thickness 525 μm. The length and depth of the channels are 85 mm and 100 μm, respectively. The fabrication process was described in chapter 3. The silicon channel was sealed with PVC foil and the sealed channels were coated with Parylene. Afterward, the channels were diced (Kulicke & Soffa Industries Inc., USA), at 3 mm distances. The PVC foil was gently peeled off from the silicon surface. To measure the AF4 thickness, the surface of the Parylene coated PDMS chip was milled by a focused ion beam (FIB). Before the milling process, a thin layer of gold (10 nm) was deposited on top of the AF4 layer, which prevented charging during the FIB process. The thickness of the AF4 was measured in each section by scanning electron microscopy (SEM) (Zeiss, Germany) and electron high tension (EHT) of 10 kV was used for each measurement.

The deposition principle of Parylene into a long narrow channel can be described by the molecular flow during the vapor deposition process [110]. The mean free path λ of the Parylene monomer in the vacuum deposition chamber is far larger than the characteristic size (i.e., the hydraulic diameter Dh) of the microfluidic channel. In other word, the Knudsen number λ is much larger than 1, hence the free molecular flow condition is satisfied, for which intermolecular collisions rarely happen. The Knudsen diffusion coefficient for the free molecular flow is only dependent on the molecular weight, the deposition temperature and the channel size. The results show that the penetration depth of AF4 is higher than of Parylene C, which is consistent with literature [86, 106]. Parylene AF4 has the highest in-tube penetration ability because of its lower coefficient of friction (static: 0.15, dynamic: 0.13) and lower molecular weight (244 gram/mol). Parylene C possesses a higher coefficient of friction (static and dynamic: both 0.29) and higher molecular

weight (277 gram/mol) [84, 86]. The measured thickness in the silicon channel is presented in Fig.4.5(c,d). The thickness of the deposited layer decreases as a function of increasing distance from the entrance of the microchannel. In Fig.4.5, the measurement results are depicted showing the penetration ability of Parylene C and AF4 in silicon etched microchannels. To achieve a deposited thickness of at least 4 μm in a channel with a cross-section of 100 $\times$ 300 μm^2, the maximum channel length for Parylene C and AF4 are 11 mm and 24 mm, respectively (Parylene enters the microchannel from both sides). The kilogram price of AF4 dimer is about twenty times higher than that of Parylene C. In addition, Parylene AF4 requires twice the amount of dimer to achieve the same deposited thickness. However, the measurement results show that the penetration ability of Parylene AF4 is two to three times as much as that of Parylene C. This allows longer storage channels to accommodate micro-droplets. Additionally, Parylene AF4 has a continuous service temperature of 350°C, whereas Parylene C can only withstand 125°C [86]. PDMS has a continuous service temperature of approximately 200°C. Therefore, AF4 coated PDMS channels can be used for applications where higher working temperatures or device sterilization is required.

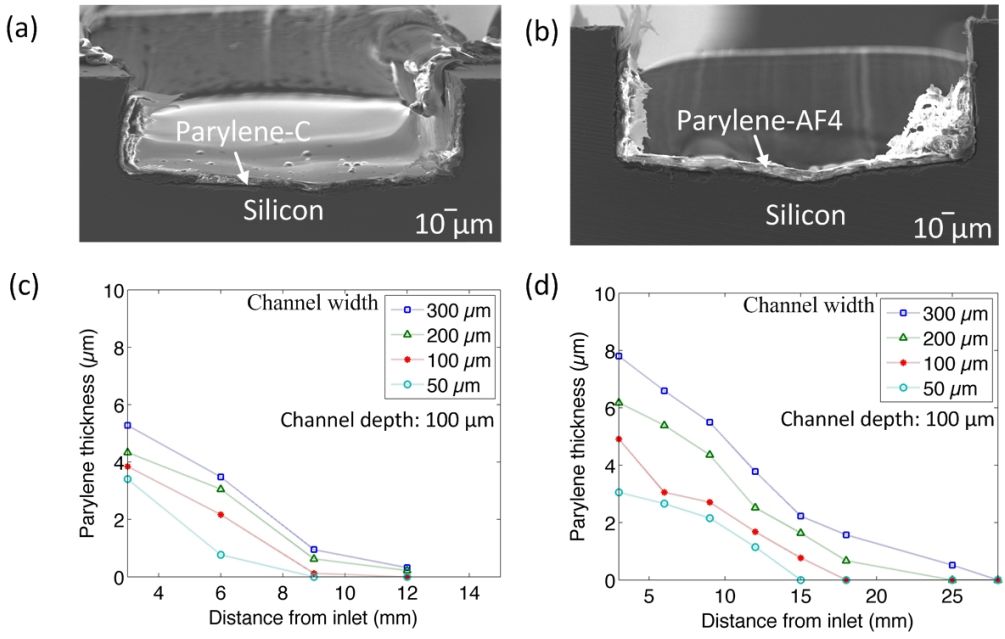

Figure 4.5: SEM photographs of Parylene C on silicon (a); Photograph of Parylene AF4 on silicon (b); The measured thickness along the channel for Parylene C (c). The measured thickness along the channel for Parylene AF4 (d).

4.4.3 Diffusion of Rhodamine B into PDMS and Parylene coated PDMS

Absorption of florescent and other organic molecules is a troublesome property of PDMS. Small molecules diffuse and absorb into the PDMS surface and bulk, which limits the application of PDMS. Non-porous coating of Parylene on PDMS suppresses molecules absorption into the PDMS. A solution of Rhodamine B was stored in Parylene AF4 coated PDMS channels and in non-coated PDMS channel. Rhodamine B is an organic fluorescent substance, with excitation and emission wavelength of 553 nm and 627 nm, respectively [111]. It diffuses into the cured PDMS, and was used as an indicator to characterize the diffusion and absorption barrier of the AF4 coating in the channel. A coated and a non-coated channel of 85 mm long with depth and width of 100 $\times$ 200 μm, are used in this measurement setup. A 1% (w/v) solution of Rhodamine B in DI water was prepared and injected into the channels at a flow rate of 100 μl/hr. The chips were placed on the fluorescent microscope stage (Nikon, Japan) such that the field of view was the same for each chip. A reference image was taken at t=0, immediately after the solution was injected. A sequence of images was taken every 10 minutes to monitor the diffusion and absorption of Rhodamine B molecules into the PDMS. Fluorescent emission of the Rhodamine B was filtered out using a 521-565 band-pass filter and images were taken using a camera (Nikon D5100) mounted on a microscope. At time t=0, no absorption and diffusion of Rhodamine B was observed in both non-coated PDMS and AF4 coated PDMS channels. After some minutes Rhodamine B absorption into PDMS in the non-coated channel becomes visible. It results in a broader fluorescent profile of the channel width, which can be seen in Fig.4.6(b). A quantitative analysis of the diffusion length of Rhodamine B into the PDMS was conducted by comparing the intensity profile at t=0 and t=10 min, see Fig. 4.6(c). The diffusion length of Rhodamine B into PDMS is estimated by calculating the pixel value of the fluorescent intensity along the x-axis (shown in Fig.4.6 (a)) using a customized software script (MATLAB). The diffusion length of Rhodamine B into the bulk PDMS after 10 min. is 100$\pm$20 μm. Three successive measurements were conducted to obtain each data point.

The same test was conducted to investigate the possible improvement of the absorption and diffusion barrier performance of Parylene AF4 coatings in PDMS channels (Fig.4.6(d-f)). At t=10 min, no diffusion or absorption of Rhodamine was observed. The storage time was prolonged and a sequence of images was captured every hour. Figure 4.6(f) depicts that the intensity profile of AF4 coated PDMS channel at t=0 and t=12 hours overlap each other, which shows that diffusion of Rhodamine B into the AF4 coated PDMS

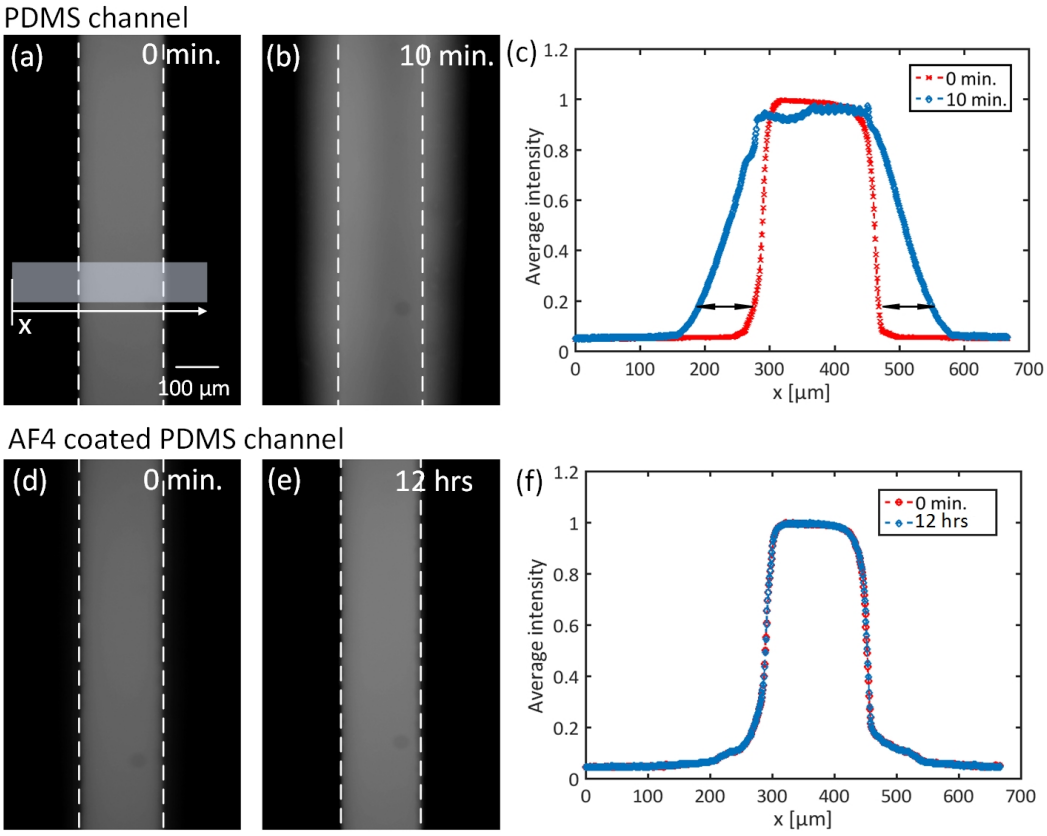

Figure 4.6: (a,b): Diffusion of Rhodamine B molecules into the PDMS for non-coated channels; (c): Intensity profile of Rhodamine B diffused into the PDMS in non-coated channels at t=0 and t=10 mins; (d,e): Storage of Rhodamine B in a Parylene AF4 coated PDMS channel; (f): Intensity profile of Rhodamine B in the AF4 coated PDMS channel at t=0 and t=12 hours.

channel did not occur.

The penetration length during Parylene AF4 deposition is higher than for Parylene C, which is presented in Fig.4.5. A measurement was conducted by storing Rhodamine B solution both in AF4 coated PDMS channels and C coated PDMS channels. For both cases the channel was 85 mm long with depth and width 100 $\times$ 200 μm, respectively, which is shown in Fig.4.7(a). Both channels were filled with 1% (w/v) Rhodamine B solution with a flow rate 100 μl/hr and the solution was stored in the channels for 60 min. A noticeable change of Rhodamine B diffusion into the PDMS is found at a channel length of 20 to 22 mm distance from the inlets of the AF4 coated channel, whereas in Parylene C coated channel it was at a channel length of

4 to 6 mm. At this location Rhodamine B molecules start diffuse into the PDMS in the Parylene coated PDMS channel (Fig.4.7(b,c)). A quantitative measurement of Parylene thickness in an assembled channel has been conducted. The AF4 layer thickness at a channel length 22 mm is approximately 1.2 μm. On the contrary, there is no Parylene C layer visible after 12 mm of the channel length from the inlets.

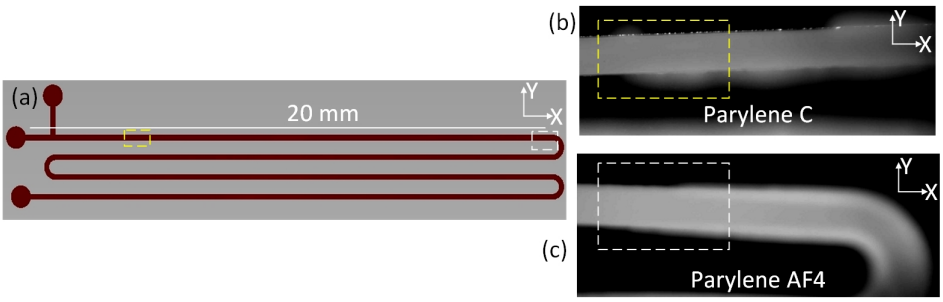

Figure 4.7: A schematic diagram of an 85 mm long channel with depth and width of 100±20 μm (a). The location of C coated channel length, where Rhodamine B starts to diffuse into the channel material (b). The location of C coated channel length, where Rhodamine B starts to diffuse into the channel material (c)

4.5 Droplet generation and storage

Extensive experiments have been conducted to study droplets in a Parylene coated microchannel, storage of droplets in the channel and culturing cells in the stored droplets. This section is dedicated to the study of droplets in a micro channel. The uniformity of droplets size is one of the important advantage of droplet microfluidics. The size and shape of droplets has been studied and the result will be presented in the following section. The channel properties play an important role on the flow of droplets through a channel. The effect of Parylene coated surface on the flow of droplets was studied and will be discussed in this section. At the end of the section, experimental result of droplets storage and culturing cells in the stored droplets will be presented.

4.5.1 Size and shape of droplets in a microchannel

The size and shape of droplets in a microchannel depend on the channel geometry, channel materials, flow rate of the continuous and droplet phase, density of the liquids, and the concentration of the surfactant. If these properties are kept constant, the size and shape of droplets vary with the droplet generation structure such as T-junction and flow focusing. The mathematical explanation of the size of the droplets in a microchannel has been presented in section 2.3.4. During experiments, it was observed that the larger droplets have a flattened shape and smaller droplets have a spherical shape. The findings are linked to the surface tension and gravitational force. For the larger droplets both forces act on the shape of droplets, whereas, for the smaller droplets only surface tension is an active force. This can be explained by the Bond number [112], which is

$$B_0 = \frac{\rho g R^2}{\gamma}, \tag{4.1}$$

where γ is the surface tension, ρ is the density, g is the gravitational force, and R is the droplet radius. If $B_0 < 1$, the droplet is spherical in shape, otherwise the gravitational force flattens the droplets. Droplets of different size and shape are presented in Fig.4.8 and Fig.4.9. However, in a narrow rectangular microchannel, where the radius of the droplet is larger than the width of the channel, the shape of the droplets cannot be explained by the Bond number. The larger droplets take flattened shape because of the narrow channel. The experimental result of agarose droplets presented in the chapter 5 agrees with this conclusion. Figure 5.5 showed that the flattened shape

agarose droplets in a microchannel take spherical shape when they are taken out of the chip.

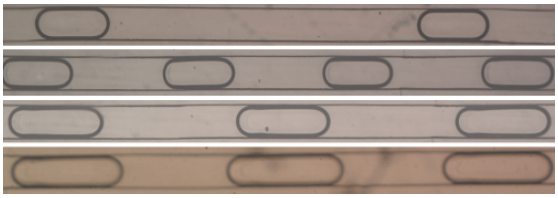

Figure 4.8: The size and shape of aqueous droplets at different flow rate.

4.5.2 Flow of droplets in a microchannel

The transport of droplets in confined fluidic networks in microchannels is necessary for many droplets applications such as PCR, chemical reactions, and bioengineering. However, less research has been conducted on the understanding of flow characteristics and their related factors for the systems involving the flow of droplets. Rectangular microchannels were used for the storage and for the other applications of droplets in this research work. Therefore, only droplet flow through a rectangular microchannel will be discussed. Several factors influence the flow of droplets in a microfluidic network, such as the density of the fluids, the flow rate of both fluids, and the interfacial tension between them, which is explained in section 2.4. Channel roughness also has a significant impact on the flow of droplets in a microchannel. It is directly related to the frictional resistance imparted on the droplets by the channel surface. As the channel size decreases, surface roughness becomes an important parameter. The SU-8 mold to produce the PDMS channel is fabricated using photolithography to ensure a smooth surface. Typically, the microchannels imprinted in the PDMS layer are closed with a glass slide or with another piece of PDMS. This bonding is usually done by a plasma process. Due to the plasma process, the smoothness of the channel can be affected. However, the conformal pinhole-free coatings of Parylene into the PDMS channel ensures a smooth surface of the channel. Therefore, the influence of the surface roughness on the flow of droplets is very small, so small that we have not detected it in our experiments.

The travel speed of droplets depends on the size and viscosity of the droplets. Smaller droplets travel faster than larger droplets. The smaller droplets are located in the middle of the channel where the flow velocity is the highest. Whereas the larger droplets are near to the channel wall/in contact where the flow velocity is zero. The flow profile of a liquid in pressure

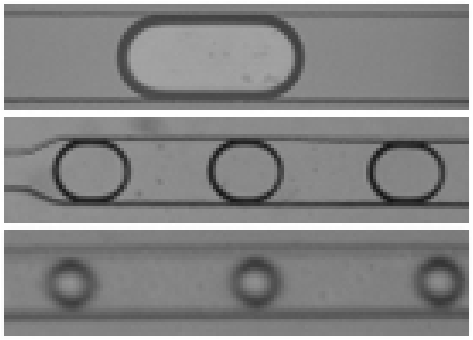

Figure 4.9: Various sizes of droplets and their flow in Parylene coated a PDMS microchannel. The larger droplets are in contact/near to the channel wall, where the flow velocity is zero. The smaller droplets are located in the middle of the channel, where the flow velocity is the highest.

driven flows was explained in chapter 2.

4.5.3 Storage of droplets

PDMS is permeable to liquid and gas, which causes shrinkage of water droplets in the channels, whereas Parylene AF4 coated PDMS suppresses the shrinkage. Droplets were stored both in AF4 coated and non-coated PDMS microchannels for several hours and the volume loss of droplets in time was measured. In both cases, 23 mm long microfluidic channels of depth and width 100 $\times$ 300 μm, respectively, were used. The fabrication steps of PDMS and Parylene coated PDMS channel is discussed in details in chapter 3. The inter-droplets distance was maintained at a distance of at least the droplet diameter to prevent undesired merging of the stored droplets. The droplets were generated in the microchannel using a T-junction geometry, the principle of T-junction has been discussed in chapter 2. Mineral oil with a viscosity of 30-60 mPa.s (20°C) and a density of 1.06 g/mL at 20°C was used as the continuous phase. DI water was used as the droplet phase for the on-chip droplets storage measurement. The continuous phase (oil) and the droplet phase (DI water) were kept in two separate 1 ml glass syringes (Hamilton) at room temperature. The syringes were fixed in two separate syringe pumps (Legato 180 dual, KD-scientific), which continuously supplied the liquid into the microchannel. PEEK microtubings of 250 μm inner diameter carried liquid from the syringes to the microchip. The microchip was fixed on the inverted routine microscope stage (TS100 Nikon, Japan). A camera (Nikon D5100) was fixed with the microscope to analyze and take photographs of the stored-droplets. The experimental setup of droplets generation and storage

is presented in Fig.4.10.

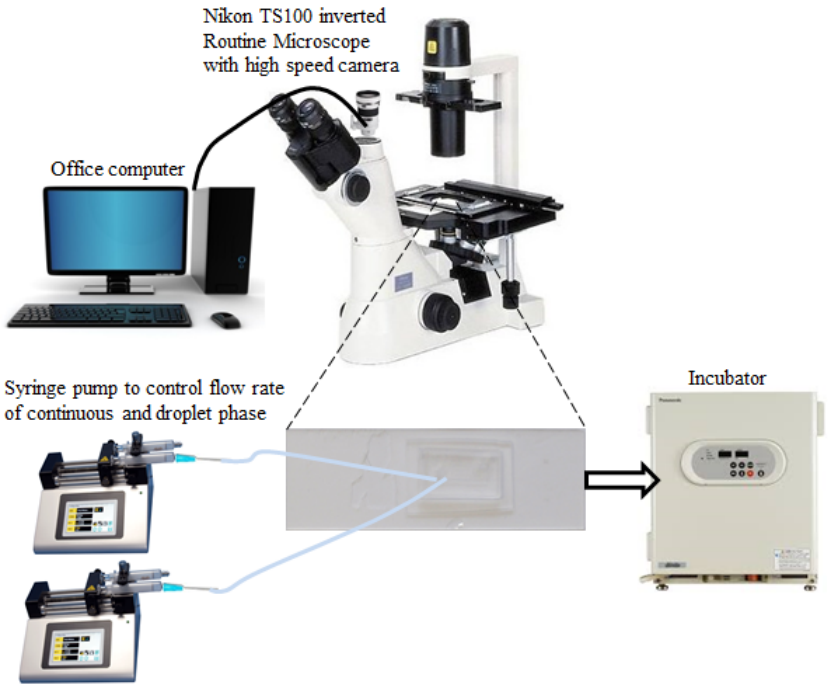

Figure 4.10: Experimental setup for the generation and storage of droplets.

The continuous phase and the droplet phase were pumped to the microchannel at a flow rate 10 μl/hr and 4μl/hr, respectively. After filling the microchannel with the droplets, the inlet and outlet tubes were removed and the chip was completely sealed with water-resistant adhesive tape (Farnell, Germany). Depending on the droplets size approximately 20 droplets were stored in the microchannel for each storage measurement. Reference images of the droplets were taken at t=0, just after disconnecting the microtubes from the chip, then the chip was kept at 37°C in an incubator (Panasonic MCO-5AC-PE). A sequence of images was taken every hour up to 48 hours of droplets storage. The microscope stage was fixed in such a way that the field of view was the same for each measurement. Five successive measurements of droplets storage were conducted maintaining the same environmental condition. The coalescence of stored-droplets in the microchannel was prevented by adding a surfactant (span 80) of a concentration of 1% (v/v) to the mineral oil. A significant decrease in droplet shrinkage in the AF4 coated PDMS channel compared to the non-coated PDMS channel was noticed. As PDMS is porous, water diffused away from the droplets into the PDMS and eventually evaporates. After four hours of storage, the droplets were com-

pletely gone (Fig.4.11(a)). On the other hand, in the AF4 coated channel the droplets lose less than 10% of their initial volume. AF4 has the lowest water absorption properties (< 0.01 %, for a thickness of 25 to 76 μm) among the different types of Parylene [84, 86]. The AF4 layer on PDMS suppresses water molecules to diffuse into the PDMS (Fig.4.11(b)). The comparison of droplets volume reduction in non-coated PDMS and in AF4 coated PDMS channels is presented in Fig.4(d). Each data point presented in Fig.4.11(d) is the average normalized value of approximately 100 stored droplets. In the AF4 coated PDMS channel the droplets showed only 20$\pm$2 % volume reduction after 48 hours of storage time. The volume of droplets was calculated by using a customized software script (MATLAB) that counts pixels from captured images.

It must be taken into account that the droplets also lose volume to the surrounding oil. It has been reported in literature that water molecules from the droplets dissolve into the surrounding hydrocarbon oil [113]. To reconfirm this statement, an additional measurement was conducted to analyze the diffusion of water molecules from the droplet into the surrounding oil during the storage. For this, smaller droplets (not touching the channel wall) and comparatively bigger droplets (touching the channel wall) were stored using the same setup and environmental condition as used for long-term droplets storage. In this case, the oil-surrounded droplets are approximately 100 μm in diameter, which is less than half of the size of the channel width. Droplets were then stored in the same condition as for larger droplets. The shrinkage of the smaller droplets were measured in time and compared with the larger droplets shrinkage (Fig.4.11(e)). The volume loss for small droplets is five times higher than the volume loss of larger droplets. The surface area to volume ratio and the higher inter-droplets distance between the smaller droplets results in a higher dissolving rate. It is noted that in the first five hours droplets lose 50% of their total volume-loss measured in 48 hours (Fig.4.11(d)). By reducing the inter-droplets distance the droplets shrinkage in AF4 coated channel can be reduced. However, during the storage measurement, it was noticed that the droplets are more stable when the inter-droplets distance is at least the diameter of the stored droplets.

4.5.4 Storage of bacteria in droplets

Storage of a biological sample in a droplet is an application for on-chip storage of droplets among the many other applications. To demonstrate the on-chip storage of a biological sample, bacterial populations of *E. coli* and *E. faecalis* were encapsulated in droplets and stored for several hours in a Parylene AF4 coated PDMS channel. The encapsulation of bacteria in droplets followed

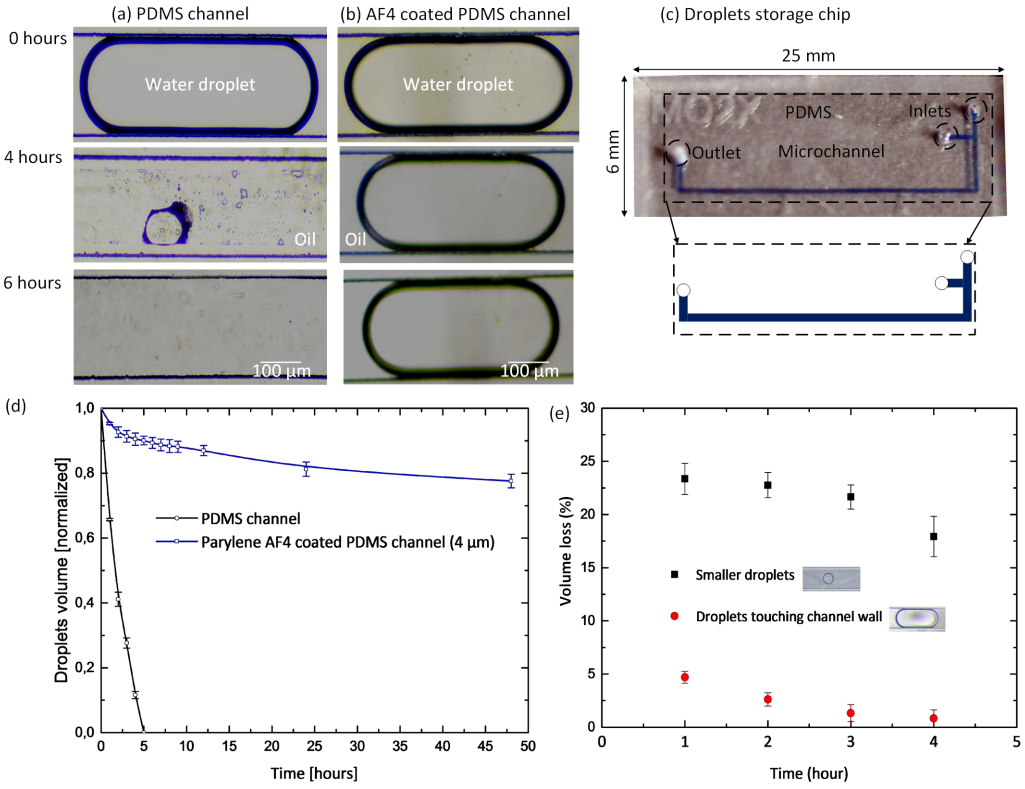

Figure 4.11: Photograph of a stored droplet in a non-coated PDMS channel and an AF4 coated PDMS channel, taken at t=0, at t=4 and at t=6 hours (a,b); Photos show that Parylene AF4 coating significantly improves the channels storage properties. Photograph of the droplets storage chip (c); Change of droplets volume over time (d); At 5 hours of droplets storage at 37°C, there is no droplet phase visible any more in the PDMS channel, whereas in the Parylene AF4 coated channel the droplet loses only a small part of its volume; The comparison of volume loss of smaller and larger droplets (e).

the Poisson distribution equation, which is explained else where [114]. Since each droplet encapsulated a sufficient amount of cells, they have well followed the Poisson distribution ratio. 25% (w/v) Lysogeny broth (LB) medium with 14% (w/v) sucrose in DI water was used as a culture medium to grow *E. coli*. At first *E. coli* was cultured in agar gel. Later a loop cluster of cells was taken with an inoculating loop holder (1 mm inner diameter), and diluted in 1 ml LB medium. Afterwards, cells were centrifuged and washed, and again diluted in another 5 ml fresh LB medium. This bacteria diluted LB medium was used as a droplet phase. The bacteria-containing droplets in oil were

generated using the same set-up and procedure as used for droplets storage measurements. After encapsulating the bacteria in the droplets, the inlets and outlet of the chip were sealed with an adhesive tape. Reference images were taken right after the generation of the bacteria-containing droplets. The chip was kept at 37°C in an incubator. A sequence of images was taken every 30 minutes up to 12 hours. E. faecalis was stored and cultured following the same protocol as used for *E. coli*. It was observed that during the storage the population of both bacteria increased. Figure 4.12 illustrates growth of *E. coli* and *E. faecalis* in microdroplets.

E. coli is a rod-shaped bacteria with approximately 0.5 μm width and 2 μm length [115]. Immediately after transferring the cells from bulk medium (agarose) to fresh liquid medium, the populations temporarily remains unchanged. The time necessary to recover from physical damage or shock after transfer is the so-called lag-phase [116]. E. coli takes approximately one hour for the first generation to start growing including the lag-phase in the stored droplets. After the lag-phase, *E. coli* growth in droplets takes approximately 25 min. for each generation. It was found that the exponential growth phase of *E. coli* in this experiment was up to 5 hours; afterwards the bacteria stopped growing due to a lack of sufficient nutrients.

E. faecalis is spherical in shape. In growth conditions, they can elongate and appear coccobacillary as can be seen in Fig.4.12(b). *E. faecalis* form short chains or are arranged in pairs during growth [117]. Like *E. coli*, *E. faecalis* takes a longer time for the first division because of the lag-phase, it takes approximately two hours for the first generation to start growing. The experimental result shows that *E. faecalis* in droplets takes approximately 50 minutes for each generation. In practice, a single device could be used more than ten times for droplet storage experiments.

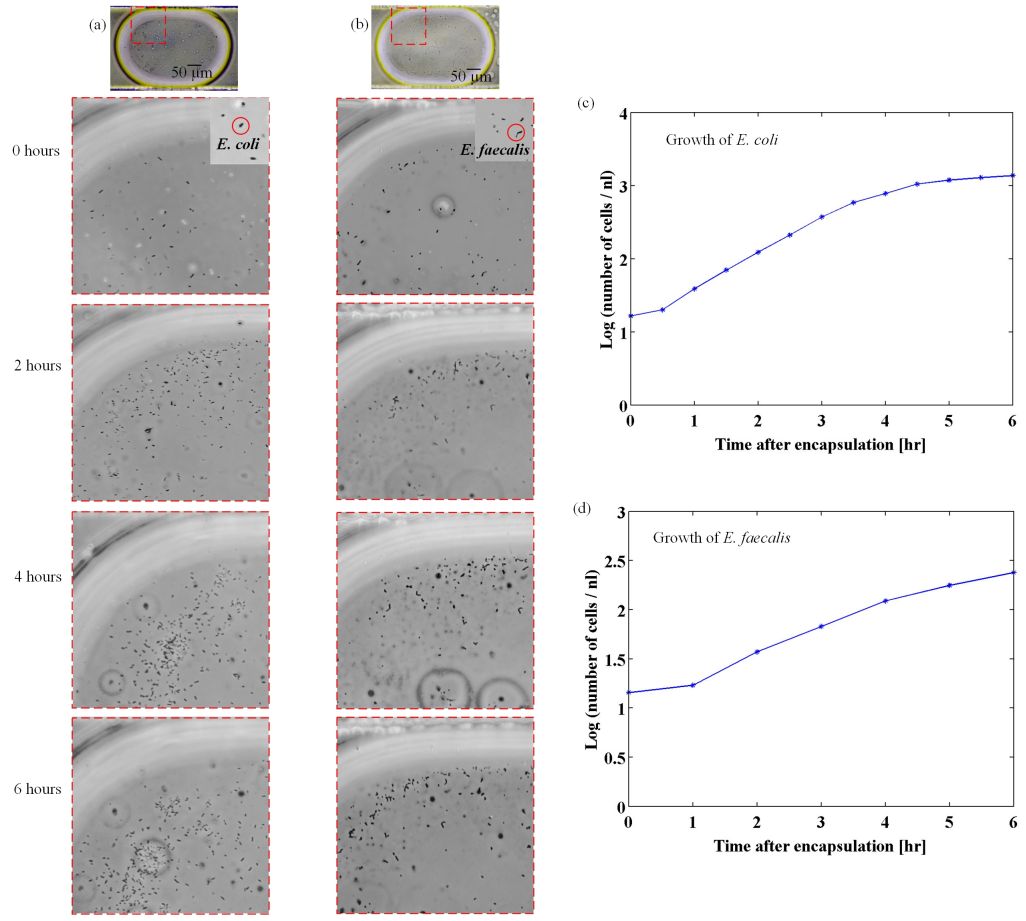

Figure 4.12: Growth of bacterial population in droplets. *E. coli* encapsulated and their growth inside a droplet (a, c); *E. faecalis* growth inside a droplet (b, d). Sufficient nutrients were present in the microdroplet for multiple generations of bacterial growth.

4.6 Conclusions

A microfluidic system for the on-chip storage of droplets was designed and fabricated. The diffusion of water into the PDMS substrate was suppressed by coating the PDMS surface with Parylene AF4. Experiments confirmed that droplets could be stored for at least two days, even at an elevated temperature of 37°C, with only a small reduction in volume. The diffusion barrier of Parylene AF4 was also examined using Rhodamine B solution, where no diffusion was observed. When storing Rhodamine B solution, it was found that the droplets did not wet or adhere to the surface of the channel wall, indicating that the hydrophobicity of Parylene AF4 coated

PDMS is maintained over time. A single device could be used more than ten times for droplet-storage experiments. After the storage measurements, the droplets were removed from the chip by applying under-pressure to the outlet. The channel was ready for the next measurement after cleaning with isopropanol. The method presented produces biocompatible materials as PDMS and Parylene AF4 are used to fabricate the microfluidic chip. The successful culturing of *E. coli* and *E. faecalis* in the stored droplets confirm that the device has practical use. The proposed method has great potential for long-term on-chip biological and chemical processing. The limitation of the proposed on-chip storage method is that it is difficult to store mammalian cells, which require a balanced environment of oxygen and carbon dioxide to survive. A solution to this will be presented, along with experimental results, in the following chapter.

Chapter 5

Agarose droplets

Agarose has been used in cell culture for several decades. Agarose solution can form a stable gel at a concentration as low as 0.3% (w/v) at room temperature. It has a very low ionic concentration and is free of contaminating impurities that may affect the growth of cells. This chapter presents a microfluidic chip to generate agarose droplets and on-chip gelation of the generated droplets. The applications of agarose droplets will also be discussed. In the last part of the chapter, the encapsulation of yeast cells in agarose droplets is presented.

5.1 Introduction

The elasticity of the microenvironment on cellular growth has a significant impact [118]. For example, elastic moduli of brain tissues (0.1-1 KPa) is different from the elastic moduli of bone tissues (1.5×10^7) [119]. Hence *in vitro* culture, some cells need a solid surface to grow whereas other cells can grow on both solid and liquid environments. Cells can sense the stiffness of the surrounding environment by adhering to and pulling upon it. Because of this, when cells are being transferred from a solid surface to a liquid medium, it takes some time to adapt to the environment which is called lag-phase.

In the past decades, microfluidics create new opportunities for studies of cell biology. It has been used for the generation of well-defined cellular microenvironments by encapsulating cells in droplets or microgels. The encapsulation strategy offers several advantages: the ability to create 3D cellular environments with well controlled dimensions and chemical and mechanical properties. The use of agar droplets allows the encapsulation of cells and culture them in a different elastic environment, which enables the investigation of the role of the mechanical properties of 3D environments on

cell behavior [120].

The primary objective of this chapter is the description of a method for throughput production of agarose droplets and on-chip gelation of the droplets. These generated droplets can be used to encapsulate cells. Agarose has been used in biological research because it is biocompatible, non-adhesive to cells and non-adsorptive to proteins. A primary analysis of the biocompatibility of the agarose droplets has been done by encapsulating yeast cells in it.

5.2 Chip design

The primary function of the device is to generate uniform agarose droplets and provide sufficient time for the on-chip gelation of the generated droplets. A T-junction device of width and height of 100 $\times 100\mu$m has been used for the generation of agarose droplets. The droplet generation principle at the T-junction has been discussed in chapter 2. The required gelation time of agarose depends on the type of agarose, the concentration of the solution, the volume of the solution and temperature of the environment [121]. The gelation time plays a significant role in the chip design. The length of the droplet phase (agarose solution) carrying channel from inlet to the T-junction should be as short as possible to prevent gelation of the agarose solution. After the generation of the agarose droplets, the droplets need time for gelation. As mentioned previously, the gelation of agarose depends on the concentration of the solution. The higher the concentration the less time it requires to solidify considering all other factors being constant. A short microchannel followed by a T-junction should be sufficient to create and solidify high concentrated agarose droplets. However, a high concentrated solution cannot be fed through a narrow channel due to the electroviscous effect [122]. A 1 wt.% agarose solution in DI water is capable to flow though the narrow channel and can encapsulate cells when droplets are generated. Therefore, a long channel preceded by a T-junction has been used to provide sufficient time for gelation and to store a large amount of droplets. A meander shape channel is used to minimize the size of the chip (Fig.5.1). The chosen material for fabricating the chip is PDMS. The advantage and disadvantage of a PDMS channel have been discussed in chapter 3 and 4 in details. The fabricated PDMS channel was bonded on a glass slide to seal the channel.

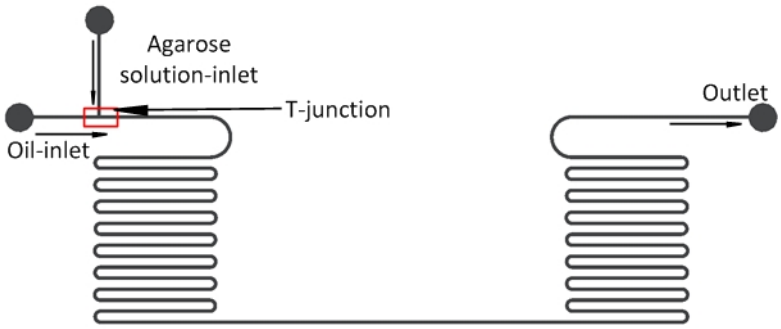

Figure 5.1: Schematic diagram of agar droplets generation chip.

5.3 Materials

For the fabrication of the device, the same materials and processing steps were applied as described in detail in chapters 3 and 4. As described in chapter 4, droplets generation requires a continuous phase and a droplet phase liquid. Mineral oil of viscosity 30-60 mPa.s (20°C) with surfactant (Span-80) was used as the continuous phase and was purchased from Sigma Aldrich, USA. An ultra-low gelling temperature agarose solution was used as the droplet phase. Agarose with gelling temperature in the range of 26-30° was also obtained from Sigma Aldrich, USA. A 1 wt.% agarose solution was prepared by dissolving 10.3 mg of powder agarose in 10 ml of DI water and then heated on a hotplate stirrer to 65° until the agarose dissolved completely. Long time exposure to a high temperature of agar solutions can lower the gel strength. The effect is accelerated by decreasing pH. Therefore, during the experiment, it was avoided to expose agar solutions to high temperatures and maintain the pH between 6 to 7. Saccharomyces cerevisiae (yeast) cells were encapsulated in agarose droplets in a microchannel. Yeast was obtained from a local supermarket, and then it was cultured in the laboratory in YPD (Carl Roth, Germany) medium at 32°C on a hot plate for 24 hours. Yeast cells were stained with acridine orange; cells were washed with phosphate buffered saline (PBS) before staining. Both chemicals were obtained from Carl Roth, Germany.

5.4 Generation of agarose droplets

A microfluidic channel of width and height 100×100 μm, respectively, were used to generate agarose droplets. The chip comprised a T-junction for the generation of droplets, which was followed by a long channel to store them.

The chip was placed on the inverted routine microscope stage (TS100 Nikon, Japan) to monitor droplets generation and gelation. A camera (Nikon D5100) was fixed with the microscope to analyze and take photographs of the agarose droplets. Since droplets generation requires a continuous flow of both liquid, syringe pumps (neMESYS low pressure) were used to feed the liquid to the microchannel inlets. Two syringes of volume 1 ml, one for continuous phase and one for droplets phase, were purchased from Braun, Germany. The agarose solution with concentrations of 1 wt.% was supplied to the droplet phase inlet of the microfluidic device using a microtube that carries agarose solution from a syringe to the chip inlet. As previously mentioned the gelling temperature of the agarose is 26-30°C. At room temperature the agar formed gel, and gel cannot be injected into the narrow microchannel. Therefore, it is necessary to maintain the temperature of the agarose solution above 30°C before injecting the solution into the microchannel. Two separate heating coils were developed, one for a syringe and one for a microtube. A 1 ml syringe (Braun, Germany) was warped by a 20cm long coil of resistance 62.4 Ω/meter. The relation of the coil temperature, applied voltage, and current will be discussed in detail in the result section. The mineral oil with 1 wt.% span 80 was supplied to another inlet of the microfluidic device using an independently controlled syringe pump. At the T-junction, the stream of the agarose solution broke up and released droplets. The gelation of agarose took place in the long channel. The microfluidic chip was kept on a cold plate at 10°C to ensure complete gelation of the agarose droplets. A schematic diagram of the agarose droplets generation setup is depicted in Fig.5.2

Cell encapsulation

Yeast cells were encapsulated in the agarose droplets to investigate the cell encapsulation rate and the behavior of cells in the droplets. Before encapsulating yeast in agarose droplets, cells were stained with fluorescence dye named acridine orange for better visualization. Acridine orange is permeable to cell membrane; therefore, it can stain both a live and dead cell. It can combine with both DNA and RNA by intercalation or electrostatic attraction respectively. The acridine orange-DNA complex is excited at 480 nm and emits at 510 nm, and RNA complex is excited at 440-470 nm and emits at 510 nm [123]. The excitation light from 440-480 nm can be used to detect the cells in droplets. To stain yeast, 0.01% (v/v) acridine orange stock solution was prepared in PBS. 2 ml of the cultured yeast solution was centrifuged at 1000 rpm at room temperature for 3 min and washed with PBS buffer. Then 200 μl stock solution was added to the washed yeast and incubated at 37° for 5 min. Afterward, the incubated yeast centrifuged at

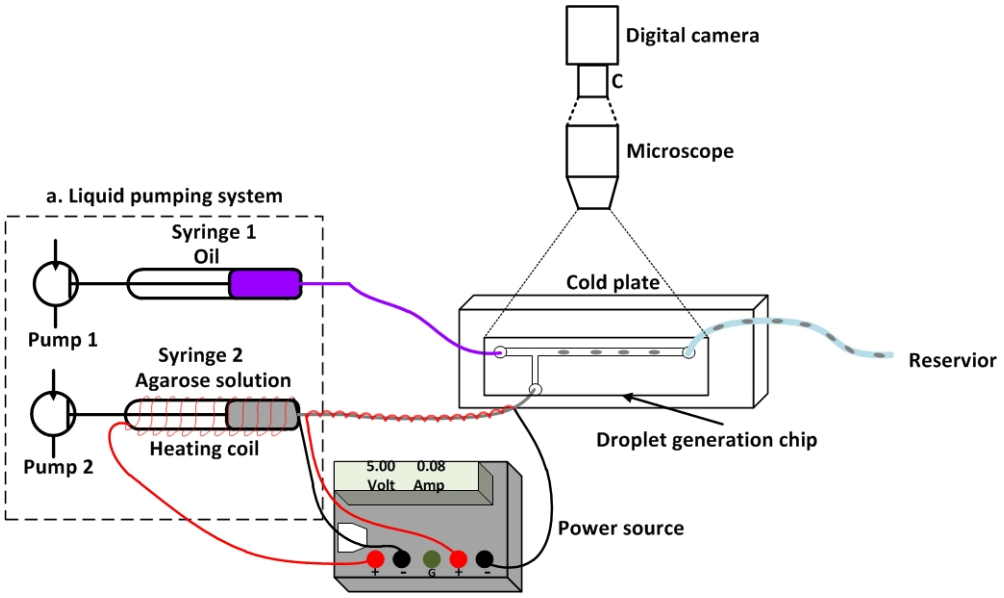

Figure 5.2: Schematic diagram of agar droplets generation setup.

1000 rpm for 3 min and washed with PBS buffer. Finally, the washed cells were suspended in 1 ml previously prepared 1 wt% agarose solution, which was used as the droplets phase for the generation of droplets. The chips were placed on the fluorescent microscope stage (Nikon, Japan) such that the field of view was the same for all the measurements. The agarose droplets encapsulated stained yeast cells in it were generated using the same setup and chip as used to produce agarose droplets in the previous section. A reference image was taken at t=0 time, immediately after the droplets were generated. A sequence of images was taken during the storage. Fluorescent emission of the acridine orange was filtered out using a bandpass filter and pictures were taken using a camera (Nikon D5100) mounted on the microscope.

5.5 Results and discussion

5.5.1 Heating coil

As described earlier, the aqueous agarose solution forms gel at a temperature below 26°C. Therefore, before generation of the droplets in the microchannel, it is necessary to maintain the solution temperature above 26°C. Heating coils have been developed for the agarose solution containing syringe and for the microtube. When current passes through a conductor, there is a generation of heat due to the ohmic loss of the conductor.

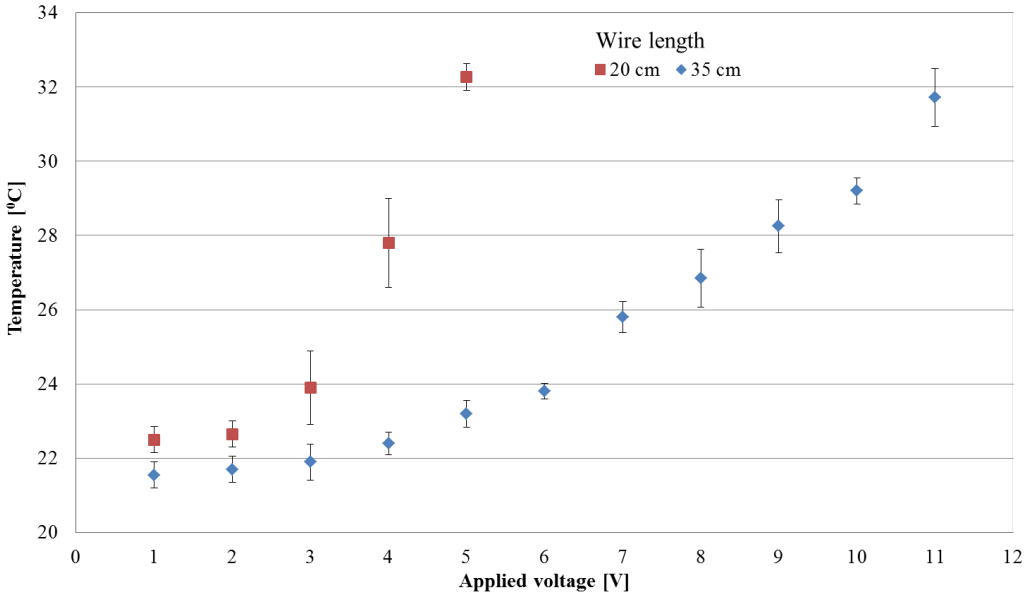

Figure 5.3: The change of temperature of the coil with the applied potential (DC).

A 20 cm long wire was wrapped around the 1ml plastic syringe and a voltage (DC) was applied across the coil. During the experiment, the applied voltage slowly increased, and the induced heat was measured. At the applied voltage 5 volt (DC) for the 20 cm long wire, the induced temperature is above 30°C to keep the agarose solution in liquid form. Each data point presented in Fig.5.3 is the average value of five successive measurements. The required time for the generation of droplets is approximately 30 min.; therefore, a sequence of measurements was conducted for each data point for 60 mins.

A microtube carries the agarose solution from the syringe to the microchip. While the solution is transported through the tube, due to the very small volume of fluid the temperature drops and the agarose solution formed gel. Therefore, a second coil was developed for heating the microtube and to get the surrounding temperature above 30°C. A 35 cm long wire was used make the coil. The result has been presented in Fig.5.3. 10 volt (DC) was applied to get the temperature above 30°C around the microtube.

5.5.2 Agarose droplets dimension

The main advantages of droplet microfluidics is its reproducibility. When droplets are used to culture cells in it, the size of the cell containing droplets is crucial. Size and shape of the generated droplets in the microchannel has been studied (Fig.5.4). It has been described in detail in chapter 2 that the size and shape of the generated droplets at T-junction depends on the channel dimension, flow rate, and the viscosity of the used liquid. Figure 5.4(a) illustrates how the size of the droplets changes with the flow rate ration of droplet and continuous phase. The size of the agarose droplets decreases with the decrease of the flow ratio decrease and the inter-droplets distance increase. Each data point presented in Fig.5.4 is the average value of 100 agarose droplets generated in a microchannel. For the droplets dimension studies, mineral oil with 1 wt.% span 80 was used a continuous phase, and agarose solution with concentrations of 1 wt.% was used as a droplet phase. An experiment has been conducted to generate droplets by changing the concentration of the agarose solution. If the solution concentration is lower than 1 wt.%, the agarose droplets are not solid enough, and it breaks while taking out of the chip. The necessity of agarose droplets out of the chip will be discussed in the following section. If the concentration is higher than 1 wt.%, it is not possible to feed the solution into the microchannel. Because of the electroviscous effect, a high concentrated solution requires higher external pressure (in pressure-driven flow) to flow through a narrow channel. The bonding between the microtube (carries liquid from syringe to the inlet of the channel) and the channel-inlet is not strong enough to survive such a high pressure, hence generation of droplets is not possible. In this study, a larger size of the droplets has been generated to encapsulate yeast cells. In a large droplet, the amount of nutrient to feed the cells is higher; therefore, cells can survive for an extended period.

5.5.3 Agarose droplets out of the chip

One of the important applications of agarose droplets is culturing cells in the droplets. Many cells require oxygen to survive and grow. The generated agarose droplets contain a limited amount of nutrients. After a certain period, additional nutrients are required to grow the cells in droplets. Once the agarose droplets are gelified additional nutrients can be added only by the diffusion process. Thus adding nutrients on-chip is a very challenging task. Taking agarose droplets out of the chip and store them in nutrients rich medium can solve the problem.

An experiment was conducted, where droplets were taken out of the chip

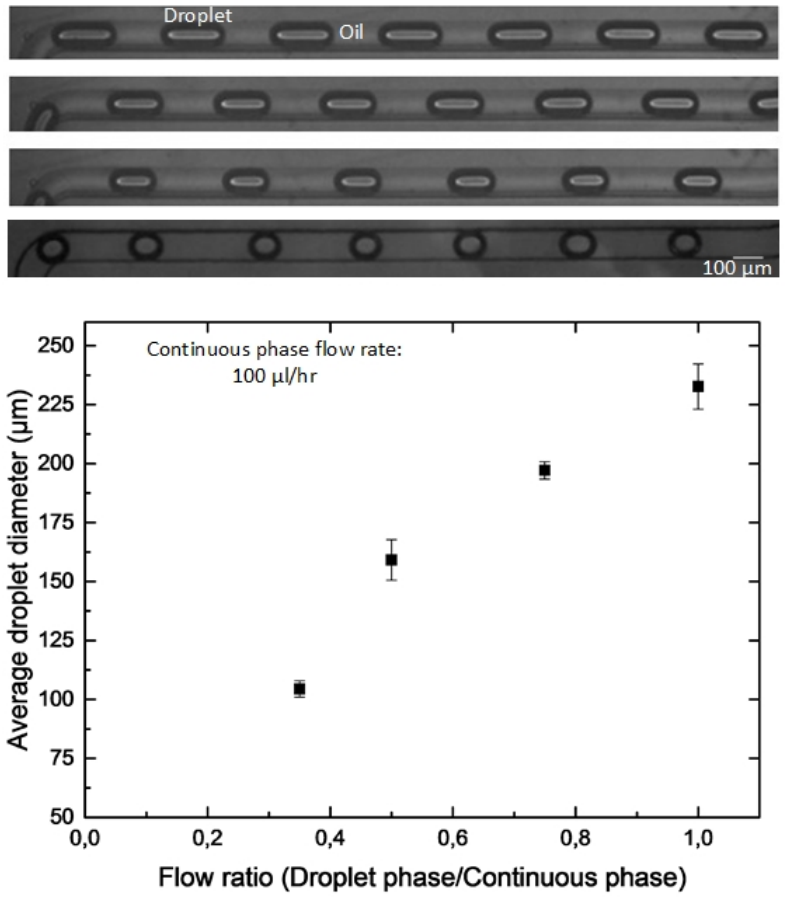

Figure 5.4: Variation of size of the agarose droplets with respect to the flow rate ration of droplet phase and continuous phase. Mineral oil with 1 wt.% span 80 was used a continuous phase and agarose solution with concentrations of 1 wt.% was used as a droplet phase.

before complete gelification; many of the droplets started to merge with each other due to the lower gel strength. To avoid the coalescence of droplets over a period of times, it was important to achieve sufficient pre-gelation of droplets in the downstream channel of the microfluidic device. Complete droplet gelation was carried out by placing the microfluidic chip, containing libraries of droplets, in the refrigerator at 4° C for at least 2 hours. Afterwards, the chip was kept at room temperature for an hour and then droplets were taken out of the chip for further examination. Figure 5.5 depicts agarose droplets out of the chip. The droplets were kept in the oil for several hours and no change of shape of the droplets was observed.

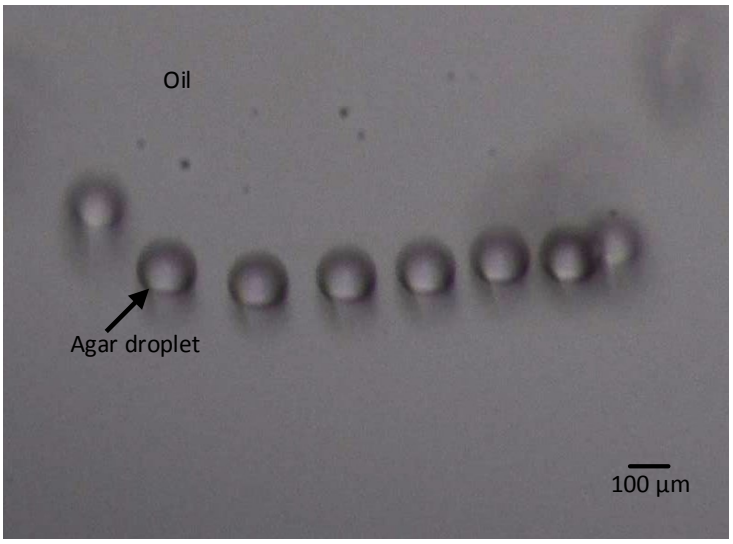

Figure 5.5: Optical microscopy image of agarose microgel droplets. The droplets were taken out of the microfluidic chip after complete gelation.

5.5.4 Encapsulation of cells in agarose droplets

Yeast (saccharomyces cerevisiae) cells haven been encapsulated in agarose droplets. The dimension of yeast cell varies with species. The dimension of the yeast used in this experiment is 3 - 4 μm in diameter. Stained yeast cells with acridine orange were encapsulated in the agarose droplets for better visualization. The stained cells were diluted in agarose solution and then the cell containing agarose solution was used to generate droplets. Cell encapsulation efficiency in agarose droplets can be explained using the Poisson distribution equation, which has been explained in chapter 4.

Yeast can not survive in an environment of more than 35°C for an extended period. Thus maintaining the right temperature is a very crucial. However, to prevent the agarose solution to become gelified, the temperature should be more than 30°C. The temperature of the yeast diluted agarose solution was precisely maintained in between 30°C to 33°C during the generation of droplets. The cells encapsulated droplets were generated using the same experimental setup that was used for generating agarose droplets.

After encapsulating yeast in agarose droplets, droplets were stored on-chip for 4 days. The photograph of the encapsulated yeast in droplets is presented in Fig.5.6. During the storage time, it has been observed that some of the stored cells have tendency to go out of the droplet. Since there is no gravitational force in a droplet, cells moves around in the liquid droplets. At

the time of encapsulation some cells are already at the edge of droplets, during the storage they break the oil/water barrier and enter into the surrounding oil, although the percentage is very low. The amount of cells where this takes place is less then 3%, which was determined by counting cells using a microscope.

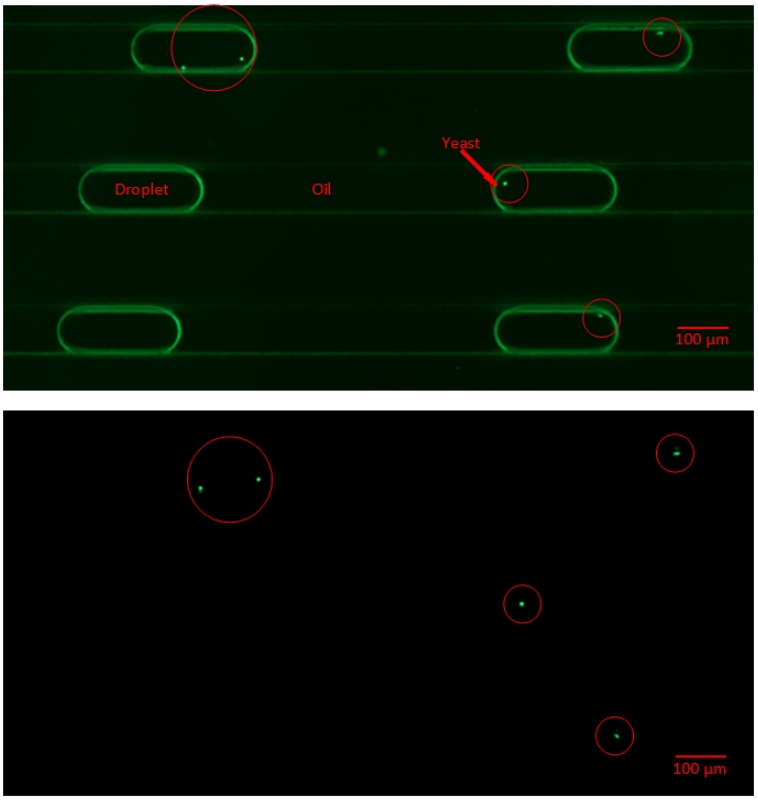

Figure 5.6: Cells encapsulated in agarose droplets.

5.6 Conclusions

We have realized a high throughput agarose droplets generation chip, where agarose droplets can be generated and stored in the same chip. A peripheral setup was realized to maintain the specific temperature to prevent the gelification of the agarose solution before entering into the chip. By changing the flow rate of the continuous and droplet phase it is possible to generate different size of droplets. The main application of the agarose droplets is cell storage and culturing. Yeast cells have been successfully encapsulated in agarose droplets. Encapsulation of yeast is one step forward towards the encapsulation of mammalian cells in agarose droplets. This method has potential to be used in storage and culturing of mammalian cells.

Chapter 6

Droplets sorting and merging

This chapter is focused on the design of a microfluidic chip where droplets of different liquids and sizes can be generated and merged independent of their size and inter-droplet separation. The application of on-chip droplets sorting and merging is presented in the introduction section of the chapter. The state of art of droplet sorting and merging methods has also been discussed in the introduction. A design of a microfluidic chip where droplets with cells can be generated and stored for several hours is presented in the chip design section. A method to generate droplets with fresh nutrients to merge with the stored droplets to supply nutrients to the cells is also discussed in the design section. Finally, realization and characterization of the designed chip are discussed. The result presented in this chapter has been published in [124].

6.1 Introduction

Droplet microfluidics has drawn attention from biological and chemical communities by offering a nano-environment for culturing cells and performing a chemical reaction, high-throughput capabilities and reducing experimental cost enormously. For example, in the macro scale, drug screening and gene expression analysis are expensive because of the use of expensive and limited available reagents. Droplet microfluidics reduces the use of reagents by 1000 times or more compared to the macro scale. Many chemical and biological reactions and cell analysis require the addition of reagents to the empirical droplets as well as sorting of droplets those are of interest.

Precise merging and mixing of droplets is of crucial importance in droplet-based systems where biological and chemical processes take place. Under normal operating conditions the mixing of fluids in micro-channels is diffi-

cult due to the laminar flow regime, which has been explained in chapter 2 in detail. Mixing is mostly determined by diffusion. Most of the studies found in literature about droplets merging and mixing are based on the inter-droplet separation or droplet size [6, 125]. In addition, many research works are dealing with integrated active elements such as microvalve or electrodes for droplets merging [126, 127]. Due to the required high voltage, active merging is not suitable for cell based assays. A method has been reported in literature where merging or mixing of different reagents to the micro-droplets was realized by injecting liquids at the time of droplets generation [128]. This method cannot be used in on-chip cell culturing and viability test of cultured cells in droplets. In on-chip cell culturing, droplets need to be stored in a micro-channel to grow cells prior to adding reagents. On-chip droplets storage significantly reduces the complexity of the hands-on inter-device operation and the sample processing time. The necessity and applications of on-chip droplets storage have been discussed in chapter 4. During the experiments, it has been found that the growth rate of the cells in the droplets decreased in time due to the decrease of available nutrients. Merging droplets with fresh nutrients to the cell containing droplets can solve this problem.

In this work, a microfluidic chip has been designed and realized where droplets with encapsulated cells can be generated from one side of the chip and stored for several hours. From the other side of the channel droplets with fresh nutrients can be generated and merged with the stored droplets to supply required nutrients.

6.2 Chip design

The aim of the droplets merging chip is to add additional nutrients/reagents to droplets in which cells have been stored for several hours. In some cases, droplets sorting is necessary before addition of reagents; therefore, a sorting area is required. The designed chip consists of a T-junction followed by a long channel, where nutrients/reagents containing droplets can be generated and stored, a droplet sorting area, a droplet merging junction, and a storage chamber where merged droplets can be stored. A schematic diagram of the designed chip is depicted in Fig. 6.1. A T-junction is used for generation of droplets and encapsulation of cells in it (left side of the chip). A 27 cm long meander shape channel serves as a storage chamber for droplets.

During the on-chip droplets storage, the neighboring droplets come closer with time and eventually merge, the details was discussed in chapter 4. The oxygen and hydrogen have a high difference in electronegativity, resulting in the water molecule polarized. Hydrogen can form 'hydrogen bond', which

is capable of creating a very strong intermolecular force and it gives the water molecule cohesive force. Because of this strong force, two droplets attract each other and the oil phase starts to drain out. There are two methods to prevent merging droplets during their storage (i) use a sufficient amount of surfactant with the continuous phase liquid (ii) increase the inter-droplets distance. A large inter-droplets distance is not very practical since the number of stored droplets will reduce significantly. A high percentage of surfactant with the continuous phase liquid will prevent the merging of the stored droplets with the fresh nutrients droplets when it is necessary. A small amount of surfactant with the continuous phase liquid was used and the inter-droplets distance was the same as the diameter of the droplets to prevent the merging of droplets during storage. An extra outlet (outlet 2) allows sorting out the desired droplets by applying external suction. The sorted droplets are driven to the merging area where reagents can be added for further analysis and can be stored for a couple of hours. The selection and the moving speed of the droplets from storage 1 and storage 2 can be controlled independently by different combinations of the pump activity at junction 1 and junction 2, and activating (blocking and unblocking) the outlets 1 and 2. For the mixing of the liquids of the merged droplets, the diffusion area between two approaching droplets has been considered. Due to the absence of turbulent flow in a microchannel mixing of liquids only takes place by means of diffusion. The diffusion of two liquids increases with the increase of the interfacial area between them. Therefore, the droplets were merged in such a way that they hit each other head-to-head and entered to the merged channel in parallel. In such a way, they get more interfacial area and the diffusion rate increase. Additionally, a serpentine channel was used to enhance the mixing of liquids in the merged droplets. The serpentine channel induces vortical motion in liquids and increases pressure on droplets, which leads to faster mixing [129].

6.3 Materials

For the fabrication of the device, the same materials and processing steps were applied as described in chapters 3 and 4. For the generation of droplets mineral oil of viscosity 30-60 mPa.s (20°C) with surfactant (Span-80) was used as the continuous phase and was purchased from Sigma Aldrich, USA. The percentage of surfactant in the oil was 0.005%. *E. coli* was stored in droplets and lysogeny Broth (LB) medium was used as the culturing medium. The process of cell preparation and the encapsulation principle has been explained in chapter 4 and 5. To visualize the mixing of liquid at the merging

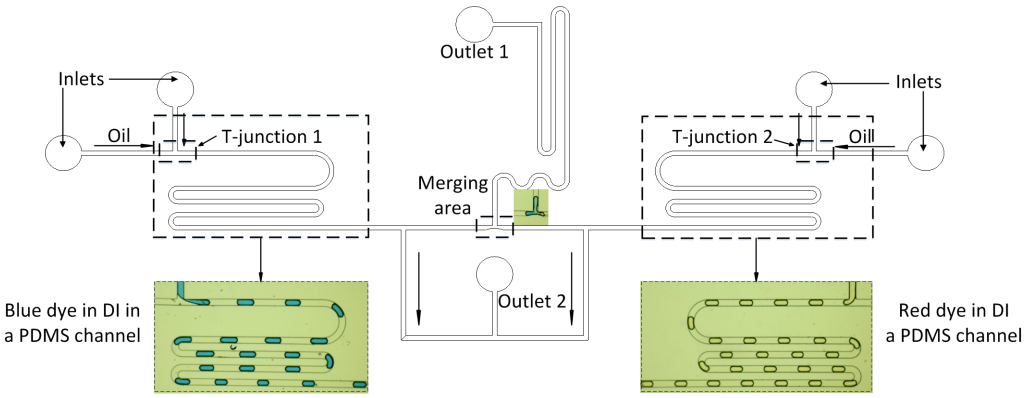

Figure 6.1: Schematic diagram of the designed chip; Blue dye containing droplets at the left side of the channel (storage1); Red dye containing droplets at the right side of the channel (storage 2); the droplets merging area is in the middle of the chip.

and mixing area, indigo carmine (blue) and rhodamine B (red) droplets were merged and mixed in the micro chip. 1 % (v/v) aqueous solution of indigo carmine droplets were generated at T-junction 1 and 1 % (v/v) aqueous solution of rhodamine B droplets were generated at the T-junction 2; afterward, they were merged and mixed at the merging junction. Both chemicals were purchased from Sigma Aldrich, Germany. In the droplets sorting experiment, fluorescent beads (Sigma Aldrich, Germany) of 10 μm diameter has been used for better visualization of the particles. The excitation and emission wavelength of the fluorescent beads are 553 nm and 627 nm, respectively.

6.4 Experimental setup

Generation of droplets requires a continuous flow of both liquids, Syringe pumps (neMESYS low pressure) were used to feed the liquid to the microchannel inlets. Syringes of 1 ml volume (Braun, Germany) were used to store both droplets and continuous phase. Microtubes of 250 μm inner diameter were used to carry the liquid from syringe to the inlet of the chip. The droplet generation chip was fixed on a fluorescent microscope stage (Nikon, Japan) to monitor the droplets. Fluorescent images of the beads were taken using a camera mounted on the microscope.

6.5 Results and discussion

As described earlier, the diffusion of molecules between two liquids increases with the interfacial area in a microchannel. An experiment has been conducted where two droplets were merged tail-to-head Fig.6.2. Hence they entered in the merging channel in series obtaining a smaller interfacial area. In another experiment, droplets were merged head-to-head; therefore, after merging they entered into the channel in parallel and got the longer interfacial area. To visualize the mixing of liquids in a droplet, a colorimetric method was used. In head-to-tail merging, the droplets do not mix properly even after passing the serpentine channel area. Whereas, the head-to-head merged droplets mixed entirely in the serpentine area of the channel. Photograph (Fig.6.2) depicts that the diffusion area improves the mixing of different liquids in droplets.

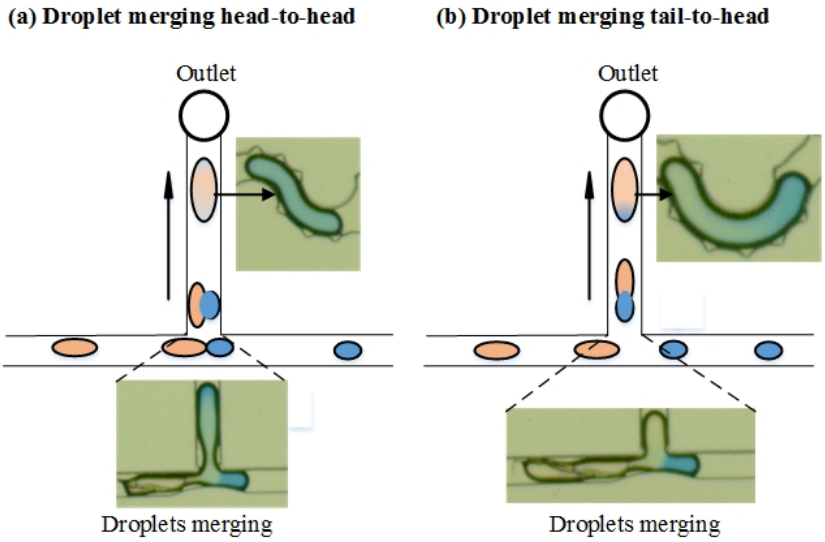

Figure 6.2: Droplets merging condition; dropets merged head-to-head, where they get more interfacial area (a); droplet merged tail-to-head, where they get less intefacial area (b).

The droplets merging chip includes a sorting area where the desired droplets have been sorted out from the randomly generated droplets. At the time of generation, the size of droplets and the number of encapsulated particles can be varied due to a slight variation of the flow rate and the random encapsulation methods. Therefore, sorting of droplets is crucial for the optimization of reagents use and to save the experimental time. Fluorescent microbeads have been encapsulated in the droplets and sorted at the sorting

area of the chip.

The chip can be represented by its equivalent electrical circuit to understand the liquid flow profile in the channel. Circuit analysis helps to predict pressure-driven laminar flow in a microchannel and to design complex microfluidic networks in advance. Consider, R_{11}, R_{12}, and R_{13} represent analogous resistance of the storage 1, resistance of the waste outlet, and resistance of the channel distance between merge and sorting area, respectively (Fig.6.3). For R_{21}, R_{22}, and R_{23} same analogy is applicable for storage 2 as for storage 1. R_{31} represents the resistance of the storage channel for the merged droplets. i_{11}, i_{12}, i_{13}, i_{21}, i_{22}, i_{23}, and i_{31} are analogies to the velocity of the droplets of the corresponding channel as shown in Fig.6.3.

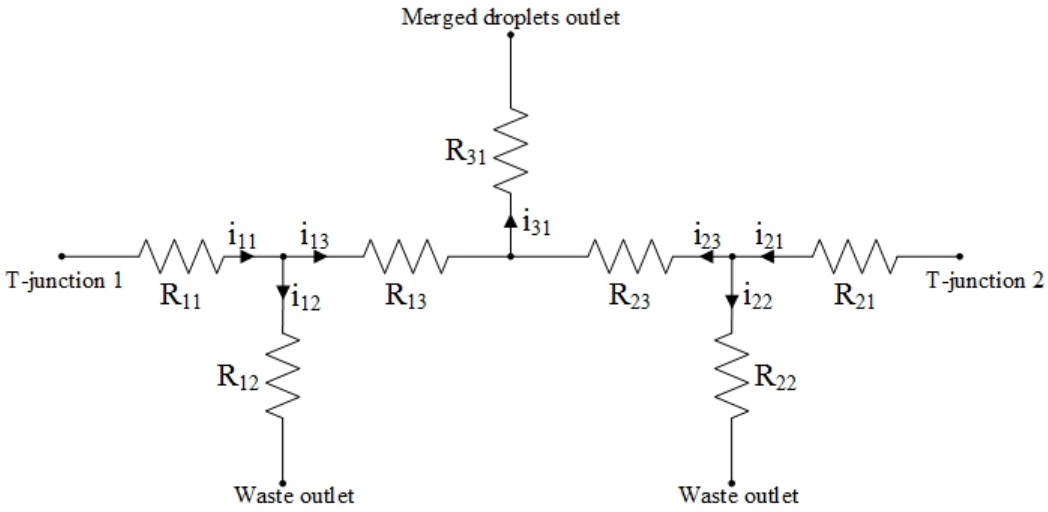

Figure 6.3: Electrical equivalent circuit of the droplets merging chip of Fig.6.1.

By applying the Kirchhoff laws we can write,

$$i_{11} = i_{12} + i_{13} \tag{6.1}$$

$$i_{21} = i_{22} + i_{23} \tag{6.2}$$

$$i_{31} = i_{13} + i_{23} \tag{6.3}$$

If we take into consideration that R_{11} and R_{21} is very large compared to the other hydrodynamic resistance present in the circuit. From the Kirchhoff's circuit law, we can say that the resistance at the waste channel is smaller than the combined resistance of the merged and sorting channel. Therefore, generated droplets coming from the T-junction 1 tend to pass

through the waste channel. The sorting of droplets has been done at this junction. Droplets of interest are being passed through the merging channel by blocking the waste channel. Other droplets are being passed through the waste channel. The same conditions are applicable for the T-junction 2.

Figure 6.4 presents the unsorted droplets in the storage 1 and sorted droplets in the storage area for merged droplets. In this chip, no sensor has been integrated. Therefore, droplets were observed through a camera attached to the microscope and sorted out by controlling the fluid pumps. The efficiency of the sorting method is low due to the manual control of the pumps.

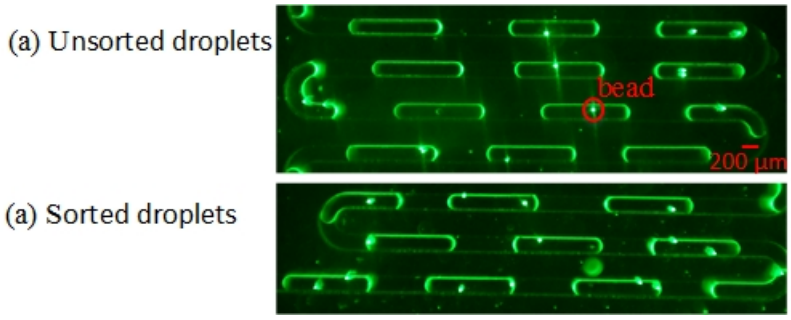

Figure 6.4: Fluorescent beads are encapsulated in droplets in a random way. Before sorting of droplets (a); after sorting of droplets (b).

The aim of the droplets merging chip is to add additional nutrients/reagents to the stored cells encapsulated in droplets. *E. coli* has been encapsulated in droplets, where droplet phase is *E. coli* diluted LB medium, and stored for 2 hours. As the time passes, the population of the cells increases and the amount of nutrients decreases. To grow the stored cells in droplets it is necessary to supply them with sufficient nutrients. It has been found that after few generations' growth of the *E. coli*, it suffers from lack of nutrients, which can be solved by adding extra nutrients droplets to the cells contain droplets Fig.6.5.

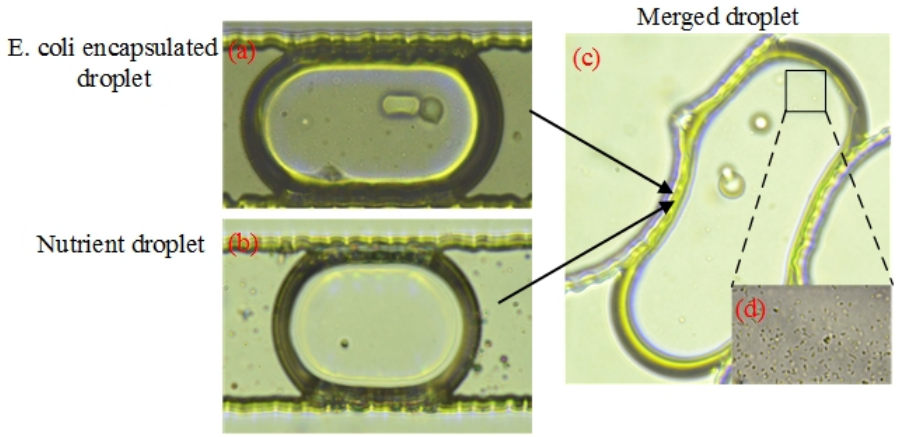

Figure 6.5: The droplet in (a) was generated from one side of the chip and has encapsulated *E-coli* bacteria in Lysogeny Broth (LB); the droplet in (b) was generated from the other side of the chip and contains LB medium; in (c), the two droplets have been merged together, providing additional nutrients to the bacteria; magnified view of the encapsulated cells in droplet (d).

6.6 Conclusion

A microchip has been designed and realized for on-chip manipulation of droplets. The functionality of the chip was proven by storing *E. coli* on-chip and later on by adding nutrients to them. Droplet encapsulated microbeads has been sorted out in the sorting area. The droplets sorting efficiency is about 60% due to the manual control. However, automatization of the whole system would increase the sorting efficiency drastically. The proposed method serves the basic needs for biological and chemical processing and has great potential, therefore. By applying image processing, the system has the potential for fully automation.

Chapter 7

Air-bubble as a gas reservoir

A new method of on-chip droplets storage in a Parylene AF4 coated PDMS channel was introduced in chapter 4. However, mammalian cells can not be stored in an AF4 coated channel for an extended period due to the lack of oxygen and carbon dioxide. A method to supply oxygen to the stored droplets in a microchannel is presented in this chapter. The introduction focuses on the necessity and the state of art of the on-chip oxygen reservoir. The chip design and realization are discussed in the latter part of the chapter. Finally, MDCK cells were stored in the droplets, and their survival in the presence of air-bubbles is discussed. Parts of this chapter have been published in [130].

7.1 Introduction

Oxygen (O_2) is an important component for many biological processes. Biological processes, such as cell division [131], enzymatic reaction [132], and the polymerase chain reaction (PCR) [133] are accomplished *in vitro*. Droplet microfluidics has been introduced to the field of biology to make the *in vitro* system more reliable, highly sensitive, and less complex. The fundamental of droplet microfluidics was discussed in chapter 2. A droplet is considered as a test tube, where biological and chemical processes can be carried out in an isolated environment, resulting in significant reductions of instrumental footprints. Droplet storage is required to conduct biological processes such as cell culturing, enzymatic reaction, and protein crystallization. A microfluidic chip made of a biocompatible material and impermeable to liquid is needed to store droplets on-chip. Microfluidic chips that are used to store droplets are fabricated using glass, Parylene, polymethylmethacrylate (PMMA), and Teflon capillary [134, 135]. However, oxygen cannot penetrate into the channel limiting droplets to be applied in biological process where

maintaining oxygen level is crucial. Different approaches were introduced to increase the oxygen levels in a microchannel. A method has been reported in literature [136], where mammalian cells were grown in a micro-chamber and the necessary gas was supplied from an adjacent chamber. The two chambers are separated by a porous membrane, which allows gas supply from one chamber to another. Another way is to use porous substrate materials like PDMS through which the gas can diffuse to the microfluidic channel. In cell cultures, where the temperature is held at 37°C, the aqueous droplets can quickly evaporate and pass through the PDMS, resulting in dramatically increased osmolality of the liquid [134]. Because of this, cells are often cultured in the chips under continuous flow. The continuous flow of liquid induces shear stress and eventually affects the cell growth [137]. An existing technique to provide oxygen in microfluidic channels is based on thin oxygen permeable PDMS layers separating aqueous channels from oxygen feeding gas channels [95]. Devices using this technique consist of multiple layers making them hard to realize because of the fragility of the thin PDMS membrane and the need for multiple lithography steps. Another existing technique to supply oxygen to the droplets is based on an off-chip (in a reservoir) droplet storage method [94, 138]. This method does not allow continuous monitoring of cells growth because for the analysis the droplets have to be transferred back into the microfluidic chip. Therefore, a simple system is desired where droplets can be generated and stored with the facility of required oxygen supply in a single microchannel. The atmosphere comprises 20.95% of oxygen which is the natural source of oxygen for the living organism. The traditional methods of the *in vitro* cells culture are a petri dish, flask, and microplate, where cells receive oxygen from the air. The similar approach can be applied to the droplets in more defined and controlled way. To achieve this, air-bubbles can be placed in a microchannel in series with the aqueous-droplets and used as a source of oxygen, and carbon dioxide. However, bubbles in a hydrophobic microchannel, necessary to generate droplets, cause problems by adhering to the channel surface hindering the flow of aqueous droplets through the channel. This incident can be prevented by using another liquid between the channel surface and the bubbles, which is immiscible with both air and water. This liquid layer should be lipophilic in nature and biocompatible. Fluorocarbon oil is a suitable material in this case, which also allows diffusion of oxygen and carbon dioxide through the oil [139]. To prevent the interaction between the bubbles and the channel surface, the bubbles should be placed in the middle of the channel that can be done by using a flow-focusing or W-junction (Fig.7.2). According to Henry's law at atmospheric pressure and room temperature (25°C), the amount of dissolved oxygen in water is 8.9 μl/liter. This amount increases with the system pressure and de-

creases with temperature, hence, by increasing the pressure the oxygen level in the culture liquid medium can be increased, literature indicates that high oxygen pressure decreases cells survival rate [140] and the temperature cannot be decreased because 37°C is the required temperature for cells to grow. In the current study, we demonstrate a new approach for regulation oxygen level in a microfluidic chip. In contrast to previous methods, air bubbles were placed close the aqueous droplets, separated by fluorinated oil, in the same microfluidic channel to modulate the oxygen level by means of diffusion. Initial investigations on air-bubbles as oxygen reservoir in microfluidic channels were presented in [130]. The oxygen level in the aqueous-droplets was monitored by a redox indicator methylene blue. Madin-Darby Canine Kidney (MDCK) cells were encapsulated and stored in the droplets with the presence of air bubbles.

7.2 Theory

Gas bubbles transport through a hydrophobic microfluidic channel

Transporting gas-bubbles through a hydrophobic microchannel should be precisely taken care of. Since the uncontrolled presence of gas bubbles can introduce significant problems in a microfluidic system by disturbing and eventually blocking the flow of liquid. When liquid and gas, are present in a microchannel, the interactions on the boundaries between gas, liquid, and solid introduce nonlinearity and instability [141, 142]. When both liquid and gas are flowing, the situation becomes rather complex because of dynamic contact angle. However, this phenomenon has been explained both in theoretically and practically in literature [141–144]. During the chip design this event was thoroughly studied and investigated. At first, the behavior of a static bubble in a polygonal capillary is discussed. The shape of the static bubble in a polygonal capillary, composed of N sides, depends on N and the contact angle. When $\theta < \pi/N$, liquid fills the channel wedges, and when $\theta > \pi/N$, gas fills the entire channel cross-section [145, 146]. In this study, we have square microchannels, hence N is 4 (Fig.7.1b), and the static contact angle of Parylene AF4 coated PDMS is about 120°. Therefore, the second case is applicable in this system. The system becomes more complex when motion is induced, which is indeed the case in this study.

In a two-phase flow system, gas and water, the contact angle in a microchannel is defined with respect to the liquids; the receding contact angle is at the front of the bubble and the advancing contact angle is at the rear

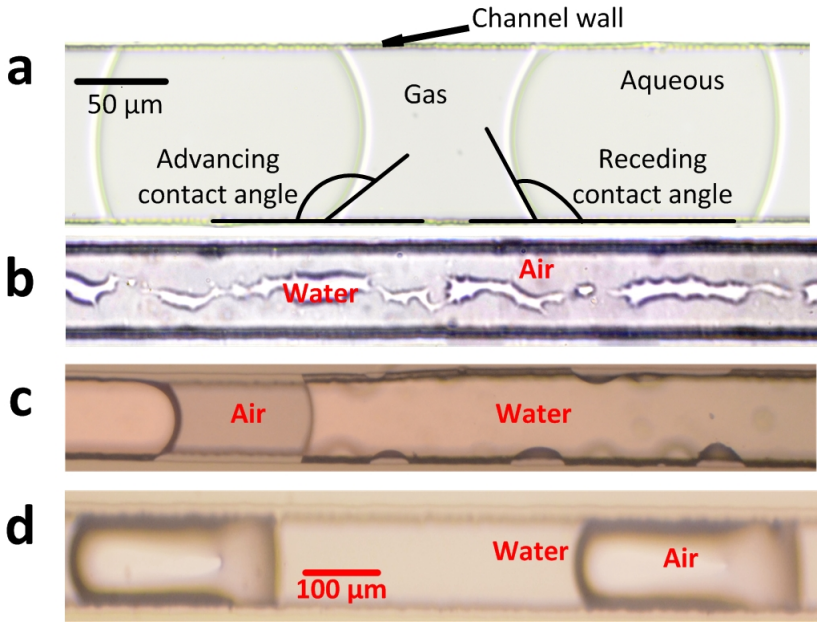

Figure 7.1: Bubbles in a hydrophobic microchannel. The photograph was taken at a resting position of bubbles and aqueous flow (a); Air and water flow in micro channel. The flow rate of air is 10 times higher than the flow rate of water. The air hindering the flow pattern of the liquid (b); the flow rate of water phase is 5 times higher than the flow rate of air. Bubbles has been generated in between aqueous phase, however, small satellite bubbles adhering to the channel surface hindering the flow of aqueous phase. Small bubbles were gather over time until a big bubble come and take them away (c); The flow rate of both gas and aqueous phase are equal, the bubbles has been generated in aqueous phase, as they travel through the hydrophobic microchannel bubbles changes its shape (d).

of the bubble. Figure 7.1a presents receding and advancing contact angle of a droplet in a square microchannel. The hydrophobic flow of gas/water is quite unsteady. When both gas and water flow through the channel, where the input flow rate of water is higher than the input flow rate of gas, small satellite bubbles generate and adhere to the channel walls due to the low surface energy. The small bubbles are driven away from the channel in two different ways- after many bubbles merge together form a bubble occupying the entire channel and is pushed by the liquid flow, or a big bubble comes and driven them away, which is demonstrated in Fig.7.1c. In the case where both water and gas flow rate is equal, bubbles are generated in water. During their flow through the channel, the advancing contact angle increases and the

receding contact angle decreases of the bubbles as velocity increases. Thus, the bubble shape loses symmetry with respect to the direction of the flow, which is depicted in Fig.7.1d. The contact angles are also influenced by the roughness of the solid surface [147]. In this study the used channel roughness effect can be ignored as after fabricating PDMS channels, the channel's surface was coated with Parylene AF4. From the above discussion, it is understood that gas/water flow in microchannel is quite unsteady and cannot be used to generate aqueous-droplets in gas or the other way around. To avoid this difficulty, a three-phase system is introduced, where gas bubbles are surrounded by fluorinated oil that prevents gas to be in contact with the aqueous phase and the channel wall.

7.3 Chip design

The microfluidic platform should allow the controlled creation of gas-bubbles and their unhindered transport through the hydrophobic microchannel. To ensure these requirements, the contact of a gas bubble to the channel surface, and to the aqueous-droplet has to be prevented. To establish these requirements, we need a third liquid which has an affinity to a hydrophobic surface (lipophilic), and also immiscible both with air and aqueous. Oil, a base chemical in droplet microfluidics, satisfies these requirements. To prevent contact of gas-bubble with the channel wall and aqueous droplets, first gas-bubbles are generated in oil by using a W-junction, where gas entered through the middle channel and oil entered through the two side channels, that prevents gas-bubbles to be in contact with the channel surface. These oil-surrounded droplets then brought to a T-junction where aqueous-droplets were inserted in between two gas-bubbles. Therefore, there is no direct contact between the gas-bubbles and aqueous-droplets. In Fig.7.2 a schematic of the microchannel layout is shown which is used in our experiments. By adjusting the flow rates of the W-junction and the T-junction, the formation of the aqueous droplets between gas-bubbles is easily achievable and also the size of the bubbles and droplets can be defined.

7.3.1 Optical setup

An S2000 fiber optic spectrometer (Ocean optics, USA) was used for optical measurements. A tungsten halogen light source of wavelength 200-1100 nm (Ocean optics, USA) is used. For optical measurements, several optical elements were integrated with the transparent polymer (Fig.7.3). The design of the optical components integrated chip is adapted from [148, 149]. The

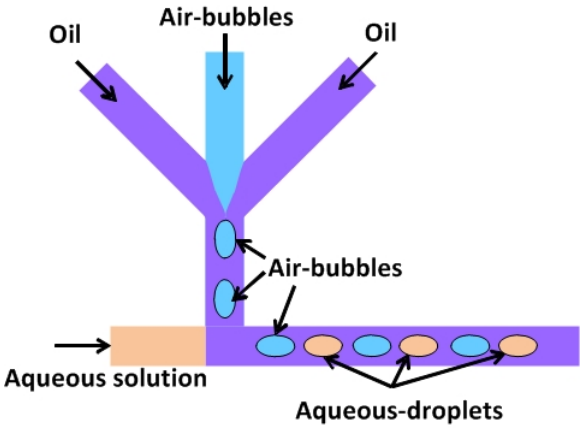

Figure 7.2: Schematic diagram of the designed microchannel consisting of a W-junction for air-bubbles generation and a T-junction for aqueous-droplets generation.

light source was coupled to a multimode optical fiber (Thorlab Inc, USA) and the other end of the optical fiber was inserted and fixed into the microchip. The light was then coupled into the on-chip polymer waveguide and guided by total internal reflection. The light exiting the waveguide is focused by a concave air lens and coupled into the microfluidic channel. The transmitted light from the sample in a microchannel is then collected and focused by another air concave lens to the optical fiber which is coupled to the spectrometer. The spectrometer measures the amount of light and the A/D converter transforms the analog data collected by the spectrometer into digital information that is passed to the software and processed.

7.4 Experimental setup and bubble generation procedure

A schematic of droplets and bubbles generation setup is shown in Fig.7.4. The system consists of a liquid pumping unit that controls the flow of liquids to the chip (Fig.7.4a), a microfluidic chip (Fig.7.4b), and a gas flow control unit (Fig.7.4c). The microchip was mounted on a microscope (Nikon, LV150). A methylene blue solution, an alkaline solution of glucose, and FC-40 oil were kept in separate glass syringes (1 ml Hamilton) connected to the microfluidic chip inlets by PEEK tubes with an inner diameter of 250 μm. The flow was driven by Nemesys syringe pumps (model). To inject gas to the chip, a gas compressor was connected to a gas reservoir, which was then connected to

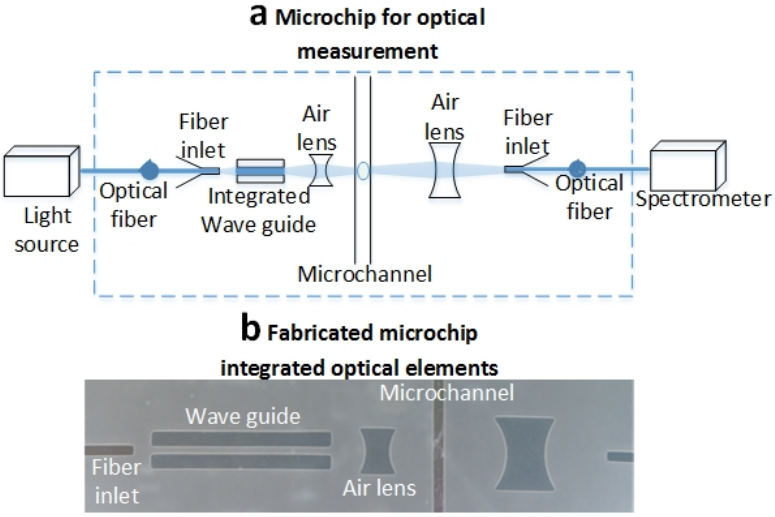

Figure 7.3: Schematic diagram of optical elements integrated in a microchip (a). Fabricated chip (b).

a pressure control unit by Tygon tubes with an inner diameter of 800 μm. Then, a PEEK tube with an inner diameter of 250 μm is connected from the pressure control unit to the chip. The gas bubbles were produced in the FC-40 oil in a W-junction and then in a T-junction aqueous-droplets were inserted between gas-bubbles as previously described. To avoid unexpected air-bubbles in the channel, the oil phase was first introduced to fill the entire channel. The movement of the bubbles and droplets were monitored by a camera (Nikon D5100).

7.5 Fabrication

The fabrication of the microfluidic chip is divided in two parts: fabrication of the PDMS microchannel and the coating of the assembled channel with Parylene AF4. The PDMS channel (width: 200μm, height: 100μm, and length: 12mm) was fabricated using standard soft lithography. The SU-8 master mold, containing channel structure, was prepared on 4" silicon wafer. Then liquid PDMS (Sylgard 184 by Dow Corning) was mixed with a curing agent in 10:1 ratio and degassed in a vacuum desiccator to remove air bubbles. The degassed PDMS was poured on the mold in a petri dish and degassed again. Subsequently, it was cured on a hot plate at 65°C for 4 hours. After inlets and an outlet holes were punched in the chips, the chips were bonded on a glass slide (width x length: 25 x 75 mm2) by oxygen plasma of 250 W,

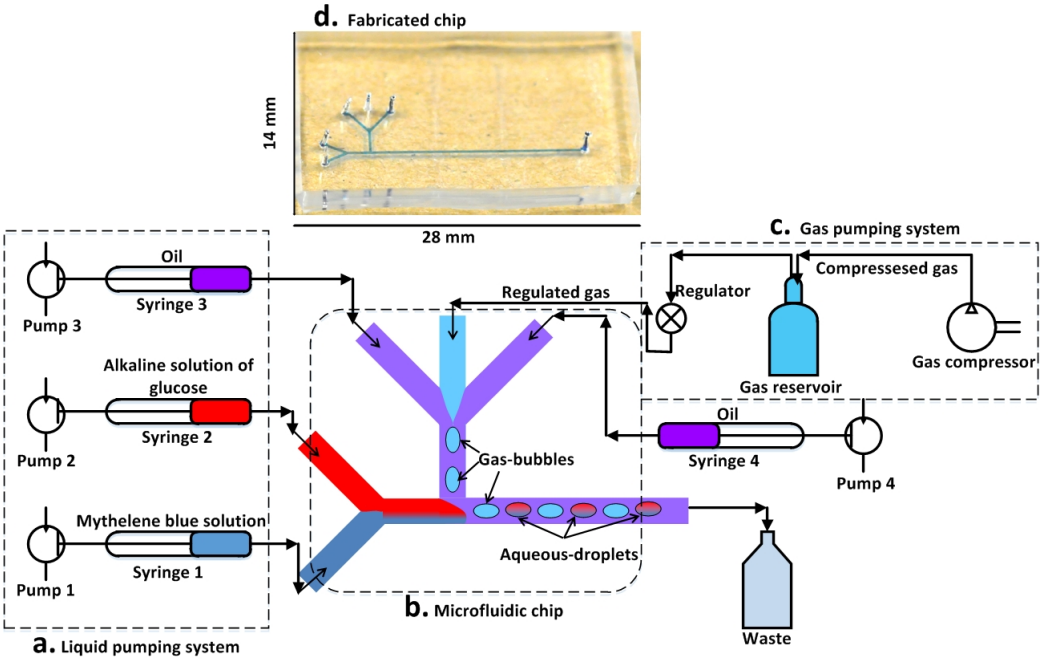

Figure 7.4: Schematic diagram of the microfluidic setup. (a) The liquid pumping system consists of micropumps, glass syringes and PEEK tubes. (b) A microfluidic chip to generate microdroplets and bubbles in fluorinated oil. (c) Gas pumping system consists of a gas compressor, a gas reservoir and a regulator that controls the flow pressure of the gas. (d) Fabricated microchip, the channel was filled with blue dye for better visualization.

for 10s. At the final step, this assembled PDMS channel was coated with Parylene AF4 (CAS 3345-29-7, 94.6%, PPS, Germany). The deposition of Parylene AF4 is described in detail in chapter 4.

7.6 Reagents

An alkaline solution of glucose in DI water was prepared and mixed with a solution of methylene blue in a microchannel to measure the presence of oxygen. Methylene blue was obtained from Merck KGaA, Germany; glucose and sodium hydroxide was brought from Carl Roth, Germany. FC-40 oil, density 1.85 g/mL at 25 °C, is obtained from sigma Aldrich, USA.

7.6.1 Fluorinated oil

Fluorocarbon oil is being used in biological applications because of its chemical inertness [150, 151]. Its strong carbon-fluorine bond results in low intermolecular forces, low surface tension, and no solvent action on a non-fluorinated compound. Therefore, its chemical composition does not shift or fraction with time, which ensures stable transport properties with time and fluid loss to the minimum. Because of the lower intermolecular bonding, it can dissolve more gases compared to hydrocarbon oil. Moreover, fluorocarbon oil can dissolve large volumes of respiratory gases and this solubility is related to the molecular volume of the dissolving gases. Its oxygen solubility is not subjected to the effect of pH, and they facilitate an effortless transfer of oxygen [152, 153]. Fluorinated oil has a 20 times higher oxygen solubility and a three times higher CO_2 solubility than pure water making the culture of living cells encapsulated in aqueous droplets particularly easy [139]. This makes fluorinated oil as a carrier oil to generate aqueous droplets in oil for molecular biology assays. In addition, as compared to hydrocarbon oils, fluorocarbon oils result in less swelling of polydimethylsiloxane (PDMS), a commonly used material for fabricating microfluidic channels.

7.6.2 Methylene blue as an oxygen indicator

Methylene blue (methylthionine chloride) is a dye that reversibly changes its color upon oxidation and reduction [154, 155]. Methylene blue (MB) is reduced by a reductant (i.e. an alkaline solution of glucose) to form a colorless (reduced) leucomethylene blue (MBH). The reactions are as follows

$$C_6H_{12}O_6 + (1/2)O_2 \longrightarrow C_6H_{12}O_7$$

$$C_6H_{12}O_6 + NaOH + MB \longrightarrow NaC_6H_{11}O_7 + MBH$$

Glucose (GL) in an alkaline solution is slowly oxidized by oxygen, forming gluconic acid. In the presence of sodium hydroxide (NaOH), gluconic acid is converted to sodium gluconate. Methylene blue speeds up the reaction by acting as an oxygen transfer agent. As the dissolved oxygen oxidizes glucose, methylene blue itself is reduced, forming the colorless leocomethylene (MBH), and the blue color of the solution disappears.

7.7 Mammalian cells preparation and encapsulation in droplets

The materials needed for preparing the growth medium are minimum essential medium (MEM), fetal bovine serum (FBS), MEM non-essential amino acid solution and penicillin-streptomycin. A 50 ml growth medium was prepared by adding 43 ml MEM, 4.8 ml FBS, 0.5 ml MEM non-essential amino acid solution and 0.5 penicillin-streptomycin. MDCK cells were obtained from Medical University of Vienna. At first, the cells were cultured in a flask. Afterwards, the healthy cells were encapsulated and stored in droplets in a microchip.

The preparation steps of healthy cells in a T25 flask are as follows:

- Separate the cells from the previous culture medium.
- Rinse the cells with 2 ml warm PBS. The PBS solution was kept in an incubator for 15 min. at 35°C.
- Remove the PBS solution.
- Add 2 ml Tryple, which protect cell's surface proteins.
- Place the cell containing flask in the incubator for 15 mins at 35°C and with 5% CO_2 presence.
- Check if the cells have detached from the bottom of the flask.
- In case cells cells have not detached from the bottom of the flask, gently hit the flask to stimulate the cell detachment.
- When most of the cells are detached, transfer 2 ml cell suspension in a 15 ml falcon tube using a pipette.
- Add 5 ml warm PBS to the cell suspension.
- Centrifuge the cell suspension for 3 minutes at 1300 rpm. The rpm value is crucial, a higher number of rpm might break the cell wall and eventually kill the cell.
- Make sure that the cell pallet is located at the bottom of the falcon tube and remove the liquid from the cell pellet.
- Re-suspend the cell pellet in 1 ml warm PBS.

- Add 7.2 ml of MDCK growth medium in a T25 flask. Add 150 μl cell suspension into the T25 flask.

The MDCK cell was cultured for three days in an incubator at 35°C and with 5% CO_2 presence. After incubation, cells were prepared for encapsulating in droplets using the same procedure except for the last two steps. A solution of 150 μl cell suspension in 5 ml MDCK growth medium was prepared in a falcon tube, which was used for MDCK cell encapsulated droplets generation. The microchip was fixed on the inverted routine microscope stage (TS100 Nikon, Japan). A camera (Nikon D5100) was fixed with the microscope to analyze and take photographs of the stored-droplets.

7.8 Results and discussion

7.8.1 Reaction time: methylene becomes colorless leucomethylene blue

A methylene blue solution and an alkaline solution of glucose were mixed at a flow rate of 40 μl and 100 μl per hour, respectively, in a long meander shape channel. The methylene blue and the reduction solutions were entered into the microchannel from the two inlets and mixed at the T-junction. The mixing volumes were varied by varying the flow rates of the two solutions. The methylene blue becomes colorless with time as dissolved oxygen is consumed by the alkaline glucose solution as depicted in Fig.7.5a. The time required for methylene blue to become colorless (reduced color) leucomethylene blue depends on the volume of methylene blue solution is being mixed with the reductant solution (an alkaline solution of glucose). In this experiment, a methylene blue solution was prepared by mixing 3 mg powder methylene blue in 10 ml DI water. A reductant solution of glucose 2.5% (w/v) and sodium hydroxide 2.5% (w/v) in DI water was prepared. At first, the reduction time was measured by mixing the two solutions in a microtube. The relation of the reduction time with the volume ratio of two liquids is presented in Figure 7.5b. Afterward, methylene blue and the alkaline solution was mixed in a microchannel. The reaction time increases with the increased volume of methylene blue (Fig.7.5b). In the microchannel, the mixing of liquids takes a longer time due to the absence of the turbulent flow.

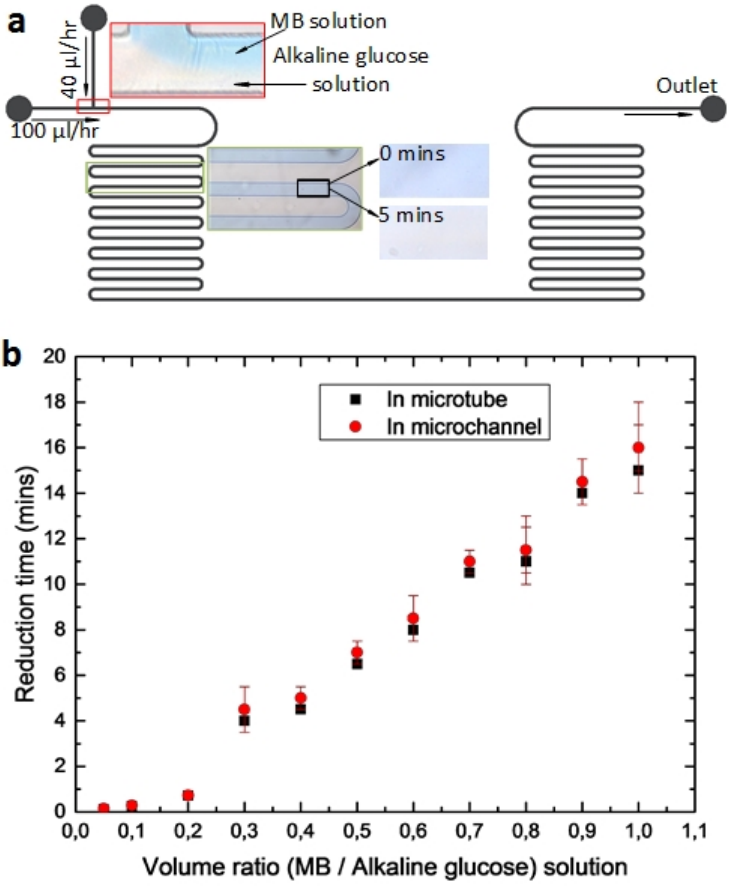

Figure 7.5: The mixing of a methylene blue and an alkaline glucose solution in a meander shape long microchannel (a). The reaction time of methylene blue to become colorless leucomethylene in a microtube and in a microchannel (b).

7.8.2 The effect of air-bubbles on the presence of oxygen in a microchannel

The oxygen levels were measured with and without the presence of air-bubbles in the microchannel. A solution of glucose and NaOH were prepared in deionized water, which had an oxygen content of 9mg/L in approximate equilibrium with the air, according to Henry's law. The methylene blue solution was also prepared in deionized water. The bubbles were generated and placed between aqueous droplets (Fig.7.6a). The methylene blue solution and the alkaline glucose solution was mixed in the microchannel in a ratio of 1:4, respectively, to generate aqueous-droplets. The methylene blue

in alkaline glucose solution droplets takes (10±1) min. to become colorless without the presence of air-bubbles (Fig.7.6b); whereas it needs (35±4) min. in the presence of air-bubbles Fig.7.6c). In these measurements, the volume of the aqueous-droplets and air-bubbles were approximately the same. In the previous measurement (Fig.7.6b), where methylene blue was mixed with the alkaline glucose solution in the microchannel, the time for methylene blue to become colorless was (5±0,5) min. With the presence of FC-40 oil, methylene blue in alkaline glucose solution droplets take (10±1) min to become colorless. As previously explained, in fluorinated oil 20 times more oxygen can be dissolved than in water. This oxygen can diffuse from the oils to the aqueous droplets.

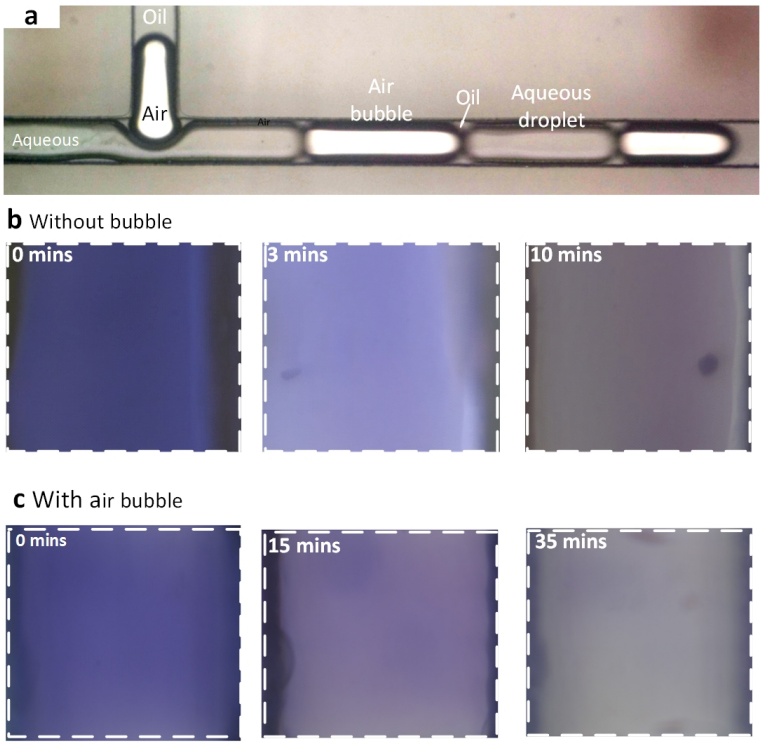

Figure 7.6: Droplets and air bubble generation in microchannel where FC-40 oil was used as continuous phase (a). Oxygen detection in aqueous droplets without air-bubbles suspended in fluorinated oil (b). Oxygen in aqueous droplets with the presence of air bubbles in microchannel (c).

7.8.3 Transmittance spectrum of methylene blue

In the experiments, spectrometry was used to follow the methylene blue reaction in an alkaline glucose solution. Droplets of methylene blue in an alkaline glucose solution were generated placed in series of air-bubbles in FC-40 oil. To measure the transmitted spectrum, droplets were positioned in front of the optical setup of the chip. The light passed through the sample, and the transmitted light was measured. Ten measurements were made on each sample, as illustrated in Fig.7.7. The transmittance signal increases as the methylene blue become reduced color leucomethylene blue. The transmittance intensity at a wavelength of 675 nm is plotted in Fig.7.7b. For all the measurements, the ratio of methylene blue and alkaline solution of glucose was 1:4. However, due to the pulsating behavior of pumps, a slight change in the volume of the two solutions is observed.

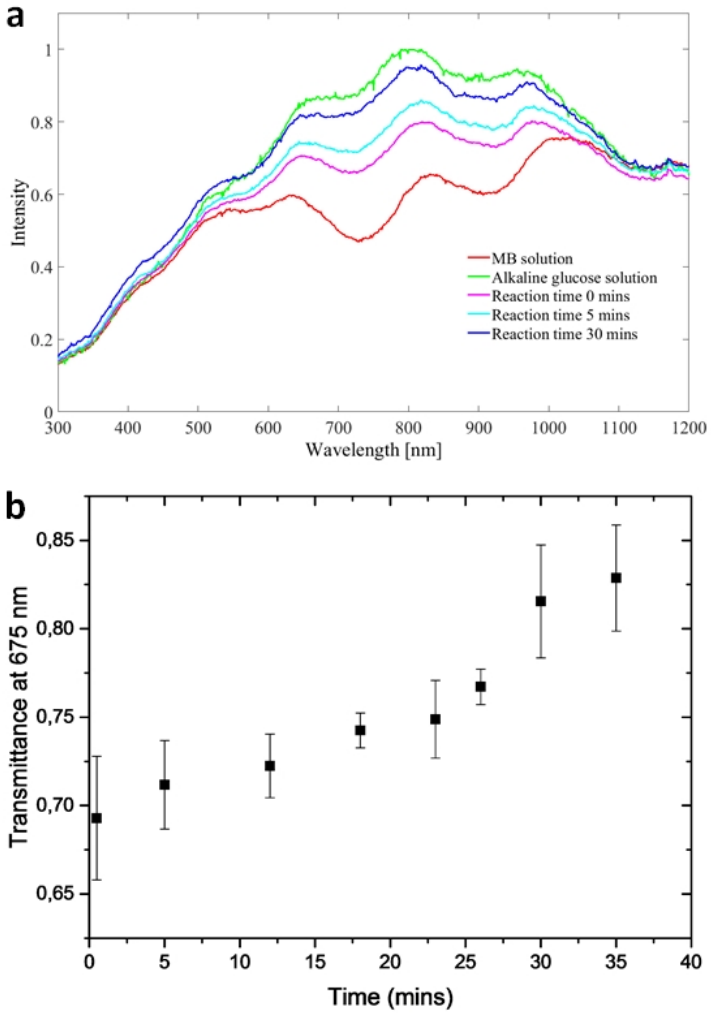

Figure 7.7: Spectrometer trace of a methylene blue solution, an alkaline glucose solution, and the reaction between the solutions in droplets (a). Spectrometer trace at 675 nm. The rate of reduction of methylene blue by an alkaline solution of glucose (b).

7.8.4 MDCK cell encapsulation and on-chip storage

The MDCK cell encapsulating droplets were produced in a microchannel using the same procedure and chip as described in Fig.7.4. The encapsulation rate of cells in droplets has been described in detail in chapter 4. After filling the channel with those, the inlet and outlet tubes were removed from the chip, and the inlets and outlets were sealed with water- resistant adhesive tape (Farnell, Germany). Depending on the droplets size approximately six

Table 7.1: MDCK cells storage in droplets with and without the presence of air bubbles

Chip Nr.	On-chip storage time [hr]
Chip 1	1
Chip 2	2
Chip 3	4
Chip 4	6
Chip 5	8
Chip 6	12
Chip 7	1 (without air bubbles)

droplets with cells in it were stored and used for the further measurements. The chip was then placed in an incubator at 35°C with 5% CO_2. Several chips, with the same dimension, have been used for the experiments.

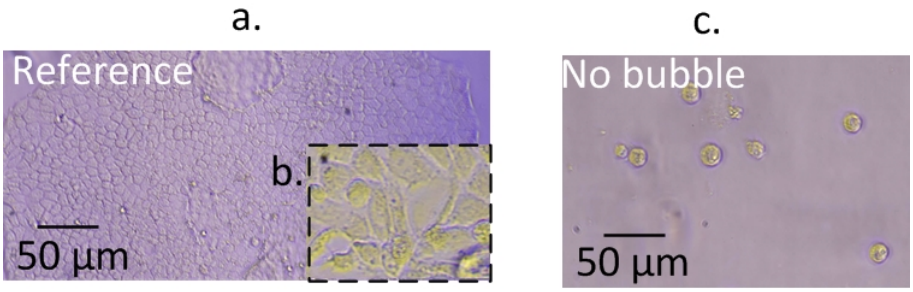

Figure 7.8: (a) Image of MDCKcells, cultured in a T25 flask; (b) Closer view of MDCK cells; (c) Cells were stored in a droplet without the presence of air-bubbles; afterward, they were transferred to microwell plate to observe the survival of cells. The picture was taken 48 hours after transferring the cells from microchip to microwell plate.

The mammalian cells are susceptible to the surrounding environment; thus, the survival of mammalian cells need very sophisticated environmental condition. The focus of this experiment is to investigate the survival rate of the mammalian cell in a microchannel. After storing the droplets in the microchannel as described in Table.7.1, the droplets were taken out of the chip 1. The cells were then washed in warm PBS, centrifuged, and transferred to a microwell plate. 1.5 ml of MDCK cell growth medium is added to the well plate and was kept in an incubator at 35with 5% CO_2. Figure 7.9 presents the pictures of cells in a droplet after one hour of storage and the same cells in the microplate plate after three days.

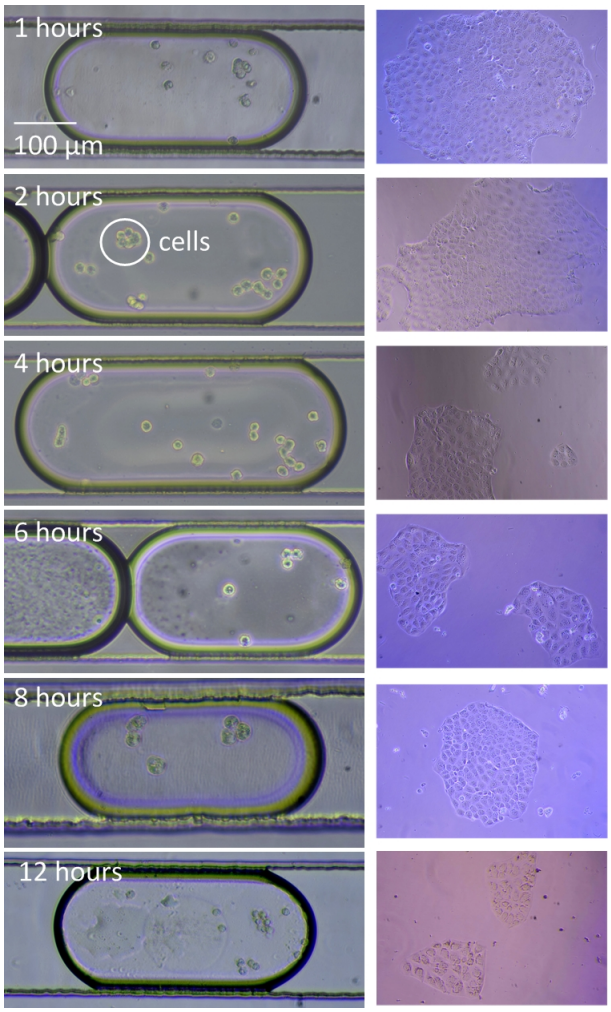

Figure 7.9: MDCK cells encapsulated in droplets. After on-chip storage, cells were transferred to microwell plate and their growth has been observed over the time.

A reference picture of cell grown in a T25 Flask without storing the cells in droplets is presented in Fig.7.8a. From chip 2 to chip 6 the same procedure as for chip 1 has been applied except for the storage time. No dead cells have been observed up to 8 hours of storage in droplets. A few dead cells have been found after 12 hours of storage time. MDCK cell encapsulated droplets with the presence of air bubbles in a chip (chip 7) has been stored on-chip for an hour, then cells were transferred to the microwell plate using the same procedure as Chip 1. No cell growth has been observed after three days of storage in a microplate (Fig.7.8c). This experiment demonstrates that

the mammalian cells can be stored at least 12 hours in a microchip in the presence of air-bubbles in the channel, which is a big step forward to on-chip culturing of mammalian cells.

7.9 Conclusion

We have designed and realized a multiphase microfluidic system that enables the diffusion of oxygen from air-bubbles to aqueous droplets without the need of changing the medium. The diffusion of oxygen from air-bubbles to aqueous-droplets suspended in fluorinated oil was successfully demonstrated using methylene blue as an indicator. MDCK mammalian cells were successfully stored in droplets with the presence of air-bubbles for 12 hours. The proposed method and device are a big step forward to long-term on-chip cultivation of mammalian cells and aerobic bacteria growth in stored droplets.

Chapter 8

Conclusions and outlook

The goal of this thesis work is the design and fabrication of a microfluidic device for on-chip storage and manipulation of droplets. Droplet microfluidics represents a promising new tool for cell culturing, drug screening, and high throughput analysis. The applications of such a system is yet to be explored. In this thesis work, an on-chip droplets storage method and its application have been presented. Based on the storage chip, other applications of droplets such as agarose droplets generation and storage, and methods that provide nutrients and oxygen to the stored droplets have been developed. The novel methods for on-chip droplets storage and manipulation of droplets that have been realized allow general conclusions to be drawn from the achieved results in terms of applicability and performance. Since designs evolve over time and since they are never final when they are being researched, it is necessary to find a way to produce a prototype that is inexpensive and easy to fabricate. Before going to the fabrication processes, each fabrication process has been thoroughly investigated in terms of suitable materials and fabrication techniques. Since the application of the developed chip is the storage of cells or biological reagents on-chip, the chip material should be biocompatible in nature. The investigation of droplets has been conducted mainly by optical microscopy, hence a transparent material is required to develop the chip. Considering those requirements and ease of fabrication techniques, PDMS as base material has been chosen for the primary development of the chip.

In the following sections, the major achievements of this research work are shortly summarized and future perspectives for the continuation of the further research in the relevant fields are discussed.

On-chip droplet storage

Droplet storage is required for cell cultivation, drug screening, and chemical reactions to be conducted in droplets. Methods addressed in literature for storage of droplets are off-chip. In those methods droplets were generated in a chip and transferred to a micro-tube/Teflon tube to be stored. These methods are difficult to use where continuous monitoring of each droplet is crucial. Therefore, an on-chip method is required for such a system. A novel storage method has been introduced in this work, where droplets were generated and stored in the same chip for 4 days. For storage chips, PDMS has been used as a base material for the chip fabrication. Since PDMS is porous a drastic volume loss of the droplets has been observed during storage. Parylene has been introduced as a new material in combination with PDMS to overcome the drawbacks of PDMS. Since there are different types of Parylene that are commercially available, an investigation has been conducted to select the best type for our specific application. The biocompatibility, hydrophobicity, and penetration depth of Parylene C and AF4 have been examined. AF4 showed a better performance, hence AF4 has been used for further study.

Water droplets in oil were generated and stored for 4 days at an elevated temperature in a Parylene AF4 coated PDMS chip. The results showed that droplets loose a very small amount of liquid from their initial volume through the surrounding oil compared to the stored droplets in PDMS, where droplets loose all their volume in only four hours. Although *E. coli* and *E. faecalis* have been encapsulated and stored in droplets, this method can be applied to other cell encapsulations and to do chemical reactions which need to be stored for several days. For instance, yeast cells that have been encapsulated in agrose droplets have been generated on chip and stored for several days.

Droplets manipulation

One of the great advantages of droplet microfluidics is that droplets can be manipulated on chip, which includes the splitting of a bigger droplet into smaller droplets, the addition of droplets, mixing liquids in one droplet, and sorting of droplets that contain substances of interest. A chip has been designed and realized that can sort and merge droplets to provide additional reagents to the sample droplets. In a microfluidic channel the Reynolds number is low. Therefore, the mixing of liquids is mainly by means of diffusion. Many methods have been introduced in literature, where acceleration of the mixing process has been investigated. In this work, a serpentine channel has been introduced to accelerate the mixing of two liquids in droplets. Fluorescent beads were encapsulated in droplets and sorted out prior to merging

with another droplet in the microchannel. Finally, E. coli has been encapsulated in droplets, stored, and merged with nutrient droplets in the microchip. The efficiency of the microchip is not optimal up to level due to the manual control of the sorting process. However, the automation of the whole system has the capability to increase its efficiency. The working principle and design of the proposed microchip has great potential to be applied in the field of biology and chemistry.

Storage of mammalian cells in droplets

Nowadays, many biological processes, including cell division, enzymatic reactions, and the polymerase chain reaction (PCR) are accomplished *in vitro*. The traditional methods of *in vitro* cells culture are petri dish, flask, and microplate, where cells receive oxygen from the surrounding air. The similar approach has been applied to droplets in a more defined and controlled way. To achieve this, air-bubbles have been placed in a microchannel in series with aqueous-droplets and used as a source of oxygen, and CO_2. We have designed and realized a multiphase microfluidic system that enables the diffusion of oxygen from the air-bubbles to the aqueous droplets through fluorinated oil without the need of changing the medium. The diffusion of oxygen from air-bubbles to the aqueous-droplets suspended in fluorinated oil was successfully demonstrated using methylene blue as an indicator. The presence of an air-bubble increased the oxygen in an aqueous-droplet up to 7 times compared to the oxygen in an aqueous-droplet without an air-bubble present in the channel. An MDCK cell line has been stored in droplets with sufficient nutrients in it with and without the presence of air-bubbles in the microchannel. The result showed that with the presence of air-bubbles cells can survive in droplets more that 12 hours whereas with the absence of air-bubbles these cells can not survive more than 2 hours. The presented method has a great potential in the field of on-chip drug screening and storage of mammalian cells for a longer period of time.

Outlook

The storage, sorting, merging, mixing, and oxygen supplementation to the stored droplets are individually presented in this work. Although the successful implementation of all the devices has been conducted, little attention has been given to the integration of the whole system. An outlook is provided here for the further continuation of the project. Droplet microfluidics has tremendous potential to be applied in various branches of science. However, until now, most of the processes take place only in the research lab.

Droplet generation on a microchip requires an external setup, including syringe pumps, syringes, and microtubes. The external setup increases the required sample volume and affects the size of the generated droplets. Thus, it is necessary to integrate an on-chip droplet generation setup.

The droplet sorting and merging chip can be automated by integrating optical and electrical sensors and by controlling the micropump with signals from the sensors. Image processing is another area for further automation of the sorting and merging processes.

Mammalian cells have been successfully stored in droplets for several hours. However, the growth of mammalian cells in droplets needs to be further investigated..

The results presented in this work may provide tools and techniques for the successful application of droplet microfluidics.

Acknowledgments

It has been an incredible experience to work at IMSAS and with the Eng-CaBra fellows. I have gained significant experience from my colleagues on how to face scientific and professional challenges. This thesis work would not have been possible without the help and encouragement of several people to whom I am incredibly grateful.

Firstly, I would like to express my sincere gratitude to my advisor Prof. Dr.-Ing. Michael J. Vellekoop for his continuous support, patience, and motivation during my Ph.D. studies and related research. He introduced me to the field of microfluidics and encouraged me to pursue research in this field. Under his supervision, I learned how to define research problems, solve them, and finally publish the results. Further, I would like to thank him for taking time off his busy schedule to read this thesis.

I would like to thank my committee members Prof. Dr.-Ing. Karl-Ludwig Krieger, Prof. Dr. Walter Lang, and Prof. Dr. Steffen Paul for taking time out of their busy schedule to participate in my defense.

My sincere thanks go to Dr. Sander van den Driesche for his constant guidance, motivation, and support. He taught and helped me to conduct experiments on cells culturing in a microfluidic system. I owe a lot of gratitude to him for always being there for me.

I am grateful to my office and lab mate Dr. Ing. Lukas Brandhof for his continuous support during my Ph.D. study. He was also my Master's thesis supervisor for a short period. I benefited immensely from his laboratory experience.

I want to thank Valeria Fioravanti and Dr. Reza Ebrahimifard for the productive discussions and for all the fun we have had in the last three years. A special thanks to Marta Di Salvo for teaching me how to work with mammalian cells. She has been an excellent office mate. Thanks Marta, for bringing local coffee from your home town and introducing me to the Moka pot.

I would like to thank Dr. Frieder Lucklum for the introduction of the 3D printer and for the support to prepare and print microchannels. I would like

to thank Dr. Frank Bunge and Martin Oellers for the support in the lab. I express my gratitude to all IMSAS employees for their help while working in the microfabrication lab and characterization lab. I am also pleased to say thank to Gnana Ganesh Ekambaram, Mohammad Towshif Rabbani, Baris Babaoglu, whom I supervised in their Master thesis/project and their contribution to this Ph.D. thesis.

I would also like to extend my gratitude to all EnCaBra fellows with whom I traveled. This has been a fantastic opportunity to work with energetic, motivated, and friendly researchers.

I express my cordial thanks to my colleagues Simone Duwe, Matthias Orlob, and Dr. Poornachandra Papireddy Vinayaka for their inspiration and support. A special thank you to Simone, who proofread the abstract (in German) of this thesis.

Finally, words cannot express how grateful I am to my family, especially my mother, for all the sacrifices that she has made on my behalf. I would also like to thank all of my friends who supported me in writing this thesis and encouraged me to strive towards my goal. I would also like to express appreciation toward my husband, Mir Mamunuzzaman, who spent countless sleepless nights with me and was always my support when I needed it the most.

List of publications

Journal papers (peer reviewed)

1. Akhtar M, van den Driesche S, Boedecker A, Vellekoop MJ, “Long-term storage of droplets on a chip by Parylene AF4 coating of channels”, Sensors Actuators B, online 2017, Volume 255, Part 3, 2018, 3576-3584, doi: 10.1016/j.snb.2017.08.032.

International conferences

1. Akhtar M, Brandhoff L, van den Driesche S, Vellekoop MJ, "Air-droplets as Gas Reservoir to Provide O2 to the Stored-Aqueous Droplets in Micro-channels", Procedia Engineering, Volume 120, 2015, 92-95. doi: 10.1016/j.proeng.2015.08.573.

2. Mahmuda Akhtar, M. Towshif Rabbani, and Michael J. Vellekoop. Merging of droplets in micro-channel independent of the droplet size and inter-droplet separation. Progress in Biomedical Optics and Imaging - Proceedings of SPIE, 9518, 2015.

3. Mahmuda Akhtar, Sander Driesche, and M.J. Vellekoop. On-chip storage of droplets in parylene-AF4 coated pdms channels. 18th International Conference on Miniaturized Systems for Chemistry and Life Sciences, MicroTAS 2014, pages 1641-1643, 01 2014.

Other publications

1. Abdallah A, van den Driesche S, Brandhoff L, Bunge F, Akhtar M, Clara S, Jakoby B, Vellekoop MJ, “Microfluidic device for Acoustophorisis and Dielectrophoresis Assisted Particle and Cell Transfer between Different Fluidic Media”, Procedia Engineering, Volume 120, 2015, 691-694. doi: 10.1016/j.proeng.2015.08.754.

2. Clara S, Abdallah A, Jakoby B, Akhtar M, Vellekoop M, "Improved Droplet Size Stability Using Phase- Guide Structures", Proc. of the IEEE Sensors Conference (2015), Korea, 1469-1472.

3. Brandhoff L, Akhtar M, Bülters M, Bergmann RB, and Vellekoop MJ, "Running Droplet Optical Multiplexer", Optofluid. Microfluid. Nanofluid.; 1:62-68 (2014); doi: 10.2478/optof-2014-0007.

Bibliography

[1] S. C. Terry, J. H. Jerman, and J. B. Angell, "A gas chromatographic air analyzer fabricated on a silicon wafer," *IEEE Transactions on Electron Devices*, vol. 26, no. 12, pp. 1880–1886, Dec 1979.

[2] A. Manz, N. Graber, and H. Widmer, "Miniaturized total chemical analysis systems: A novel concept for chemical sensing," *Sensors and Actuators B: Chemical*, vol. 1, no. 1, pp. 244 – 248, 1990.

[3] T. Thorsen, S. J. Maerkl, and S. R. Quake, "Microfluidic large-scale integration," *Science*, vol. 298, no. 5593, pp. 580–584, 2002.

[4] P. Tabeling, *Introduction to Microfluidics*, 2006.

[5] T. M. Squires and S. R. Quake, "Microfluidics: Fluid physics at the nanoliter scale," *Rev. Mod. Phys*, vol. 77, pp. 977–1026, October 2005.

[6] D. Ferraro, M. Serra, D. Filippi, L. Zago, E. Guglielmin, M. Pierno, S. Descroix, J.-L. Viovy, and G. Mistura, "Controlling the distance of highly confined droplets in a capillary by interfacial tension for merging on-demand," *Lab Chip*, vol. 19, pp. 136–146, 2019. [Online]. Available: http://dx.doi.org/10.1039/C8LC01182F

[7] M. A. Maleki, M. Soltani, N. Kashaninejad, and N.-T. Nguyen, "Effects of magnetic nanoparticles on mixing in droplet-based microfluidics," *Physics of Fluids*, vol. 31, no. 3, p. 032001, 2019. [Online]. Available: https://doi.org/10.1063/1.5086867

[8] F. Ahmadi, K. Samlali, P. Q. N. Vo, and S. C. C. Shih, "An integrated droplet-digital microfluidic system for on-demand droplet creation, mixing, incubation, and sorting," *Lab Chip*, vol. 19, pp. 524–535, 2019. [Online]. Available: http://dx.doi.org/10.1039/C8LC01170B

[9] H. N. Joensson, M. Uhlen, and H. A. Svahn, "Droplet size based separation by deterministic lateral displacement-separating droplets by cell-induced shrinking," *Lab Chip*, vol. 11, pp. 1305–1310, 2011.

[10] P. Garstecki, M. J. Fuerstman, H. A. Stone, and G. M. Whitesides, "Formation of droplets and bubbles in a microfluidic t-junction-scaling and mechanism of break-up," *Lab Chip*, vol. 6, pp. 437–446, 2006.

[11] S. L. Anna and H. C. Mayer, "Microscale tipstreaming in a microfluidic flow focusing device," *Physics of Fluids*, vol. 18, no. 12, 2006.

[12] N. Wu, Y. Zhu, S. Brown, J. Oakeshott, T. S. Peat, R. Surjadi, C. Easton, P. W. Leech, and B. A. Sexton, "A pmma microfluidic droplet platform for in vitroprotein expression using crude e. coli s30 extract," *Lab Chip*, vol. 9, pp. 3391–3398, 2009.

[13] F. Courtois, L. F. Olguin, G. Whyte, A. B. Theberge, W. T. S. Huck, F. Hollfelder, and C. Abell, "Controlling the retention of small molecules in emulsion microdroplets for use in cell-based assays," *Analytical Chemistry*, vol. 81, no. 8, pp. 3008–3016, apr 2009.

[14] P. Kumaresan, C. J. Yang, S. A. Cronier, R. G. Blazej, and R. A. Mathies, "High-

Throughput Single Copy DNA Amplification and Cell Analysis in Engineered Nanoliter Droplets," *Analytical Chemistry*, vol. 80, no. 10, pp. 3522–3529, may 2008.

[15] C. W. Pan, D. G. Horvath, S. Braza, T. Moore, A. Lynch, C. Feit, and P. Abbyad, "Sorting by interfacial tension (sift): label-free selection of live cells based on single-cell metabolism," *Lab Chip*, vol. 19, pp. 1344–1351, 2019. [Online]. Available: http://dx.doi.org/10.1039/C8LC01328D

[16] D. RanChen, ZeyongSun, *Microfluidics for Pharmaceutical Applications*, 2019.

[17] X. Leng, W. Zhang, C. Wang, L. Cui, and C. J. Yang, "Agarose droplet microfluidics for highly parallel and efficient single molecule emulsion pcr," *Lab Chip*, vol. 10, pp. 2841–2843, 2010.

[18] R. Williams, S. G. Peisajovich, O. J. Miller, S. Magdassi, D. S. Tawfik, and A. D. Griffiths, "Amplification of complex gene libraries by emulsion PCR," *Nat Meth*, vol. 3, no. 7, pp. 545–550, jul 2006.

[19] M. Ildefonso, N. Candoni, and S. Veesler, "A cheap, easy microfluidic crystallization device ensuring universal solvent compatibility," *Organic Process Research & Development*, vol. 16, no. 4, pp. 556–560, apr 2012.

[20] J. H. Tsui, W. Lee, S. H. Pun, J. Kim, and D.-H. Kim, "Microfluidics-assisted in vitro drug screening and carrier production," *Advanced Drug Delivery Reviews*, vol. 65, no. 1112, pp. 1575 – 1588, 2013, design production and characterization of drug delivery systems by Lab-on-a-Chip technology.

[21] R. E. G. J P Brody, P Yager and R. H. Austin, "Biotechnology at low reynolds numbers," *Biophys J.*, vol. 71, no. 6, pp. 3430–3441, December 1996.

[22] O. Reynolds, "An experimental investigation of the circumstances which determine whether the motion of water shall be direct or sinuous, and of the law of resistance in parallel channels," *Philosophical Transactions of the Royal Society*, vol. 174, no. 0, p. 174, 1883.

[23] J. P. Holman, "Heat transfer," *McGraw-Hill*, p. 207, 2002.

[24] S. T. W. Nam-Trung Nguyen, *Fundamentals and Applications of Microfluidics*. Artech House, Boston, London, 2002.

[25] F. R. . D. Einstein A, "Investigations on the theory of the brownian movement," *Publications, New York*, 1956.

[26] M. B. E. V. Christoph Erbacher, Fiona G. Bessoth and A. Manz, "Towards integrated continuous-flow chemical reactors," *Mikrochim. Acta*, vol. 131, pp. 19–24, 1999.

[27] J. Berthier, *Microdrops and Digital Microfluidics*. William Andrew Inc., 2008.

[28] D. Q. Pierre-Gilles de Gennes, Franse Brochard-Wyart, *Capillarity and Wetting Phenomena: Drops, Bubbles, Pearls, Waves*. Springer, 2003.

[29] P. J. M. Fermigier, "An experimental investigation of the dynamic contact angle in liquidliquid systems," *J. Colloid Interface Sci.*, vol. 146, p. 226241, 1990.

[30] F. R. J. Berthier, "Numerical modeling of ferrofluid flow instabilities in a capillary tube at the vicinity of a magnet," *in: Proceedings of the 2002 MSM Conference*, 2002.

[31] P. S. J. Berthier, *Microfluidics for Biotechnology*. Artech House Publishers, Norwood, MA,, 2006.

[32] R. Hilfer and P. E. Oren, "Dimensional analysis of pore scale and field scale immiscible displacement," *Transport in Porous Media*, vol. 22, no. 1, pp. 53–72.

[33] P. Garstecki, H. A. Stone, and G. M. Whitesides, "Mechanism for flow-rate controlled breakup in confined geometries: A route to monodisperse emulsions," *Phys. Rev. Lett.*, vol. 94, p. 164501, Apr 2005.

[34] http://mathworld.wolfram.com/heavisidestepfunction.html.

[35] P. Guillot, A. Colin, A. S. Utada, and A. Ajdari, "Stability of a jet in confined pressure-driven biphasic flows at low reynolds numbers," *Phys. Rev. Lett.*, vol. 99, p. 104502, Sep 2007.

[36] A. M. Ganan-Calvo and J. M. Gordillo, "Perfectly monodisperse microbubbling by capillary flow focusing," *Phys. Rev. Lett.*, vol. 87, p. 274501, Dec 2001.

[37] W. Lee, L. M. Walker, and S. L. Anna, "Role of geometry and fluid properties in droplet and thread formation processes in planar flow focusing," *Physics of Fluids*, vol. 21, no. 3, 2009.

[38] T. Cubaud and T. G. Mason, "Capillary threads and viscous droplets in square microchannels," vol. 20, no. 5, 2008.

[39] D. Funfschilling, H. Debas, H.-Z. Li, and T. G. Mason, "Flow-field dynamics during droplet formation by dripping in hydrodynamic-focusing microfluidics," *Phys. Rev. E*, vol. 80, p. 015301, Jul 2009.

[40] S. L. Anna, N. Bontoux, and H. A. Stone, "Formation of dispersions using flow focusing in microchannels," *Applied Physics Letters*, vol. 82, no. 3, pp. 364–366, 2003.

[41] G.-P. R. R.-G. A. B.-A. T. C. A. C. S. F.-M. M. Ga?Calvo AM, MartBanderas L, "Straightforward production of encoded microbeads by flow focusing: potential applications for biomolecule detection," *Int J Pharm.*, vol. 324, no. 1, pp. 19–26, Oct 31 2006, pub 2006 May 22.

[42] J.-P. Raven and P. Marmottant, "Periodic microfluidic bubbling oscillator: Insight into the stability of two-phase microflows," *Phys. Rev. Lett.*, vol. 97, p. 154501, Oct 2006.

[43] C. Zhou, P. Yue, and J. J. Feng, "Formation of simple and compound drops in microfluidic devices," *Physics of Fluids*, vol. 18, no. 9, 2006.

[44] P. Garstecki, I. Gitlin, W. DiLuzio, G. M. Whitesides, E. Kumacheva, and H. A. Stone, "Formation of monodisperse bubbles in a microfluidic flow-focusing device," *Applied Physics Letters*, vol. 85, no. 13, pp. 2649–2651, 2004.

[45] A. S. U. Elise Lorenceau, M. J. Darren R. Link, Galder Cristobal, and D. A. Weitz, "Generation of polymerosomes from double-emulsions," *Langmuir*, vol. 21, no. 20, pp. 9183–9186, 2005, pMID: 16171349.

[46] W. J. Milliken, H. A. Stone, and L. G. Leal, "The effect of surfactant on the transient motion of newtonian drops," *Physics of Fluids A*, vol. 5, no. 1, pp. 69–79, 1993.

[47] I. B. Bazhlekov, P. D. Anderson, and H. E. Meijer, "Numerical investigation of the effect of insoluble surfactants on drop deformation and breakup in simple shear flow," *Journal of Colloid and Interface Science*, vol. 298, no. 1, pp. 369 – 394, 2006.

[48] B. Ziaie, A. Baldi, M. Lei, Y. Gu, and R. A. Siegel, "Hard and soft micromachining for biomems: review of techniques and examples of applications in microfluidics and drug delivery," *Advanced Drug Delivery Reviews*, vol. 56, no. 2, pp. 145 – 172, 2004, biosensing and Drug Delivery at the Microscale.

[49] G. M. A. W. Y. Xia, "Soft lithography," *Chem., Int. Ed.*, vol. 37, pp. 550–575, 1998.

[50] S. M. Usama M. Attia and J. R. Alcock, "Micro-injection moulding of polymer microfluidic devices," *Microfluidics and Nanofluidics*, vol. 71, no. 1, pp. 1–28, July 2009.

[51] J. Kim and X. Xu, "Excimer laser fabrication of polymer microfluidic devices," *JOURNAL OF LASER APPLICATIONS*, vol. 15, no. 4, pp. 255–260, November 2003.

[52] J. W. W. W. W. L.-G. A. Ming Li, Shunbo Li, "A simple and cost-effective method for fabrication of integrated electronicmicrofluidic devices using a laser-patterned

pdms layer," *Microfluidics and Nanofluidics*, 2012.

[53] N. S. Bruce L. Carvalho, Eric A. &hilling and G. J. Kellogg, "Soft embossing of microfluidic devices," in *7th lnternat onal Conference on Miniaturized Chemical and Blochemlcal Analysts Systems October 5-9, 2003, Squaw Valley, Callfornla USA*, 2003.

[54] J. H. J. Stephen C. Terry and J. B. Angell, "A gas chromatographic air analyzer fabricated on a silicon wafer," *IEEE Trans. Electron Devices*, vol. 26, pp. 1880–1886, 1979.

[55] D. Nieto, R. Couceiro, M. Aymerich, R. Lopez-Lopez, M. Abal, and M. T. Flores-Arias, "A laser-based technology for fabricating a soda-lime glass based microfluidic device for circulating tumour cell capture," *Colloids and Surfaces B: Biointerfaces*, vol. 134, pp. 363 – 369, 2015.

[56] . David Erickson, X. Liu, U. Krull, , and D. Li, "Electrokinetically controlled dna hybridization microfluidic chip enabling rapid target analysis," *Analytical Chemistry*, vol. 76, no. 24, pp. 7269–7277, 2004, pMID: 15595869.

[57] S. Lai, S. Wang, J. Luo, L. J. Lee, S.-T. Yang, , and M. J. Madou, "Design of a compact disk-like microfluidic platform for enzyme-linked immunosorbent assay," *Analytical Chemistry*, vol. 76, no. 7, pp. 1832–1837, 2004, pMID: 15053640.

[58] S. K. F. Z. E. C.-M. A. Harrison DJ, Fluri K, "Micromachining a miniaturized capillary electrophoresis-based chemical analysis system on a chip," *Science*, vol. 261, no. 5123, pp. 895–897, 1993.

[59] Z. S. D. n. Jaroslav Kotowski, VNavrl, "Fast and simple fabrication procedure of whole-glass microfluidic devices with metal electrodes," *Microelectronic Engineering*, vol. 110, pp. 441 – 445, 2013.

[60] W. H. Ren K, Zhou J, "Materials for microfluidic chip fabrication," *American Chemical Society*, vol. 46, no. 11, pp. 2396–2406, 2013.

[61] H. Becker and C. Gärtner, "Polymer microfabrication technologies for microfluidic systems," *Analytical and Bioanalytical Chemistry*, vol. 390, no. 1, pp. 89–111, 2008.

[62] H. Sato, H. Matsumura, S. Keino, and S. Shoji, "An all su-8 microfluidic chip with built-in 3d fine microstructures," *Journal of Micromechanics and Microengineering*, vol. 16, no. 11, p. 2318, 2006.

[63] J. C. McDonald, , and G. M. Whitesides*, "Poly(dimethylsiloxane) as a material for fabricating microfluidic devices," *Accounts of Chemical Research*, vol. 35, no. 7, pp. 491–499, 2002, pMID: 12118988.

[64] A. D. Stroock, , and G. M. Whitesides*, "Controlling flows in microchannels with patterned surface charge and topography," *Accounts of Chemical Research*, vol. 36, no. 8, pp. 597–604, 2003, pMID: 12924956.

[65] A. M. Ghaemmaghami, M. J. Hancock, H. Harrington, H. Kaji, and A. Khademhosseini, "Biomimetic tissues on a chip for drug discovery," *Drug Discovery Today*, vol. 17, no. 3–4, pp. 173 – 181, 2012.

[66] F. G. O. D. L. K. Peter Domachuk, Konstantinos Tsioris, "Bio-microfluidics: Biomaterials and biomimetic designs," *Adv Mater.*, vol. 22, no. 2, p. 2490, Jan 12 2010.

[67] D. P. C. Y. Yeshaiahu Fainman, Luke Lee, Ed., *Optofluidics: Fundamentals, Devices, and Applications: Fundamentals, Devices, and Applications.* McGraw Hill Professional, 2009.

[68] Y. Xia and G. M. Whitesides, "Soft lithographys," *Annu. Rev. Mater. Sci.*, vol. 28, pp. 153–84, 1998.

[69] M. Geissler and Y. Xia, "Patterning: Principles and some new developments," *Advanced Materials*, vol. 16, no. 15, pp. 1249–1269, 2004.

[70] B. D. Gates, Q. Xu, D. R. Michael Stewart, C. G. Willson, , and G. M. Whitesides, "New approaches to nanofabrication: Molding, printing, and other techniques," *Chemical Reviews*, vol. 105, no. 4, pp. 1171–1196, 2005, pMID: 15826012.

[71] X. Ye, H. Liu, Y. Ding, H. Li, and B. Lu, "Research on the cast molding process for high quality {PDMS} molds," *Microelectronic Engineering*, vol. 86, no. 3, pp. 310 – 313, 2009, the Fourth {IEEE} International Symposium on Advanced Gate Stack Technoiogy (ISAGST 2007).

[72] H. Schift, L. J. Heyderman, M. A. der Maur, and J. Gobrecht, "Pattern formation in hot embossing of thin polymer films," *Nanotechnology*, vol. 12, no. 2, p. 173, 2001.

[73] B. M. Kalay, G., "Processing and physical property relationships in injection-molded isotactic polypropylene. 2. morphology and crystallinity." *Journal of Polymer Science Part B: Polymer Physics,*, vol. 35, no. 2, pp. 265–291, 1997.

[74] A. del Campo and C. Greiner, "Su-8: a photoresist for high-aspect-ratio and 3d submicron lithography," *Journal of Micromechanics and Microengineering*, vol. 17, no. 6, p. R81, 2007.

[75] K. V. Nemani, K. L. Moodie, J. B. Brennick, A. Su, and B. Gimi, "In vitro and in vivo evaluation of su-8 biocompatibility," *Materials science & engineering. C, Materials for biological applications*, vol. 33, no. 7, p. 10.1016/j.msec.2013.07.001, oct 2013.

[76] W. Dai, K. Lian, and W. Wang, "A quantitative study on the adhesion property of cured SU-8 on various metallic surfaces," *Microsystem Technologies*, vol. 11, no. 7, pp. 526–534, 2005.

[77] Linear polydimethylsiloxanes cas no. 63148-62-9. EUROPEAN CENTRE FOR ECOTOXICOLOGY AND TOXICOLOGY OF CHEMICALS.

[78] A. Colas and J. Curtis, "Biomaterials science," *Silicone Biomaterials History and Chemistry*, 2004.

[79] U. W. K. Z. Marciniec B, Gulinski J, *Comprehensive handbook on hydrosilylation*. Pergamon Press, 1992.

[80] A. Esteves, J. Brokken-Zijp, J. Laven, H. Huinink, N. Reuvers, M. Van, and G. de With, "Influence of cross-linker concentration on the cross-linking of {PDMS} and the network structures formed," *Polymer*, vol. 50, no. 16, pp. 3955 – 3966, 2009.

[81] M. A. Schmidt, "Wafer-to-wafer bonding for microstructure formation," *Proceedings of the IEEE*, vol. 86, no. 8, pp. 1575–1585, Aug 1998.

[82] T. Y. Chang, . Vikramaditya G. Yadav, and Sarah De Leo, a. C.-L. C. a. S. S. a. M. R. D. Agustin Mohedas, and Bimal Rajalingam, , and A. Khademhosseini, "Cell and protein compatibility of parylene-c surfaces," *Langmuir*, 2007.

[83] E. J. T. Y.-P. J. Tooker, Meng E, "Biocompatible parylene neurocages. developing a robust method for live neural network studies," *IEEE Eng Med Biol Mag.*, vol. 24, no. 6, p. 30, 2005.

[84] Specialty coating systems. [Online]. Available: http://scscoatings.com/

[85] J. Gao, T. Chen, C. Dong, Y. Jia, P.-I. Mak, M.-I. Vai, and R. P. Martins, "Adhesion promoter for a multi-dielectric-layer on a digital microfluidic chip," *RSC Adv.*, vol. 5, no. 60, pp. 48 626–48 630, jun 2015.

[86] Plasma-parylene systems gmbh, rosenheim, germany. [Online]. Available: http://www.plasmaparylene.de/

[87] W. Gorham, "Para-xylylene polymers," Sep. 19 1967, uS Patent 3,342,754.

[88] M. Akhtar, S. Driesche, A. Bdecker, and M. J. Vellekoop, "Long-term storage of droplets on a chip by parylene af4 coating of channels," *Sensors and Actuators B: Chemical*, vol. 255, 08 2017.

[89] M. Akhtar, S. Driesche, and M. Vellekoop, "On-chip storage of droplets in parylene-af4 coated pdms channels," *18th International Conference on Miniaturized Systems for Chemistry and Life Sciences, MicroTAS 2014*, pp. 1641–1643, 01 2014.

[90] H.-S. Moon, K. Je, J.-W. Min, D. Park, K.-Y. Han, S.-H. Shin, W.-Y. Park, C. E. Yoo, and S.-H. Kim, "Inertial-ordering-assisted droplet microfluidics for high-throughput single-cell rna-sequencing," *Lab Chip*, vol. 18, pp. 775–784, 2018. [Online]. Available: http://dx.doi.org/10.1039/C7LC01284E

[91] F. Ma, M. T. Chung, Y. Yao, R. Nidetz, L. M. Lee, A. P. Liu, Y. Feng, K. Kurabayashi, and G.-Y. Yang, "Efficient molecular evolution to generate enantioselective enzymes using a dual-channel microfluidic droplet screening platform," *Nature Communications*, vol. 9, no. 1, p. 1030, Mar. 2018. [Online]. Available: https://doi.org/10.1038/s41467-018-03492-6

[92] J. B. Wacker, I. Lignos, V. K. Parashar, and M. A. M. Gijs, "Controlled synthesis of fluorescent silica nanoparticles inside microfluidic droplets," *Lab Chip*, vol. 12, pp. 3111–3116, 2012.

[93] T. Nisisako and T. Hatsuzawa, "Microfluidic fabrication of oil-filled polymeric microcapsules with independently controllable size and shell thickness via janus to coreshell evolution of biphasic droplets," *Sensors and Actuators B: Chemical*, vol. 223, pp. 209 – 216, 2016.

[94] J. C. B. A. E.-H. O. J. M. L. F. J. B. K. J. H. S. K. H. D. C. H. D. A. W. A. D. G. J. Clausell-Tormos, D. Lieber and C. A. Merten, "Droplet-based microfluidic platforms for the encapsulation and screening of mammalian cells and multicellular organisms," *Chem. Biol.*, vol. 15, no. 5, p. 427437, 2008.

[95] A. L. M. Polinkovsky, E. Gutierrez and A. Groisman, "Fine temporal control of the medium gas content and acidity and on-chip generation of series of oxygen concentrations for cell cultures," *Lab Chip*, vol. 9, no. 8, p. 107384, Apr 2009.

[96] G. Firpo, E. Angeli, L. Repetto, and U. Valbusa, "Permeability thickness dependence of polydimethylsiloxane (pdms) membranes," *Journal of Membrane Science*, vol. 481, pp. 1 – 8, 2015.

[97] A. B. Theberge, E. Mayot, A. El Harrak, F. Kleinschmidt, W. T. S. Huck, and A. D. Griffiths, "Microfluidic platform for combinatorial synthesis in picolitre droplets," *Lab Chip*, vol. 12, pp. 1320–1326, 2012.

[98] J. P. Urbanski, W. Thies, C. Rhodes, S. Amarasinghe, and T. Thorsen, "Digital microfluidics using soft lithography," *Lab Chip*, vol. 6, pp. 96–104, 2006.

[99] K. E. A.P. Debon, R.C.R. Wootton, "Droplet confinement and leakage: Causes, underlying effects, and amelioration strategies," 2015.

[100] Y. Zhang and H. Jiang, "A review on continuous-flow microfluidic pcr in droplets: Advances, challenges and future." *Analytica Chimica Acta*, vol. 914, no. 5, pp. 7–16, 2016-03-31 00:00:00.0.

[101] C. Ybert and J.-M. di Meglio, "Ascending air bubbles in protein solutions," *The European Physical Journal B - Condensed Matter and Complex Systems*, vol. 4, no. 3, pp. 313–319, 1998.

[102] C.-L. T. Koji Takahashi, Jian-Gang Weng, "Marangoni effect in microbubble systems," *Microscale Thermophysical Engineering*, vol. 3, no. 3, pp. 169–182, 1999.

[103] T. Fortin, J.B.; Lu, *Chemical Vapor Deposition PolymerizationThe Growth and Properties of Parylene Thin Films.* Kluwer Academic Publishers: Norwell, MA, USA, 2004.

[104] H. Sasaki, H. Onoe, T. Osaki, R. Kawano, and S. Takeuchi, "Parylene-coating in pdms microfluidic channels prevents the absorption of fluorescent dyes," *Sensors*

and Actuators B: Chemical, vol. 150, no. 1, pp. 478 – 482, 2010. [Online]. Available: http://www.sciencedirect.com/science/article/pii/S0925400510005964

[105] H.-S. Noh, Y. Huang, and P. J. Hesketh, "Parylene micromolding, a rapid and low-cost fabrication method for parylene microchannel," *Sensors and Actuators B: Chemical*, vol. 102, no. 1, pp. 78 – 85, 2004, selected papers from Transducers 03. [Online]. Available: http://www.sciencedirect.com/science/article/pii/S0925400504004769

[106] W. Wang, D. Kang, and Y. C. Tai, "Study of parylene penetration into microchannel," in *2015 Transducers - 2015 18th International Conference on Solid-State Sensors, Actuators and Microsystems (TRANSDUCERS)*, June 2015, pp. 1307–1310.

[107] Q. Y. Y. Zhao, G. Chen, "Liquid-liquid two-phase flow patterns in a rectangular microchannel," no. 52, p. 40524060, 2006.

[108] G. Liu, X. Wang, K. Wang, C. P. Tostado, and G. Luo, "Effect of surface wettability on internal velocity profile during droplet formation process in microfluidic devices," vol. 80, pp. 188 – 193, 2016.

[109] A. Tracton, *Coatings Materials and Surface Coatings*. CRC Press, 2006.

[110] E. M. Tolstopyatov, S. H. Yang, and M. C. Kim, "Thickness uniformity of gas-phase coatings in narrow channels: Ii. one-side confined channels," *Journal of Physics D: Applied Physics*, vol. 35, no. 21, p. 2723, 2002.

[111] A. Minta, J. P. Kao, and R. Y. Tsien, "Fluorescent indicators for cytosolic calcium based on rhodamine and fluorescein chromophores." *Journal of Biological Chemistry*, vol. 264, no. 14, pp. 8171–8178, 1989.

[112] S. Li, "Dynamics of viscous entrapped saturated zones in partially wetted porous media," 2018.

[113] M. He, C. Sun, , and D. T. Chiu*, "Concentrating solutes and nanoparticles within individual aqueous microdroplets," *Analytical Chemistry*, vol. 76, no. 5, pp. 1222–1227, 2004, pMID: 14987074.

[114] D. J. Collins, A. Neild, A. deMello, A.-Q. Liu, and Y. Ai, "The poisson distribution and beyond: methods for microfluidic droplet production and single cell encapsulation," *Lab Chip*, vol. 15, pp. 3439–3459, 2015. [Online]. Available: http://dx.doi.org/10.1039/C5LC00614G

[115] E. N. Z.W. El-Hajj, "An escherichia coli mutant that makes exceptionally long cells," no. 197 (2015), p. 15071514, 2015.

[116] D. Madar, E. Dekel, A. Bren, A. Zimmer, Z. Porat, and U. Alon, "Promoter activity dynamics in the lag phase of escherichia coli," *BMC Systems Biology*, vol. 7, no. 1, p. 136, 2013. [Online]. Available: http://dx.doi.org/10.1186/1752-0509-7-136

[117] M. P. P.R. Murray, K.S. Rosenthal, *Medical Microbiology*, 7th ed. Elsevier Health Sciences, 2012.

[118] X.-q. Y. Y.-f. L. Y.-c. C. X.-y. C. M. Xian-feng Jiang, Kai Yang and M. Yue Tu, "Elastic modulus affects the growth and differentiation of neural stem cells," *Neural Regen Res*, 2015.

[119] F. Han, C. Zhu, Q. Guo, H. Yang, and B. Li, "Cellular modulation by the elasticity of biomaterials," *J. Mater. Chem. B*, vol. 4, pp. 9–26, 2016.

[120] A. Kumachev, J. Greener, E. Tumarkin, E. Eiser, P. W. Zandstra, and E. Kumacheva, "High-throughput generation of hydrogel microbeads with varying elasticity for cell encapsulation," *Biomaterials*, vol. 32, no. 6, pp. 1477 – 1483, 2011.

[121] L. Martyn R and D. A. Young, "The gelation of agarose," *J. Chem. SOC*, 1981.

[122] D. Li, "Electro-viscous effects on pressure-driven liquid flow in microchannels," *Colloids and Surfaces A: Physicochemical and Engineering Aspects*, vol. 195, no. 1, pp. 35 – 57, 2001. [Online]. Available:

http://www.sciencedirect.com/science/article/pii/S0927775701008287
[123] A. L. Givan, *Flow Cytometry: First Principles*, second edition ed. Wiley-Liss, Inc, Dec 2001.
[124] M. Akhtar, M. T. Rabbani, and M. J. Vellekoop, "Merging of droplets in microchannel independent of the droplet size and inter-droplet separation," pp. 95 180Y–95 180Y–6, 2015.
[125] B.-J. Jin, Y. W. Kim, Y. Lee, and J. Y. Yoo, "Droplet merging in a straight microchannel using droplet size or viscosity difference," *Journal of Micromechanics and Microengineering*, vol. 20, no. 3, p. 035003, 2010.
[126] H. Babahosseini, T. Misteli, and D. L. DeVoe, "Microfluidic on-demand droplet generation, storage, retrieval, and merging for single-cell pairing," *Lab Chip*, vol. 19, pp. 493–502, 2019. [Online]. Available: http://dx.doi.org/10.1039/C8LC01178H
[127] B. Xu, T. N. Wong, D. Zhang, and X. Shen, "Experimental and numerical investigation on a simple droplet coalescence design in microchannels," *Heat and Mass Transfer*, vol. 55, no. 6, pp. 1553–1562, Jun 2019. [Online]. Available: https://doi.org/10.1007/s00231-018-02539-0
[128] C. Chen, Y. Zhao, J. Wang, P. Zhu, Y. Tian, M. Xu, L. Wang, and X. Huang, "Passive mixing inside microdroplets," *Micromachines*, vol. 9, no. 4, 2018. [Online]. Available: https://www.mdpi.com/2072-666X/9/4/160
[129] S. Hossain and K.-Y. Kim, "Mixing performance of a serpentine micromixer with non-aligned inputs," *Micromachines*, vol. 6, no. 7, p. 842, 2015.
[130] S. v. d. D. M. Akhtar, L. Brandhoff and M. J. Vellekoop, "Air-droplets as gas reservoir to provide o2 to the stored-aqueous droplets in micro-channels," *Procedia Eng.*, vol. 120, pp. 92–95, 2015.
[131] C. W.-H. N. J. M. A. Khorshidi, P. K. P. Rajeswari and H. A. Svahn, "Automated analysis of dynamic behavior of single cells in picoliter droplets," *Lab Chip*, vol. 14, no. 5, pp. 931–7, Mar. 2014.
[132] P. Bao, D. A. Paterson, P. L. Harrison, K. Miller, S. Peyman, J. C. Jones, J. Sandoe, S. D. Evans, R. J. Bushby, and H. F. Gleeson, "Lipid coated liquid crystal droplets for the on-chip detection of antimicrobial peptides," *Lab Chip*, vol. 19, pp. 1082–1089, 2019. [Online]. Available: http://dx.doi.org/10.1039/C8LC01291A
[133] C.-Y. Ou, T. Vu, J. T. Grunwald, M. Toledano, J. Zimak, M. Toosky, B. Shen, J. A. Zell, E. Gratton, T. J. Abram, and W. Zhao, "An ultrasensitive test for profiling circulating tumor dna using integrated comprehensive droplet digital detection," *Lab Chip*, vol. 19, pp. 993–1005, 2019. [Online]. Available: http://dx.doi.org/10.1039/C8LC01399C
[134] S. R. R. P. C. Thomas and S. P. Forry, "Regulating oxygen levels in a microfluidic device," *Anal. Chem*, vol. 83, no. 22, pp. 8821–8824, 2011.
[135] S. B. J. O. T. S. P. R. S. C. E.-P. W. L. N. Wu, Y. Zhu and B. A. Sexton, "A pmma microfluidic droplet platform for in vitro protein expression using crude e. coli s30 extract," *Lap Chip*, vol. 9, no. 23, p. 33913398, 2009.
[136] F. Bunge, S. van den Driesche, and M. J. Vellekoop, "Pdms-free microfluidic cell culture with integrated gas supply through a porous membrane of anodized aluminum oxide," *Biomedical Microdevices*, vol. 20, no. 4, p. 98, Nov. 2018. [Online]. Available: https://doi.org/10.1007/s10544-018-0343-z
[137] X. F.-M. A. Tourovskaia and A. Folch, "Long-term micropatterned cell cultures in heterogeneous microfluidic environments," *Conf. Proc. IEEE Eng. Med. Biol. Soc.*, vol. 4, p. 26758, 2004.
[138] S. S. F. G. J. Y. K. X. N. J. B. E. S. I. C. R. C. R. W. K. S. E. S. Cho, D. K. Kang

and A. J. Demello, "Droplet-based microfluidic platform for high-throughput, multi-parameter screening of photosensitizer activity," *Anal. Chem*, vol. 85, no. 18, p. 88668872, 2013.

[139] J. G. Riess and M. P. Krafft, "Advanced fluorocarbon-based systems for oxygen and drug delivery, and diagnosis," *Artificial Cells, Blood Substitutes, and Biotechnology*, vol. 25, no. 1-2, pp. 43–52, 1997. [Online]. Available: https://doi.org/10.3109/10731199709118896

[140] S. V. S. J. J. Casciari and J. C. R. M. Sutherland, "Variations in tumor cell growth rates and metabolism with oxygen concentration, glucose concentration, and extracellular ph," *J. Cell. Physiol.*, vol. 151, no. 2, pp. 2386–94, May 1992.

[141] T. Cubaud and C.-M. Ho, "Transport of bubbles in square microchannels," *Physics of Fluids*, vol. 16, no. 12, pp. 4575–4585, 2004.

[142] J. Ratulowski and H.-C. Chang, "Transport of gas bubbles in capillaries," *Physics of Fluids A*, vol. 1, no. 10, pp. 1642–1655, 1989.

[143] A. J. C. S., J. Toro-Mendoza, and M. Garcia-Sucre, "Correction to the interfacial tension by curvature radius: Differences between droplets and bubbles," *The Journal of Physical Chemistry B*, vol. 113, no. 17, pp. 5891–5896, 2009, pMID: 19338313.

[144] P. C. J. . Xu and T. . Zhao, "Gasliquid two-phase flow regimes in rectangular channels with mini/micro gaps," *Flow, vol*, vol. 25, no. 3, pp. 411–432, Apr 1999.

[145] T. Cubaud, U. Ulmanella, and C.-M. Ho, "Two-phase flow in microchannels with surface modifications," *Fluid Dynamics Research*, vol. 38, no. 11, p. 772, 2006.

[146] P. Concus and R. Finn, "On capillary free surfaces in the absence of gravity," *Acta Math.*, vol. 132, no. 1, pp. 177–198, 1974.

[147] T. Cubaud and M. Fermigier, "Advancing contact lines on chemically patterned surfaces," *Journal of Colloid and Interface Science*, vol. 269, no. 1, pp. 171 – 177, 2004.

[148] M. Rosenauer and M. J. Vellekoop, "A versatile liquid-core/liquid-twin-cladding waveguide micro flow cell fabricated by rapid prototyping," *Applied Physics Letters*, vol. 95, no. 16, 2009.

[149] F. K. E. Weber, D. Puchberger-Enengl and M. J. Vellekoop, "In-line characterization and identification of micro-droplets on-chip," *Optofluidics, Microfluid. Nanofluidics*, vol. 1, no. 1, Jan 2014.

[150] J. E. Squires, "Artificial blood," *Science*, vol. 295, no. 5557, p. 10021005, 2002.

[151] J. G. Riess, "Blood substitutes and other potential biomedical applications of fluorinated colloids," *Journal of Fluorine Chemistry*, vol. 114, no. 2, pp. 119 – 126, 2002, 13th European Symposium on Fluorine Chemistry (ESFC-13).

[152] K. C. Lowe, "Perfluorochemical respiratory gas carriers: benefits to cell culture systems," *Journal of Fluorine Chemistry*, vol. 118, no. 1–2, pp. 19 – 26, 2002, a special industrial research section.

[153] V. S. G. B. A. G. H. L. E. M. S. Inayat, A. C. Bernard and O. R. Oakley, "Oxygen carriers: A selected review," *in Transfusion and Apheresis Science*, vol. 34, no. 1, pp. 25–32, 2006.

[154] A. J. Pons, O. Batiste, and M. A. Bees, "Nonlinear chemoconvection in the methylene-blue–glucose system: Two-dimensional shallow layers," *Phys. Rev. E*, vol. 78, p. 016316, Jul 2008.

[155] M. a. B. A. J. Pons, G. Sorensen and F. Sagu "Pattern formation in the methylene-blue-glucose system," *J. Phys. Chem. B*, vol. 104, p. 22512259, 2000.